Title
The role of hyaluronic acid in ductal branching morphogenesis of the prostate gland

Author
Gakunga, Peter T.

Publication Date
1996

Peer reviewed|Thesis/dissertation

The Role of Hyaluronic Acid in Ductal Branching Morphogenesis of the Prostate Gland

by

Peter T. Gakunga

DISSERTATION

Submitted in partial satisfaction of the requirements for the degree of

DOCTOR OF PHILOSOPHY

in

Oral Biology

in the

GRADUATE DIVISION

of the

UNIVERSITY OF CALIFORNIA

San Francisco

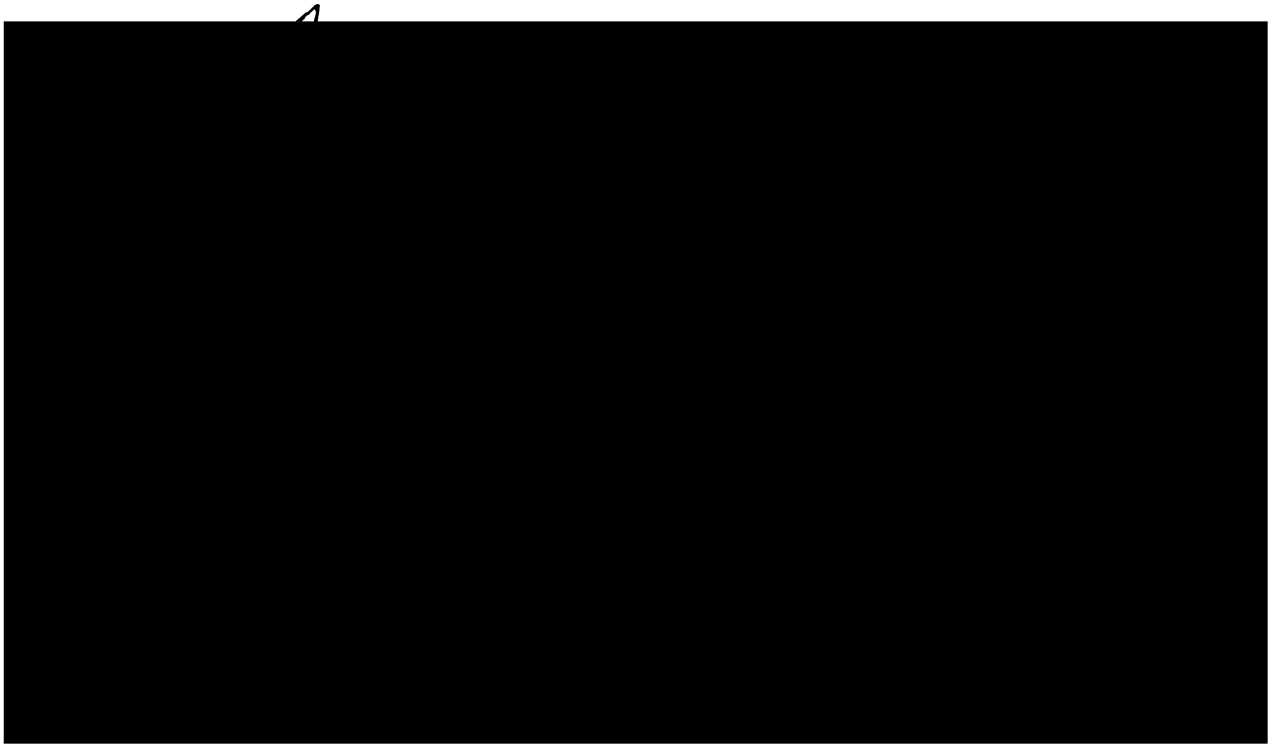

DEDICATION

To my parents, Wangui na Gakunga, who taught me how to walk;
to my wife, Wanjiku, who gave me two more feet to walk on.

Gũtirĩ kĩega kiumaga hega.
-From the Gikuyu people of Kenya

ACKNOWLEDGEMENTS

Dr. Robert Stern pointed out the steep and narrow way, but did not fail to also point out the rainbow.

Members of the Stern lab, past and present, this work is built by your bricks.

Dr. Gerald Cunha and members of his lab guided me into the world of developmental biology.

Members of my committee, Dr. Susan Hawkes and Dr. Bent Formby, gave incisive and critical input that shaped the form and content of this dissertation.

Dr. John Greenspan and Dr. Caroline Damsky recruited me into the program, and always marshalled significant support for me, every step of the way.

Ahsante sana

The role of Hyaluronic Acid in Ductal Branching Morphogenesis of the Prostate Gland

Peter T. Gakunga

Abstract

Hyaluronic acid is prominent in the extracellular matrix early in embryogenesis. Increased levels of HA correlate with rapid tissue growth and cell movement, while disappearance of hyaluronic acid coincides with the onset of tissue differentiation. CD44, a transmembrane glycoprotein, is the major receptor for hyaluronic acid on the surface of vertebrate cells. This molecule, encoded by a single gene locus, is composed of 20 exons, 10 of which are expressed variably due to alternative splicing of the nuclear RNA. The variant isoforms are restricted in their distribution compared to the standard CD44 (CD44S). Mouse anterior prostate glands obtained at various postnatal timepoints were examined for the expression of hyaluronic acid and CD44. Reverse transcriptase polymerase chain reaction analysis was used to map the temporal regulation of specific CD44 variant isoforms. In each age group, hyaluronic acid was localized exclusively in the stromal matrix. Hyaluronic acid deposition was particularly prominent in the early stages, localizing predominantly around the proliferating distal ductal tips; hyaluronic acid was greatly reduced in the later ages, and was entirely absent around the developmentally quiescent proximal regions of the ducts. Early in prostate development, CD44 was prominent in the mesenchyme. However, in the later phases, CD44 expression became associated with membranes of epithelial cells, predominantly on cells at the distal tips of invading ducts. During these stages, levels of hyaluronic acid in the stroma correlated with levels of CD44 on epithelial cells. Using a serum-free organ culture system, and computerized morphometrics, the significance of hyaluronic acid-CD44 interaction on ductal branching morphogenesis of the mouse anterior prostate, from birth to six days-of-age, was examined. In the presence of optimal levels of

testosterone, the organs underwent ductal branching morphogenesis. Treatment with either neutralizing anti-CD44 antibodies, hyaluronic acid hexasaccharides, or the enzyme hyaluronidase inhibited androgen-stimulated ductal branching morphogenesis.

A role for hyaluronic acid and CD44 interaction in the developing prostate is suggested for both the initial proliferative, and the later differentiating stages during branching morphogenesis. These results are suggestive of the significant role played by hyaluronic acid-CD44 interactions in mediating androgen-induced prostatic growth and morphogenesis.

Table of Contents

List of Figures

Chapter I

Chapter II

Chapter III

1.0 INTRODUCTION

The study of morphogenesis draws its roots from the contributions of Aristotle (translation by Platt, 1912). Through time, the field has evolved from purely descriptive observations, and now encompasses an understanding of the cascades of molecular cues responsible for the diverse signals that unfold during development.

Grobstein (1954) made the initial proposal that the extracellular matrix (ECM) mediates interactions between adjacent tissues during the embryogenesis of parenchymal organs. Consistent with a role in both tissue development and homeostasis, the ECM turns over slowly in mature tissue, providing scaffolding, while in the embryo the changes occur rapidly. This implies the existence of mechanisms for remodeling, in which not only quality, but also rates of ECM turnover play a critical role.

Tissue remodeling is influenced by a wide repertoire of factors. Evidence from several model systems, e.g. the mouse salivary gland (Bernfield, et al., 1984; Cutler, 1990), and the mammary gland (Bissell and Hall, 1987; Daniel and Silberstein, 1987; Imagawa, et al., 1990; Kratochwil, 1987; Snedeker, et al., 1991), indicates that several factors, including hormones and growth factors, in addition to the ECM, provide the information required for ductal branching morphogenesis. The overall process is characterized by the invasion of epithelial ducts into the mesenchyme, accompanied by changes in the basement membrane. Simultaneously, the mesenchymal interstitial matrix is constantly being remodeled to accommodate the expanding epithelium.

The extracellular (ECM) is rich in proteoglycans, glycoproteins (GP) and glycosaminoglycans (GAGs). In addition, it contains a dynamic network of structural and adhesive molecules as well as cytokines, glycosidases, proteinases, and their inhibitors. The interstitial ECM is synthesized primarily by fibroblasts, and contains structural and

adhesion GPs (collagens, fibronectins, the B chains of laminin, and entactin), and the GAGs, **hyaluronic acid,** heparan sulfates, chondroitin sulfates, and dermatan sulfates. The basal lamina synthesized mainly by the epithelial cells, is composed of collagens IV and V, laminin, entactin, and heparan sulfate proteoglycans such as syndecan.

Classically, ECM glycoproteins are designated the role of providing structural support. However, there is mounting evidence that they also impart biochemical information critical to several biological processes, including glandular morphogenesis (Guan, et al., 1991; Werb, et al., 1989). Several studies have documented the roles of the various components of the ECM in the development of glandular organs with an epithelial parenchymal structure (Bernfield and Banerjee, 1982; Bernfield et al., 1973; Cutler, 1990; Kratochwil, et al., 1986; Wessells, 1977). Immunocytochemical evidence from the work of Nakanishi et al. (1988) strongly suggests that collagen III has a role in the ductal branching morphogenesis of embryonic salivary glands. Purified collagenase inhibits branching morphogenesis, while collagenase inhibitor stimulates branching morphogenesis of the salivary gland (Nakanishi, et al., 1986).

Ductal branching morphogenesis, in the embryonic salivary gland model, is associated with the remodeling of GAG-containing substances in both the interstitial ECM of the mesenchyme as well as in the basal lamina. It has been suggested that GAG degradation in the basal lamina is achieved through the action of a neutral hyaluronidase (Bernfield et al., 1984). The difference in synthesis and degradation of GAGs in the developing salivary gland results in higher concentrations of HA and heparan sulfate in clefts, compared to the lobules. The continuous dialogue between epithelial and mesenchymal cells as reflected in their attendant ECMs is the focus of this study.

The prostate gland of the mouse undergoes a pattern of ductal branching morphogenesis similar to that observed in virtually all parenchymal glands including the bulbourethral gland and mammary glands. The prostate gland develops under the influence of testosterone, or the more active metabolite, dihydrotestosterone. This study utilizes the prostate gland as an experimental model to study the role of HA and its cell surface receptor, CD44, in hormone-dependent ductal branching morphogenesis.

1.1 Hyaluronic acid

Hyaluronic acid (HA) is a high-molecular-weight, negatively charged polysaccharide that is ubiquitously distributed in the ECM of all animals. HA was initially isolated from the vitreous of the eye (Meyer, 1934). The most important sources for the isolation of HA are the vitreous body, umbilical cord, joint fluid, rooster comb, and Streptococci. HA, a member of the glycosaminoglycan family, is distinctively different from the rest of the family in that it lacks a covalently linked peptide.

The structure of HA is a linear polymer built from repeating disaccharide units with the structure [D-glucuronic acid, N-acetyl-D-glucosamine] and a polydisperse molecular mass averaging several million. This helical molecule is stabilized by hydrogen bonds parallel with the chain axis (Scott, 1989), giving it an expanded coil structure in solution. The water immobilized within the coil is not chemically bound to the polysaccharide. The proposed secondary structure of HA is composed of a clustering of hydrophobic groups that potentially are involved in chain-chain interactions (Scott, 1989).

The classical technique for the detection of HA is the carbazole method for uronic acids. However, this technique has disadvantages in that it requires hyaluronan in quantities of at least 100 µg. A more sensitive battery of assays are those based on RIA or ELISA-like techniques, which can detect nanograms of HA (Lindqvist et al., 1992). These employ

HA-binding proteins (from the HA-binding region of cartilage proteoglycan, cartilage link protein, or hyaluronectin) in place of primary antibodies.

-1,4-glcUA-β-1,3-glcNAc-β-

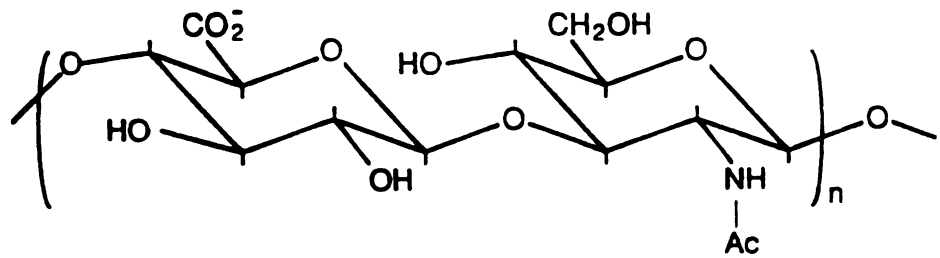

Fig i, The chemical structure of hyaluronan. The polymer is composed of the alternating disaccharide unit of glucuronic acid (GlcUA) and N-acetylglucosamine (GlcNAc).

HA is synthesized on the inner surface of plasma membrane, in contrast with the other GAGs which are made in the golgi. This was first suggested by Clarris and Fraser (1968), who described a hyaluronidase-sensitive coat surrounding synovial cells in culture. This coat is synthesized *de novo* even in the presence of HA-free medium. HA chains grow at the reducing end by the addition of sugar residues from the respective UDP-derivatives. This is carried out within the plasma membrane and subsequently the chain is translocated to the pericellular space (Prehm, 1990). In contrast, all the other GAGs grow by addition of sugars to the nonreducing end. The molecular details of the mechanisms that regulate the biosynthesis of HA remain to be worked out.

By injecting HA labeled with [^{3}H] in the acetyl group into rats intravenously, it has been established that circulating HA comes from the peripheral tissues through the lymph. The polymer is cleared from circulation primarily through the liver, with a half-life of approximately 5 minutes (Laurent and Fraser, 1986; Fraser and Laurent, 1989). By separating the various rat liver cells, it has been demonstrated that endothelial cells are responsible for taking up, and degrading HA (Smedstrod et al., 1984). The enzymatic degradation of HA is achieved by the concerted activity of three families of enzymes; hyaluronidases, which are endoglycosidases; and two groups of exoglycosidases. The initial cleavage is accomplished by hyaluronidase. Two categories of vertebrate hyaluronidases have been described; those active at neutral pH, such as testicular hyaluronidase; and enzymes active at acid pH, presumably of lysosomal origin. Following endocytosis, HA is routed to lysosomes with the resultant end-products being glucuronic acid and N-acetylglucosamine (Roden et al., 1989). There is evidence suggesting that circulating HA is also metabolized in kidney and the spleen (Laurent and Fraser, 1986), as well as the lymph nodes (Fraser and Laurent, 1989).

An important aspect of HA turnover occurs locally in various tissues. This has been documented in joints, skin, intestines, and the eye (Reed et al., 1990; Brown et al., 1991). Using [^{125}I] tryamine celloboise-labeled HA, it has been definitively demonstrated that HA is internalized into cells locally, and degraded with rapid turnover in lysosomes (Laurent et al., 1991). The rapid turnover of HA, which is uncharacteristic of structural components of connective tissue, is suggestive of additional regulatory roles for HA in cellular function.

The classical view of the biological function of HA has been that of a space filler. However, increasingly a greater role for HA in cell biology and pathology is being elucidated. The production of HA is elevated during periods of cell proliferation, with

synthesis being maximal during mitosis. This observation draws credence from several studies which provide evidence that endogenously produced HA weakens cellular attachment to the substrata (Barnhart et al., 1979; Erickson and Turley, 1983). The concentration of HA increases in compartments in which cellular migration takes place. HA creates hydrated pathways through cellular and fibrous barriers, facilitating tissue invasion. Indeed, invasion of cells during embryonic development, tumorigenesis, and tissue regeneration occurs into highly hydrated, HA-rich matrices (Comper and Laurent, 1978; Toole, 1971; Robert Stern, personal comm.). Several studies by Turley have shown unequivocally that HA promotes locomotion. An HA-binding protein (RHAMM) isolated from the conditioned medium of chick fibroblast cultures (Turley et al., 1990), and subsequently cloned and characterized (Hardwick et al., 1992) confers to cells properties akin to those of virally transformed cells.

1.2 Hyaluronic acid receptors (hyaladherins)

HA influences various biological phenomena by interacting with specific HA-binding proteins (HABPs). The HABPs described thus far can be divided into structural macromolecules embedded in the extracellular matrix; and cell surface receptors. There are distinctive differences between cell-surface HA receptors and matrix receptors: the minimum size of an HA oligosaccharide that cell-surface HA receptors (CD44, RHAMM, IVd4, LEC) bind to is the hexasaccharide (HA_6), while the matrix hyaladherins require deca- and dodecasaccharides of HA (HA_{10-12}) (Knudson, 1993). The affinity of HA-cell surface receptor binding increases with increased HA length, suggesting multivalent interaction (Toole , 1990; Underhill, 1993).

The most extensively characterized HA-binding macromolecules are link proteins and the cartilage proteoglycan, aggrecan (Goetinck et al., 1987). The tandemly repeated domains (B and B' loops) at the carboxy terminus of cartilage link protein contain the HA-binding

region. Four peptides obtained from two corresponding regions of the tandem repeats block binding of HA to link protein, thus suggesting that all four regions are involved in the binding. Each of these peptides is characterized by a cluster of positively charged amino acids, and binding decreases with increasing ionic strength, suggesting that binding is ionic. Homologies similar to those of the HA binding regions of link protein have been described in versican, which is produced by human fibroblasts (Zimmermann and Ruoslahti, 1989); in hyaluronectin, an HABP produced by human glial cells (Delpech and Halavent, 1981; Perides et al., 1989); and the N-terminus of the adhesive proteins that have variously been described as CD44, Pgp-1, Hermes antigen, and ECMRIII (Stamenkovic et al., 1989; Goldstein et al., 1989). However, RHAMM, which binds HA with high affinity, does not contain regions homologous to the HA binding domains described above. A more compelling HA binding motif that is common to all HA binding proteins has recently been described (Yang et al., 1994). HA binds optimally to an amino acid sequence that is described by the motif B(X_7)B. B is either arginine or lysine, and X is any amino acid except acidic residues. The precise spacing within the motif is critical. Substitution of arginine or lysine residues with histidine diminishes HA binding. The specificity of this motif and not just the effect of a cluster of basic charges is evidenced by the fact that HA does not bind efficiently to polylysine (Goetinck et al., 1987). Sequence analysis indicates that this motif occurs in versican between amino acids 2319 and 2327; and within the B region (aa 150-162) and the cytoplasmic domain (aa 292-300) of CD44. These are regions that have been shown to bind HA. However, the HA-binding motif does not account for all the HA binding properties of these proteins. It is interesting to note that when CD44, link protein and aggrecan are chemically reduced, they bind HA poorly (Toole, 1990), while RHAMM shows no changes in its binding abilities (Hoare et al., 1993). This suggests that a three-dimensional configuration may be important in some of the binding.

Link protein and aggrecan are structural macromolecules which, through interactions with HA, form ternary complexes that endow cartilage with its distinctive physical properties. Structural complexes involving HA and versican are important in building the matrices of connective tissues (Gallagher, 1989). A separate but related group of HABPs on cell surfaces mediates the effects of HA on cell behavior. Cell surface hyaladherins have been detected on several cell types and tissues (Toole, 1990), and a convergence of several studies has determined that many of these receptors are indeed CD44.

The first cell surface receptor for HA described was an 85 kDa protein on the surface of SV-40 transformed 3T3 cells, and also on BHK cells (Underhill, 1989). The monoclonal antibody K-3 that blocks the binding of HA to the 85 kDa receptor was used to demonstrate by immunohistochemistry, the distribution of this receptor in hamster epithelia and on members of the mononuclear phagocytic family of cells (Underhill, 1989). Subsequent studies identified the 85 kDa receptor reactive with K-3 as being CD44, and multiple forms of CD44 have been found and characterized (Aruffo et al., 1990; Culty et al., 1992).

Although CD44 is the most extensively studied HABP, other cell surface receptors have been reported that do not belong to the CD44 family. A novel HA receptor that mediates HA-induced cell locomotion has been characterized (Turley et al., 1989; Hardwick et al., 1992; Yang et al., 1994). The receptor is part of an HA receptor complex (HARC) that is found both at the cell surface of fibroblasts and as soluble proteins of M_r 72, 68, 58, and 52 kDa. The 58 kDa protein of the HARC is the HA-binding component and it has been termed RHAMM, an acronym for Receptor for HA-Mediated Motility. The cDNA sequence of RHAMM is unrelated to the previously described hyaladherins, and it is not recognized by anti-CD44 antibodies (Turley and Auersperg, 1989). Increased expression of RHAMM stimulates locomotion 6- to 10-fold in *ras*-transformed cells, in the presence of

HA. This locomotion is blocked by anti-RHAMM antibodies as well as by hyaluronidase digestion (Turley et al., 1991).

Other cell-surface HA receptors include a group of cell surface proteins recognized by a monoclonal antibody, IVd4, described by Banerjee and Toole (1991). These antibodies were raised against a novel soluble hyaladherin purified from embryonic chick brain and unrelated to previously described brain HABPs. These antibodies recognize cell-surface HABPs on several cell types and these resolve on Western analysis as three major proteins ranging from M_r 50-95 kDa (Banerjee and Toole, 1991; Banerjee and Toole, 1992). Another family of HA receptors unrelated to CD44 and RHAMM is primarily localized to endothelial cells of liver sinusoids and is involved in the clearance of HA from the circulation (Smedsrod et al., 1984) These are termed liver endothelial cell (LEC) receptors.

1.2.1 CD44

CD44 is a widely distributed family of cell surface glycoproteins which has been studied and described by different investigators in several different tissues. It is a cell adhesion molecule with functions that include ECM binding, cell migration, lymphopoiesis, and lymphocyte homing. CD44 has been characterized on several cell types including macrophages, fibroblasts, keratinocytes and epithelial cells. The functions of CD44 are based on its ability to mediate cell-cell and cell-substrate interactions involving components of the ECM and the pericellular matrix. Although most of the functions of CD44 are consequences of this primary function, the downstream events are modified depending on the cell type and the cellular environment. This observation has been detailed in endothelial cells and erythrocytes in which both $CD44^+$ (Trowbridge et al., 1982; Ahlo and Underhill, 1989) and $CD44^-$ (Bourguignon et al., 1992) phenotypes have been described. Although this apparent discrepancy may be the result of differences in cell culture methods, it may also reflect the influence of environmental cues on the expression

of CD44. The tissues that have been consistently CD44 $^-$ are cardiac muscle, liver hepatocytes, kidney tubular epithelium, and testis (Picker et al., 1990; Heider et al., 1993). In addition to human and mouse, CD44 has been described in a variety of species including hamster, baboon, rat, sheep, dog and cow (Aruffo et al., 1990; 1990; Gunthert et al., 1991).

Multiple forms of CD44 have been described. The most abundant type, referred to as "standard", CD44S or "hematopoietic", CD44H has a relative molecular mass of 85-95 kDa on non-reducing SDS-PAGE. This standard CD44 is synthesized as a polypeptide of M_r 42 kDa which undergoes N- and O-linked glycosylation (Brown et al., 1991; Lokeshwar and Bourgignon, 1991) and, in some instances, phosphorylation (Isacke et al., 1986; Neame and Isacke, 1992). The high molecular weight forms of CD44 on lymphocytes are sensitive to chondroitinase ABC. This identifies CD44 as a proteoglycan and suggests a diversity of ligand-binding properties (Jalkanen et al., 1988). Further size differences in CD44 are as a result of glycosylation and alternative exon splicing (Quackenbush et al., 1990; Camp et al., 1991).

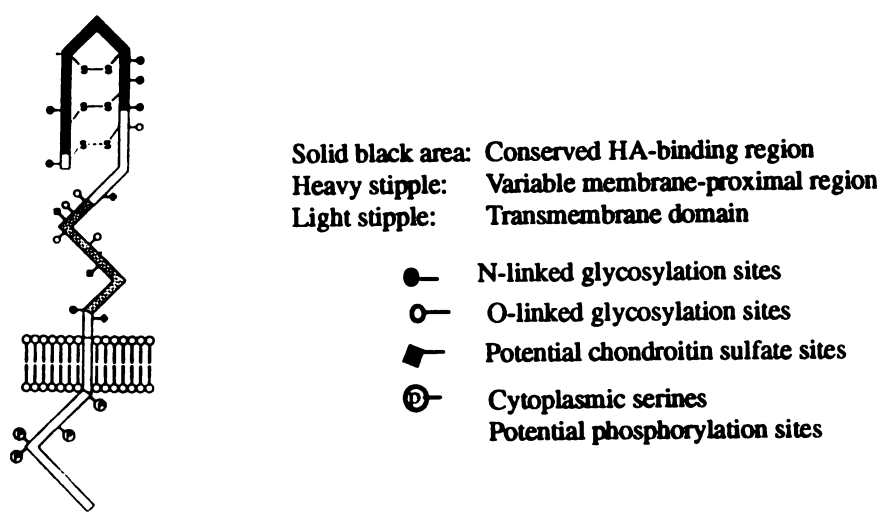

Fig ii, Representation of the mature core protein of CD44.

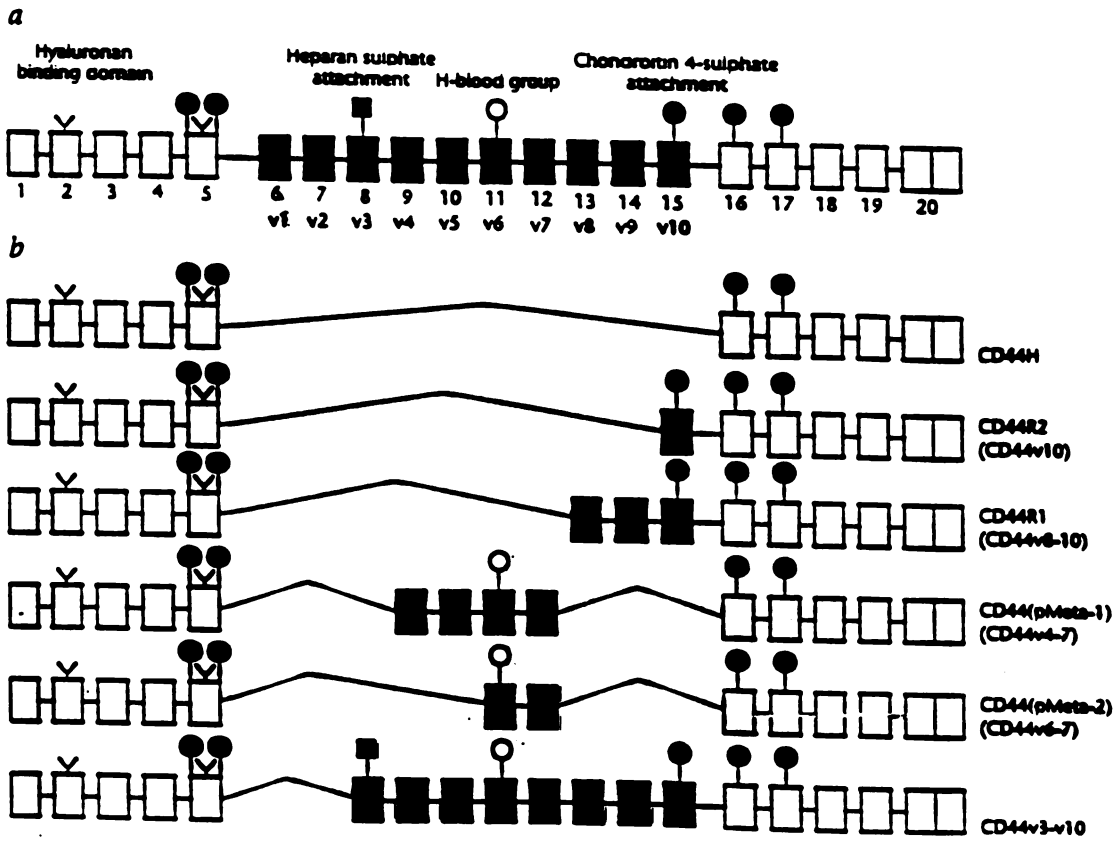

Fig iii. Map of the 20 exons of the CD44 gene. **Fig ii a,** Clear boxes represent constituitively expressed exons. Solid boxes represent alternatively spliced exons. **Fig iii b,** Exons representing alternatively spliced CD44 isoforms.

The mature core protein of CD44 can be subdivided into multiple domains. The potential trans-membrane domain is highly conserved among different species. The amino terminus of the extracellular domain is composed of 90 relatively hydrophobic residues with homology to cartilage link protein, and other HA-binding proteins (Stamenkovic et al.,

1989; Wolffe et al., 1990). The human molecule has six sites for N-linked glycosylation within this domain. The membrane-proximal domain, which is not as well conserved among species, is characterized by many potential O-glycosylation sites and three sites for chondroitin sulfate attachment. The cytoplasmic domain is highly conserved among human, baboon, and mouse (Stamenkovic et al., 1989; Zhou et al., 1989). There are five conserved residues that are potential sites for serine phosphorylation in the human protein (Isacke et al., 1986; Carter and Wayner, 1988). Ser 291 is part of a protein kinase C consensus site, and Ser 316 lies in a protein kinase A consensus site. However, experimental mutagenesis shows that these sites are not phosphorylated. The critical serine phosphorylation sites are Ser 323 and Ser 325 which lie in typical casein kinase-II consensus sites (Neame and Isacke., 1992; Pure et al., 1995). The function of this kinase in stabilizing the CD44 variable region has recently been demonstrated (Stern et al., submitted).

CD44 represents a single gene located on the short arm of chromosome 11 in humans (Goodfellow et al., 1982) and on chromosome 2 in mice (Lesley and Trowbridge, 1982). There are 20 exons of which exons 1-5 and 16-20 encode standard CD44 sequences. The ten exons between 5 and 16 are subjected to exon shuffling by alternative splicing, a phenomenon originally described in the pancreatic rat cell line BSp73ASML (Matzku et al., 1983).

1.2.2 CD44 as a receptor for HA

The N-terminal domain of CD44 is at least 30% homologous to the second (B) subdomain of cartilage proteoglycan core and link proteins (Goldstein et al., 1989; Stamenkovic et al., 1989). There is also some degree of sequence similarity to the B_1 subdomain of proteoglycan core and link proteins (Goldstein et al., 1989). This sequence homology is suggestive of a role in binding HA. However, both link protein and the two proteoglycan

core proteins, aggrecan and versican contain disulfide-bonded subdomains that form tandem-repeated structures, which suggests that the binding of HA is a product of more than one subdomain (Goetinck et al., 1987). The interaction between link protein and HA which is of an ionic nature (Goetinck et al., 1987).

Several cell types are surrounded by a pericellular matrix, and experimental formation of the pericellular matrix can be initiated by the addition of HA and cartilage proteoglycan monomer to cells in culture (Knudson and Knudson, 1993). Matrix formation is conditional on the ability of the cell to bind HA through a very specific HA-binding cell surface receptor (Knudson and Knudson, 1991). This receptor has been described in a variety of cells and tissues. It is expressed on proliferating epithelial cells such as the basal layers of stratified epithelium and the basolateral surfaces of cells at the base of the crypts of Lieberkuhn (Ahlo and Underhill, 1989). This receptor has also been described on fibroblast cell lines as an 85 kDa glycoprotein that binds to a six sugar residue on the HA polypeptide. A portion of this molecule is associated with cytoskeletal actin filaments and its properties are synonymous with those of CD44 (Lacy and Underhill, 1987; Lesley et al., 1990).

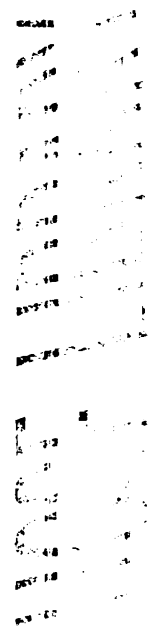

$CD44^+$ cell lines aggregate in the presence of exogenous HA, a property that can be attenuated by preincubation of these cells with antibody to the fibroblast HA receptor or with a CD44-specific monoclonal antibody (Green et al., 1989; Lesley et al., 1990; Miyake et al., 1990). The gene product of the expression of a soluble human CD44-IGg construct in COS cells binds to the high endothelial cells of lymph nodes in culture. This binding is significantly reduced by pretreatment of the cells with HA-degrading hyaluronidase and by excess HA. When a cDNA clone for the hamster CD44 molecule is transfected into COS cells, the transfected cells react with antibody specific for the hamster fibroblast HA receptor (Aruffo et al., 1990). Further, when the $CD44^-$ human Burkitt B

cell lymphoma cell line is transfected with the CD44H isoform, the cell line acquires the ability to bind to lymph node high endothelial cells. The binding is blocked by the presence of excess HA, hyaluronidase, or CD44 antibodies (Stamenkovic et al., 1989). There is therefore, sufficient evidence that CD44 functions as a receptor for HA. However, not all cells that express CD44 consistently display the HA-binding phenotype.

In experiments designed to examine the regions of CD44 mediating HA-binding, various modified mouse CD44 constructs were transfected into mouse T cell lymphoma AKRI. It was determined that the amino-terminal two-thirds of the CD44 molecule is sufficient for recognizing HA (He et al., 1992). This is consistent with observations that this region has sequence similarity to proteoglycan core and link protein (Goldstein et al., 1989). Constructs lacking most of the cytoplasmic domain do not bind HA from solution to the same extent as the wild type (Lesley et al., 1992), suggesting that cytoskeletal interactions may be crucial in mediating this interaction. Interestingly, AKRI transfectants expressing a molecule without most of the cytoplasmic tail and unable to bind HA, can be induced to do so by pretreatment with the CD44-specific monoclonal antibody IRAW 14 (Lesley et al., 1992).

Although most $CD44^+$ cell lines studied bind HA in a CD44-dependent manner, there are several other CD44 expressing cell lines that do not bind HA. In $CD44^+$ developing B cell lines, HA binding was determined only in the mature immunoglobulin-secreting cell types (Lesley et al., 1990; Miyake et al., 1990). Further evidence is the conversion of cell surface CD44 molecules from non-HA-binding to HA-binding states by the function of the mAb IRAW 14 (Lesley et al., 1992). T cell lines treated with phorbol esters can be induced to increase their HA-binding capacity without changes in the specific CD44 isoforms expressed (Lesley et al., 1990; Hyman et al., 1991). There is a clear distinction between phorbol ester-mediated induction, which occurs over several hours at 37 °C, and

results in increased CD44 expression, and activation by CD44-specific mAb which occurs at 0 °C, is rapid and can be achieved in prefixed cells. It is suggested that CD44 mAbs upregulate the HA-binding function of CD44 by clustering the molecule into multivalent structures (Hyman et al., 1991; Lesley et al., 1990; Lesley and Hyman, 1992). The level of expression of CD44 is apparently not a critical factor in accounting for differences in HA-binding. This is evidenced by the observation that a CD44 ^{hi} variant selected by fluorescence-activated cell sorting for high levels of CD44 expression binds HA to a significantly lower level than a low CD44 expressing cell line from the same parental stock (Hyman et al., 1991).

1.3 Hyaluronic acid and CD44 in morphogenesis

The exquisitely controlled series of cellular events involved in morphogenesis are influenced at each stage by ECM macromolecules. The role of GAGs in morphogenesis has been elucidated by several studies correlating changes in GAG quality, concentration, and distribution with evolving morphogenetic events, as well as by experimental manipulations designed to identify the direct role of GAGs.

Cell-cell and cell-ECM interactions play a major role in several biological processes including wound healing, maintenance of tissue homeostasis, tumor progression, embryonic development, and morphogenesis. Cells adhere to each other and to the ECM utilising specific cell surface receptors such as integrins, cadherins, selectins, and members of the immunoglobulin superfamily. Members of the CD44 family are also involved in these cell-surface receptor mediated events (Gunthert et al., 1991; Pals et al., 1993; Ruiz et al., 1995).

Several developmental systems have been used to study specific HA-related interactions in morphogenesis. These include kidney mesenchyme (Belsky and Toole, 1983), chick

embryo cornea (Hay, 1980; Trelstad et al., 1971), and chick sclerotomal cells (Kvist and Finnegan, 1970).

Branching morphogenesis is a process common to the development of several parenchymal organs including mammary gland, lung, kidney and salivary gland. It is dependent on epithelial-mesenchymal interaction (Spooner et al, 1986). Inhibition of proteoglycan synthesis in salivary gland or kidney primordia using beta-xyloside blocks branching morphogenesis (Spooner et al., 1985; Lelongt et al., 1988). This is also achieved by treatment of embryonic salivary gland epithelium with hyaluronidase (Banerjee et al., 1977). During branching of salivary gland primordia, there is a difference in the distribution of GAGs between the quiescent clefts and the active branching sites at the distal tips of lobules. Type I and III collagen accumulate in, and presumably stabilize the clefts (Bernfield et al., 1984; Spooner et al., 1986). The basal lamina of the lobules is enriched in HA and chondroitin sulfate, and is low in heparan sulfate proteoglycan and type IV collagen. A neutral hyaluronidase has been reported to mediate the turnover of lobular GAGs (Bernfield et al., 1984). The differential distribution and turnover of the epithelial and mesenchymal ECM elements leads to coordinated epithelial proliferation and stabilization, resulting in clefting and branching.

Increased HA concentration within confined compartments leads to increased tissue hydration, pressure, and ultimately to tissue expansion. This may be the mechanism responsible for the changes in the neural folds. There is compelling evidence to suggest that HA plays a role in the elevation and folding of the neural plate during the formation of the neural tube. HA accumulates in the mesenchyme of cranial neural folds (Morris-Wiman and Brinkley, 1990), and treatment of early chicken embryos with HA-specific hyaluronidase results in open neural tube defects (Schoenwolf and Fisher, 1983).

However, similar results have not been obtained with rat embryos (Morriss-Kay et al., 1986).

Embryonic limb development is initiated by the proliferation and migration of mesodermal cells followed by cellular condensations in the myogenic and chondrogenic regions, with eventual differentiation. During premyogenic and prechondrogenic condensation, the subectodermal mesoderm is uncondensed and HA-rich spaces are maintained between cells. Condensation of the mesenchyme is a critical step in the formation of cartilage and muscle. When the chondrogenic and myogenic areas of the limb bud are condensed, the mesodermal cells do not exhibit pericellular coats in culture. However, during chondrocyte differentiation, which is characterized *in vivo* by large intercellular spaces, prominent pericellular coats reappear *in vitro.* At the time of condensation there is a significant decrease in the ratio of HA to chondroitin sulfate proteoglycan produced by the condensing mesoderm (Knudson and Toole, 1985). Interestingly, this is accompanied by increased expression of cell-surface HA binding receptors (Knudson and Toole, 1987). In the light of evidence showing that cell surface HA receptors are involved in HA endocytosis prior to lysosomal degradation, it is presumed that the HA binding receptors expressed coincident with condensation are involved in receptor-mediated endocytosis of HA.

Studies by Toole and his colleagues (Banerjee and Toole, 1992) provide evidence that interaction of HA with the surface of endothelial cells is involved in endothelial cell morphogenesis. Endothelial cell morphogenesis is blocked by treatment of the cells with either mAb IVd4, an antibody specific to a newly described HA binding protein, or with a hexasaccharide. Both these reagents interfere with binding of HA to HABP, a limiting step in matrix assembly. Several studies have also documented the major role played by HA in matrix assembly by chondrocytes. The structure of cartilage matrix is based on the interaction of HA with link protein and aggrecan. Chondrocyte coats are disseminated by

treatment with hyaluronidase, and this is accompanied by loss of the aggrecan within the chondrocyte cell layer. This indicates that aggrecan is retained through interaction with HA.

In the developing chick embryo cornea, at 4-5 days of development, mesenchymal cells of neural crest origin migrate beneath the primary stroma and form the corneal endothelium (Hay, 1980). Subsequent to this event, HA is secreted by the endothelium into the stroma (Toole and Trelstad, 1971). Beyond day 9 of development, hyaluronidase activity increases in the cornea with an inverse drop in levels of HA. This time point correlates with the differentiation of mesenchymal cells to corneal keratocytes, the major producers of the extracellular macromolecules in the later stages (Toole and Trelstad, 1971). Further evidence accrues from the histochemical study of the translocation of chick sclerotomal cells from the embryonic somite to the notochord, and the subsequent formation of the cartilaginous precursors of the vertebral bodies (Kvist and Finnegan, 1970). HA is the major GAG in the matrix surrounding the migrating sclerotomal cells. Increased hyaluronidase activity, and decreased HA synthesis coincide with the point at which the cells differentiate and begin producing cartilage matrix (Toole, 1972). Similar observations have been reported in association with tissue remodeling as in skin wound healing (Bertolami and Donoff, 1978; Longaker et al., 1991). This conforms with the paradigm, that the process of tissue repair is analogous to a strategic retreat to an embryological status, to facilitate efficient return to normal function. In all the systems studied thus far, the GAG- and HA-rich structures are associated with the cell surface. This suggests that the mesenchymal cell plasmalemma contains HA receptors that link the migrating cells to the matrix.

Oncogenic transformation by *ras* promotes synthesis of HA, and tumor cells respond positively to HA-stimulating factors. The increase in locomotion of these transformed cells

has been shown to be mediated by several complex mechanisms, including the release of autocrine motility factors and growth factors (Liotta et al., 1986; Schor et al., 1989), as well as HA (Schor et al., 1989; Turley et al., 1991). It has been further demonstrated that this locomotion requires the presence of RHAMM (Hardwick, et al., 1992; Turley et al., 1991). This receptor is expressed only on the leading lamellae and the perinuclear region of cells in locomotion (Turley, 1989). The regulation of the expression of RHAMM by the *ras* oncogene suggests that this receptor plays a role in morphogenesis.

During embryogenesis, the blastocyst develops post-implantation embryonic structures, it utilizes mechanisms that are akin to those employed by disseminating tumor cells and activated lymphocytes. These involve detachment from primary sites, invasion of surrounding tissue, cell migration, and colonization of secondary sites. The role of the adhesive process early in embryogenesis is to maintain the organizational patency of new distinct tissues (Fleming et al., 1994).

In new born rats, CD44-6v-containing isoforms are expressed only in the proliferating cells. A rat exon 6v specific mAb reacts with the epidermal basal layer, the hair follicles, and the crypts of the colon mucosa (Wirth et al., 1993).

Immunohistological analysis of the expression of CD44 in 10 week human fetal tissue using variant-specific mAbs shows that exon 9v-containing isoforms are predominantly expressed in epidermis, trachea, lung, mesonephric and paramesonephric ducts, while exon 6v-containing isoforms are detectable in epidermis and trachea (Terpe et al., 1994). In adult murine tissues, CD44S is expressed predominantly in spleen, adrenal gland, thymus, uterus, liver, intestine, stomach and ocular choroid. In addition to being reactive to CD44S, the trachea, esophagus, lung and salivary gland also express high-molecular-weight isoforms (Kennel et al., 1993).

Analysis of CD44 variant expression in the mouse is currently confined to RNA analysis, since variant-specific mAbs are not yet available. Wheatley et al. (1993) examined CD44 expression during early mouse development by wholemount immunohistochemistry combined with immunoblot analysis, using mAbs IM7.8 and KM201 which recognize a CD44S epitope. Between days 9.5 and 12.5 prenatal the predominant isoform is CD44S, with some expression of higher molecular weight isoforms. CD44 expression is upregulated in the somites, the heart, and the condensing limb-bud mesenchyme during significant morphogenetic stages, correlating with the morphoregulatory function of HA in these tissues. However, the expression of CD44 does not always correlate with the expression of HA. This is more so in epithelia involved in epithelial mesenchymal interactions such as the odontogenic placodes and the apical ectodermal ridge of the developing limb bud (Wheatley et al., 1993).

The major CD44 ligand, HA, is associated with cell migration in tumour metastasis and embryogenesis (Laurent and Fraser, 1992; Knudson et al., 1993). HA is increased in tissues undergoing cell proliferation and migration. It is postulated that HA promotes cell migration by forming highly hydrated pathways which encourage cell-ECM rather than cell-cell interactions. It has also been suggested that the matrix organized by HA may act as a sink or concentrator of cytokines (Tanaka et al., 1993). In the developing mouse embryo, HA is initially observed at day 5.5 to 6.5 p.c. in the basement membranes of the primitive ecto- and endoderm and also in the yolksac. At day 7.5 p.c. (neural plate and pre-somite stage), HA is observed in the basement membrane of embryonic ectoderm and visceral endoderm, in the amnion, and the extraembryonic visceral yolk sac. At day 9.5 p.c., HA is detected in the cranial mesenchyme, but is significantly absent in the branchial bars, somites, limb buds and neural plate. A major difference that occurs after day 9.5 p.c. is the shifting of HA expression from cavities to the intercellular spaces surrounding

mesenchymal cells of neural crest and mesodermal origin. HA is expressed in the axial skeleton, endocardial cushions of the heart, craniofacial mesenchyme and general connective tissue after mid-gestation (Fenderson et al., 1993). After day 9.5 p.c. HA and CD44 are coexpressed. However recent analyses by RT-PCR have revealed that several variant isoforms are expressed in the headfolds, an area devoid of HA (Ruiz et al 1995). This suggests that CD44 may, in some situations, have a functional role that does not involve interaction with HA.

It has been suggested that receptor-mediated degradation of HA plays a critical role in embryonic morphogenesis and organogenesis in several developing organs (Orkin et al., 1982; Culty et al., 1992). This can be attenuated by disrupting the binding of HA to the cell surface prior to internalization and lysosomal degradation, by antibodies to CD44 (Culty et al., 1992). In the developing hair follicle CD44 is expressed on the mesenchymal cells during the induction phase and is significantly downregulated in the adult stage. The pattern of expression of HA follows an exactly inverse pattern. It is logical to speculate that CD44 is expressed in areas associated with HA degradation and morphologic changes.

1.4 Normal development of the prostate gland

The reproductive tract goes through an undifferentiated ambisexual stage during which the internal genitalia are composed of the urogenital sinus (UGS), mesonephric tubules, and Wolffian and Mullerian ducts (Cunha, 1986). These diverse structures form and undergo differentiation at different times. In the male the gonad differentiates into testes and produces two hormones critical for normal male reproductive system development viz. testosterone and Mullerian inhibiting substance (MIS) (Jost, 1970; Jost, 1972). Both these hormones influence the development of the male genital tract. The initial role of testosterone is to prevent programmed cell death in the Wolffian duct. The androgens subsequently induce the mesodermally derived Wolffian ducts to form the epididymis,

ductus deferens, ampullary gland, seminal vesicle and ejaculatory duct (Wilson et al., 1981). Under the influence of testicular androgens the UGS, whose epithelium is endodermally derived, gives rise to the urethra, periurethral glands, prostate, bulbourethral gland, and part of the bladder.

The differentiation into the female reproductive phenotype is hormone independent during the fetal phase of development (Jost, 1953). The Wolffian ducts regress, and the Mullerian duct is sustained since MIS is not produced. The Mullerian duct develops into the uterus, cervix, oviduct, and upper vagina. The UGS gives rise to the lower vagina, the urethra, and part of the bladder. Estrogens are not essential for the differentiation of the female sexual phenotype, since estrogen receptor knockout (ERKO) transgenic mouse undergoes normal female sexual differentiation, even though it cannot respond to estrogen (Korach, 1994).

In the male mouse, the epithelial outgrowths of the endodermal UGS arise from below the developing bladder and grow into the surrounding mesenchyme to form the ductal network of the prostate. Prostatic buds arise on 17.5 days of gestation. One to three main ducts emerge on each side ventral to the UGS, and 20-25 ducts per side from the dorsolateral aspect (Timms and Sugimura). These form the ventral and dorsolateral lobes respectively. The anterior prostate develops from two buds per side, which grow cranially through the mesenchyme associated with the seminal vesicle (Lung and Cunha, 1981).

Branching of the prostate in mice occurs postnatally, a feature that makes this model ideal for the proposed study. The ventral prostate undergoes dichotomous branching as it elongates into the mesenchyme of the UGS, and the ducts of the dorsal prostate form three to six terminal branches per main duct. The differential growth involved in ductal development has been demonstrated by thymidine incorporation into DNA, which is at a

rate 10- to 500-fold higher in ductal tips as compared to the more proximal ductal regions of the mouse prostate (Sugimura et al., 1986).

The development of the male internal genitalia is dependent on androgenic stimulation and mediated via androgen receptors (AR). This has been demonstrated by several lines of evidence: (1) androgen production continues throughout the period of prostatic morphogenesis (Weniger and Zeis, 1972; Winter et al., 1981). (2) Eliminating the effect of androgens, either through the castration of fetal testes (Jost, 1953) or by antiandrogens (Neumann, 1970) results in sub-optimal development of the male accessory sexual organs. (3) The testicular feminization (Tfm) mouse which lacks functional AR due to a mutation in the gene encoding the AR does not develop male internal genitalia ((Sugimura et al., 1986). The primary androgen produced by the fetal testis is testosterone. However, DHT (dihydrotestosterone), produced by the enzymatic reduction of testosterone by 5a-reductase, appears to be the active intracellular androgen responsible for prostatic morphogenesis. Inhibition of this enzyme results in feminization of the external genitalia, and distorted prostatic morphogenesis in the rat (Imperato-McGinley et al., 1985). There is evidence that some aspects of neonatal prostatic growth may be independent of androgens, and castration of neonatal rats or mice does not completely inhibit development of the prostate (Price, 1936; Cunha and Donjacour, 1988).

Autoradiographic studies in rats and mice have demonstrated androgen receptors expressed prenatally in the mesenchyme but not in the epithelium (Shannon et al., 1981; Shannon and Cunha, 1983; Takeda et al., 1985; Wasner et al., 1983). In the mouse prostate, epithelial androgen receptors appear at the end of the first week postpartum, coinciding with the canalization of the solid prostatic ducts, and preceding secretory activity (Shannon and Cunha, 1983).

1.4.1 Mesenchymal-epithelial interactions in prostatic development

The interaction between the urogenital sinus mesenchyme and epithelium (UGM and UGE respectively) is decisive in the development of the prostate. During prostatic development, in the presence of androgens, the mesenchyme induces epithelial ductal morphogenesis and differentiation. Both instructive and permissive inductions by UGM appear to be mediated by similar signals. Prostatic differentiation occurs in heterospecific recombinants prepared with epithelium and mesenchyme from mouse, rat, rabbit, and human tissues (Cunha et al., 1983). Evidently, these interactions are highly conserved phylogenetically.

The prostate develops from the ambisexual UGS of either male or female fetuses, under the influence of androgens. Injection of testosterone into pregnant female results in induction of prostatic development (Jost, 1968). Development of prostatic buds is also induced in cultured female urogenital sinus in the presence of testosterone (Lasnitzki, and Mizuno, 1977; Takeda et al., 1986). However, the ability of the female urogenital sinus to give rise to prostate in response to androgens is temporally constrained to early development periods and is lost with maturation due to changes within the mesenchyme (Cunha, 1975). The epithelial lining of structures that are responsive to prostatic inducers is derived from the endodermal ventral portion of the cloaca (Cunha, 1986). The epithelial responsiveness to prostatic induction appears to be a property unique to the UGS endoderm, since fetal epithelia of ectodermal origin including plantar skin, mammary gland, preputial gland, salivary gland, and foregut endoderm derived adult esophagus do not form prostate when grown in association with UGM (Cunha, 1972; Norman, et al., 1986).

During prostate development, the epithelium expresses androgen receptors (AR) and undergoes cytodifferentiation leading to the expression of prostatic secretory proteins. The timing of AR expression in developing prostatic epithelium has not been described conclusively. In prostatic buds forming from the UGS, the AR are undetectable until

shortly after birth (Prins and Birch, 1993; Shannon and Cunha, 1983; Takeda and Chang 1991; Takeda et al., 1985). Substantial evidence suggests that androgens exert their effects on the epithelium by way of the AR-positive mesenchyme. The testicular feminized (Tfm) mouse, which lacks functional AR due to a mutation in the gene encoding the AR, has been utilized in tissue recombination experiments to show that the mesenchyme of the developing prostate mediates the effects of androgens on the epithelium. In homotypic recombinants of wild-type (wt) UGM and wt epithelium, the epithelium undergoes branching morphogenesis, proliferation, AR expression, and cytodifferentiation with subsequent expression of prostate specific secretory proteins (Cunha et al., 1981; Cunha and Lung, 1978; Donjacour and Cunha, 1993). On the other hand, tissue recombinants of Tfm UGM + Tfm epithelium or Tfm UGM + wt epithelium do not develop into prostate (Cunha et al., 1980). In heterotypic recombinants of wt UGM + Tfm epithelium, the Tfm epithelium undergoes ductal branching morphogenesis, proliferation, and cytodifferentiation into prostate-like epithelium. (Cunha and Chung, 1981; Cunha and Lung, 1978; Lasnitzki and Mizumo, 1980; Sugimura et al., 1986). However, although these wt UGM + Tfm epithelium recombinants, are prostate-like, they do not express prostatic-specific secretory proteins (Cunha and Chung, 1981; Donjacour and Cunha, 1993). These studies clearly demonstrate that prostatic development requires functional AR in the mesenchyme but not necessarily in the epithelium. Functional epithelial AR is however necessary and sufficient for the expression of prostatic secretory proteins.

The interactions between mesenchyme and epithelium are reciprocal. The epithelium induces mesenchymal differentiation in a process that is dependent on both androgens and the epthelium. The rat fetal UGS mesenchyme differentiates into smooth muscle sheaths that surround the epithelial ducts (Flickinger, 1972). UGM grafted with either bladder epithelium or UGE into intact male hosts results in the formation of prostatic ducts and the differentiation of mesenchyme into sheaths of smooth muscle around the epithelial ducts.

By contrast, human fetal prostates grafted into intact hosts form copious amounts of smooth muscles surrounding the epithelial ducts (Cunha et al., 1992). In human fetal prostates grafted into castrated hosts the buds present at the time ofgrafting are maintained but do not develop any further. At the same time only minimal traces of smooth muscle are seen (Hayward et al., 1995). This documents the androgen dependence of prostatic reciprocal interactions between epithelium and mesenchyme, and specifically of smooth muscle differentiation in the prostate.

Factors other than androgens also play a role in regulating prostatic DNA synthesis. This is apparent from the fact that the prostate ceases growth with maturity despite the sustained high levels of androgen. Furthermore, injection of exogenous androgens does not cause changes in the size of the adult rodent prostate (Barry and Isaacs, 1984). During the early stages of development, the mesenchyme predominates and it appears that the potential for growth is maximal when the mesenchymal : epithelial ratio is high. The epithelial ducts elongate and arborize within the mesenchyme, and ultimately the epithelium predominates (Sugimura et al., 1986). This phenomenon is also observed in several other parenchymal organs in which the epithelial component is a bulbous rudiment surrounded by a mass of mesenchyme. Castration leads to a disproportionate loss of prostatic epithelial cells compared to stromal cells, and subsequently to a change in the epithelial : stromal ratio by a factor of 10 in the prostate gland (DeKlerk and Coffey, 1978). Of particular interest is the finding that during prostatic regression, the epithelial cells of the ductal tips degenerate, while the stromal tissue becomes more prominent (Sugimura et al.,1986). This suggests that the relative loss of epithelial and stromal cells following deprivation of androgenic influence is unequal in different regions of the gland (English et al., 1985).

Morphologically, ductal branching morphogenesis is similar in all parenchymal glands studied thus far. An intact basal lamina is necessary for the maintenance of epithelial

morphology during ductal branching morphogenesis. Loss of basal lamina results in a functionally disjointed microfilament; apparently the basal lamina stabilizes intracellular microfilaments (Bernfield and Wessells, 1970). Proteoglycans, which are synthesized by the epithelium, and are composed of a protein core with GAG side chains, form part of the basal lamina. They form the molecular link between ECM components and cytoskeletal elements within the cell. During ductal morphogenesis of the developing salivary gland, there is a conspicuous difference in GAG turnover between the lobules and the clefts. This is thought to be due to increased degradation of GAGs around the distal tips of the lobules by a mesenchymal neutral hyaluronidase (Bernfield et al., 1973; Bernfield et al., 1984). Remodeling of the epithelial-derived basal lamina by the mesenchyme is a major factor in the control of ductal branching morphogenesis, and a substantial example of the role of epithelial-mesenchymal interactions in development.

In the course of ductal branching morphogenesis of the developing salivary gland, the epithelial surface forms and reabsorbs several small clefts, of which only a fraction are stabilized. Interstitial collagens (type I and III) function as stabilizers of basal lamina components during salivary gland cleft formation. Interestingly, inhibition of collagen synthesis blocks the formation of new clefts, but has no effect on established clefts (Spooner and Faubion, 1980). Treatment of developing salivary glands with collagenase reduces ductal branching both in the salivary gland and the lung (Nakanishi et al., 1986; Nogawa and Mizuno, 1981); in the same vein, treatment with collagenase inhibitors leads to enhanced ductal branching of the glands, possibly due to non-selective stabilization of the initial clefts (Nakanishi et al., 1986). These observations suggest that during ductal branching morphogenesis, regulation of both collagen deposition and degradation is important for cleft formation, and especially for cleft stabilization.

All the experimental evidence available stresses the importance of mesenchymal-epithelial interactions in regulating growth within developing parenchymal and hormonally responsive glands. Currently, there are no studies characterizing the role of HA and CD44 in branching morphogenesis, which is the main thrust of this investigation. For this purpose, the prostate offers several advantages as a model system: It can be cultured *in vitro* in chemically defined media; the hormonal levels in culture can be controlled with great precision; and the morphological changes can be analysed with ease.

The background to, and design of these studies are detailed and discussed in chapters II and III. However, in synopsis, prostate organ culture methods have been used previously to study the effects of hormones and growth factors in the absence of systemic effects (Gittinger and Lasnitzki, 1972; Lasnitzki, 1975; Martikainen and Suominen, 1983). Latsnitzki showed that regression of adult prostatic epithelium in medium without testosterone was similar to those observed in rats *in vivo* following castration. In adult prostatic cultures testosterone dependence is critical for RNA, DNA, and protein synthesis (Johansson and Niemi, 1975; Santi and Johansson, 1973). Serum free culture conditions, supplemented with the fundamental serum substitutes; insulin, transferrin, and glucocorticoids (Barnes and Sato, 1980), make it possible to isolate and study the effects of single factors (Martikainen et al., 1987).

1.5 Significance

The universal gains in life expectancy are, in the male population, translated into increased incidences of proliferative prostatic diseases. Prostate adenocarcinoma is one of the most prevalent cancers in men, and benign prostatic hyperplasia (BPH) is diagnosed in 75% of men over the age of 50 years (Coffey and Pienta, 1987; McNeal, 1983). In prostate cancer and BPH, as indeed in any cancer, the pattern of cellular proliferation observed is a reflection of the embryonic developmental program. According to McNeal (1984), the

etiology of BPH is linked to the re-expression of the embryonic inductive capacity of the prostatic stroma. BPH initiates as stromal nodes and these are then invaded by proliferating epithelium (McNeal, 1984). Epithelial-mesenchymal interactions in the mature urogenital system can induce change in the developmental program of the epithelium. Adult prostatic epithelium retains the ability to respond to the embryonic mesenchyme of urogenital sinus (Chung et al., 1984; Cunha et al., 1987). Furthermore, malignant cells can be induced to express a more normal phenotype when grown in association with normal mesenchyme(De Cosse et al., 1973; Fujii et al., 1982). From this perspective, this study provides insight into some mechanisms of prostatic hypertrophy and cancer, while at the same time furthering our understanding of parenchymal development.

CHAPTER II

TRANSITIONS IN THE EXPRESSION OF CD44 AND HYALURONIC ACID ARE IMPLICATED IN THE REGULATION OF MOUSE PROSTATE DEVELOPMENT

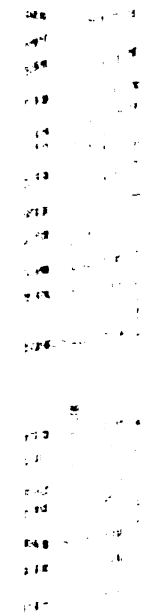

2.0 INTRODUCTION

The process of parenchymal organogenesis involves morphogenesis, growth, and functional cytodifferentiation of both the epithelial and mesenchymal components (Branham et al., 1985; Sugimura et al., 1986). The overall process is characterized by invasion of epithelial ducts into mesenchyme, accompanied by changes in the basement membrane. At the same time the mesenchymal interstitial matrix is remodeled to accommodate the expansion of the epithelium. Evidence accruing from studies of the mouse salivary gland (Bernfield et al., 1984; Cutler, 1990),and the mammary gland (Bissell and Hall, 1987; Daniel and Silberstein, 1987; Kratochwil, 1987; Imagawa et al., 1990) indicates that tissue remodeling is influenced by a wide repertoire of factors including hormones and growth factors, as well as the extracellular matrix (ECM) itself. The mesenchyme dictates the pattern of epithelial morphogenesis, resulting in the development of specialized morphological patterns, and the expression of tissue specific secretory proteins (Cunha et al., 1987; Cunha, 1995, Haffen et al., 1987; Kratochwil, 1987; Sakakura, 1987; Higgins et al., 1989 a,b).

The androgen-dependent development of the prostate occurs by way of reciprocal epithelial-mesenchymal interactions (Cunha et al., 1987). The mesenchyme induces epithelial morphogenesis and regulates the proliferation and cytodifferentiation of the epithelium. On the other hand the epithelium induces smooth muscle differentiation and patterning in the urogenital sinus (Cunha et al., 1989, 1992). In the mouse, prostatic buds arise on the 17th day of gestation (Price and Ortiz, 1965). Epithelial outgrowths of the endodermal urogenital sinus arise from below the developing bladder, and grow into the surrounding mesenchyme. Subsequent branching occurs postnatally and leads to the formation of the prostate ductal network (Sugimura et al., 1986). The androgen-dependent interaction between the urogenital sinus mesenchyme and epithelium is decisive in the development of the prostate ducts. Androgens elicit their morphogenetic effect by acting

via androgen receptors in the mesenchyme, which in turn induces morphogenesis and differentiation through paracrine mechanisms (Cunha et al., 1987).

Glycosaminoglycans (GAGs), and specifically hyaluronic acid (HA), a high molecular weight, negatively charged polysaccharide composed of the repeating disaccharide unit [D-glucuronic acid; N, acetyl-D-glucosamine], have been implicated early in morphogenesis and differentiation in a number of experimental models. These include the salivary gland (Bernfield et al., 1984), kidney mesenchyme (Belsky and Toole, 1983), chick embryo cornea (Hay, 1980; Toole and Trelstad, 1971), and chick sclerotomal cells (Kvist and Finnegan, 1970). In the embryonic salivary gland, ductal branching is associated with the remodeling of GAG-containing substances in both the interstitial ECM of the mesenchyme as well as in the basal lamina (Bernfield et al., 1984). In all the systems studied, the GAG- and HA-rich structures are associated with the cell surface. This suggests that the effect of HA on cellular behavior is mediated by plasmalemmal HA receptors that link the migrating cells to the matrix (Toole, 1990). CD44 is the predominant vertebrate cell surface receptor for HA (Goldstein et al., 1989; Stamenkovic et al., 1991; Dougherty et al., 1991). The spatial and temporal control of the expression of CD44 affects profoundly the interaction of the cell with the ECM. This molecule has been implicated in HA-dependent cell adhesion in several cell types including macrophages (Green et al., 1989), and SV-3T3 fibroblasts (Underhill and Toole, 1981). CD44 has also been localized to the surface of proliferating epithelial cells such as the basal layers of the epidermis, and the intestinal crypts (Alho and Underhill, 1989). CD44-mediated degradation of HA plays a critical role in embryonic morphogenesis and organogenesis (Culty et al., 1992). In the developing hair follicle, CD44 is expressed on mesenchymal cells during the induction phase, and is significantly downregulated in the adult stage. The pattern of HA expression is precisely the inverse, suggesting that CD44 is expressed in areas associated with HA degradation and morphological changes (Underhill, 1993). CD44 is encoded by 20 exons;

two constant regions, exons 1-5 and exons 16-20, and a 10 exon variable region ranging from exon 6 to 15 and referred to as v1-v10. These are expressed variably due to alternative splicing of the nuclear RNA resulting in numerous combinations of the variant exons which are expressed in different tissues (Screaton et al., 1993). The details of the transcriptional mechanisms that control the selection of the various splice exons have not been sufficiently described. We postulate that the modulation of CD44 isoform expression regulates key events in prostate gland development.

We report here the first study of the expression of HA and CD44 in the developing prostate gland, exploring their spatio-temporal relationship. HA and CD44 colocalized in the stroma early in the proliferating growth stage of the prostate anlagen. With further postnatal development, deposition became segregated. HA was markedly elevated in the stromal matrix and CD44 expression became confined to the epithelial cell membrane surfaces. Expression was most pronounced in association with proliferating ductal tips, compared to the more developmentally quiescent proximal ductal regions. We suggest that the switch of CD44 from stroma to epithelium is an event that is critical to the onset of branching morphogenesis.

2.1 MATERIALS AND METHODS

Animal tissues

Male Balb/c mice from Simonsen laboratories (Hollister, CA) and the Cancer Research Laboratory at the University of California (Berkeley, CA) were utilized in all experiments. After the animals were euthanised, a lower abdominal incision was made and the genital tract of each animal was removed *en bloc*. Further dissection to isolate the anterior prostate was performed in a watchmaker's depression slide, using a dissecting microscope, fine forceps, and a gauge 27 1/2 needle as a scalpel. Dissection was done in DME H-16/F-12 50:50 medium (Cell Culture Facility, University of California, San Francisco, CA).

Immunoreagents

The anti-CD44 monoclonal antibodies (mAb), KM201 and IM7.8, were generated in rats and directed against the hyaluronan CD44 receptor from mouse. The mAb KM-201 (IGg_1; Trowbridge et al., 1982), was obtained as a hybridoma (American Type Culture Collection, Rockville, MD) and purified from ammonium sulfate fractions of the hybridoma culture supernatants. The mAb IM7.8 (IgG_{2b} ; Miyake et al., 1990) was obtained from Pharmingen (San Diego, CA).

Preparation and characterization of HA-binding protein

Bovine nasal cartilage (Pelfreeze, Rogers, AK) was minced into minute pieces, and 150 g homogenized and extracted in 1000 ml 4.0 M guanidium-HCl, 0.5 M sodium acetate pH 5.8. The extract was stirred for 24 h at 4 °C and centrifuged at 9000 X g, 4 °C for 30 minutes. The supernatant fraction was exhaustively dialyzed against dH_2O, and lyophilized. This extract (1.6 g) was dissolved in 50 ml 0.1 M sodium acetate, 0.1 M Tris-HCl, pH 7.3 and incubated at 37 °C with 1.76 mg trypsin (Sigma, St. Louis, Mo) for 2h. The reaction was terminated by the addition of 1 mg soybean trypsin inhibitor (Sigma,

St. Louis, Mo). The trypsinized extract was dialyzed exhaustively against 0.5 M sodium acetate, pH 5.8.

To prepare HA-Sepharose, 300 mg human umbilical cord HA (ICN, Irvine, CA) was dissolved overnight in 45 ml dH_2O. This was stirred into 50 ml EAH-Sepharose 4B gel (Pharmacia, Piscataway, NJ) and the pH adjusted to between 4.5 and 5.8. Unoccupied amino groups were blocked by 10 ml 0.1 M acetic acid at room temperature for 1h. The gel was washed sequentially with 1.0 M sodium chloride, pH 4.5; 0.1 M Tris-HCl, 1.0 M sodium chloride pH 8.1; 0.05 M glycine, 1.0 M sodium chloride pH 3.1; dH_20; and 0.5 M sodium acetate, 1.0 M sodium chloride pH 5.7.

Trypsinized cartilage extract was added to 75 ml HA-Sepharose, and 4.0 M guanidium-HCl overnight at 4 °C, followed by dialysis against dH_2O. The extract and bead slurry was poured into a 28 x 230 mm column, washed with two sequential 150 ml washes of 1 M sodium chloride pH 5.8, and 3.0 M sodium chloride pH 5.8 to remove non-specifically adsorbed material. HA bound proteins were eluted with 400 ml 4.0 M guanidium-HCl, 0.5 M sodium acetate, pH 5.8.

Protein concentration was determined and biotinylation was achieved by reacting the protein with Sulfo-NHS at a ratio of 9:1 in 0.1M sodium carbonate/sodium bicarbonate pH 8.5, and incubating at room temperature for 2h.

HABP samples (30 ng protein) were separated under reducing conditions according to Laemmli (1970), utilising the Phastgel ® system (Pharmacia, Piscataway, NJ), and 12.5% SDS gels. The gels were treated in two ways; (1) Protein, and regular molecular weight standards (Biorad, Richmond, CA), were visualized by silver staining, and the molecular weight determined (2) Protein, and biotinylated molecular weight standards (Biorad,

Richmond, CA) were blotted from the SDS gels to nitrocellulose membranes (pore size: 0.40 μm) (Biorad, Hercules, CA) under semi-dry conditions for 15 minutes at 15 °C at a constant current of 25 mA. Additional protein binding sites on the membranes were blocked by PBS, 0.5% Tween-20. Blots were incubated with ABC peroxidase (Vectastain Kit PK 4000) (Vector, Burlingame, CA), and the biotinylated proteins visualized by staining for peroxidase activity with 3,3'-diaminobenzidine substrate (Peroxidase Substrate Kit, DAB SK-4000) (Vector, Burlingame, CA).

Immunoblotting

Anterior prostates were removed from the Balb/c mice, rinsed in PBS and homogenized in lysis buffer, 5.0 mM Hepes pH 7.4, 2.0 mM $MgCl_2$, in a Dounce homogenizer. The large cellular debris was cleared by centrifugation at 6,500 X g for 7 minutes. The membrane fraction was collected by centrifugation at 15,000 X g for 7 minutes and resuspended in sample buffer which was a modification of Laemmli's buffer (Laemmli, 1970) without ß-mercaptoethanol and without bromophenol blue. The protein content was determined by the Bradford assay, and 15 μg of each sample was resolved on 10% SDS-polyacrylamide gel. The protein was transferred onto nitrocellulose membrane (pore size: 0.40 μm) (Biorad, Hercules, CA) in the buffer 15.6 mM Tris, 120 mM glycine, pH 8.1. The membranes were blocked with 5% non-fat milk in PBS and 0.2% Tween 20 for 30 minutes (blocking solution). The protein CD44 was detected by incubation with the monoclonal antibody KM201 at a dilution of 1:100 in blocking solution, for 60 minutes at room temperature. The blots were rinsed with three changes of TBST (150 mM NaCl, 10 mM Tris-HCl, pH 8.0, 0.05% Tween-20) over 30 minutes, followed by incubation with biotinylated secondary anti-rat IGg diluted 1:200 in TBST, for 60 minutes, and further rinsing in TBST. The signal was detected with a horseradish peroxidase detection kit (Vector, Burlingame, CA)

HA Histochemistry

Mouse anterior prostates were fixed with paraformaldehyde, embedded in paraffin, sectioned (6 µl) and mounted on polylysine coated glass slides for histological staining with HABP. The specificity of the staining was determined by two methods: (1) Predigestion of sections with *Streptomyces* hyaluronidase, 100 TRU/ml, 0.1 M sodium formate buffer, 0.15 M NaCl, 1 mg/ml BSA, 0.1% Triton X-100, pH 3.7, overnight at 37 °C. (2) The biotinylated HABP was diluted 1:100 with HABP-buffer solution (0.25 M Na phosphate buffer, pH 7.0 containing 1.5 M NaCl, 0.3 M guanidine-HCl, 0.08% BSA, and 0.02% NaN_3, pH 7.0) and combined 1:1 with a solution of 0.1 mg/ml HA (Sigma, St. Louis, Mo), prior to application to the sections. The control slides, together with the experimental slides, were incubated with 3% BSA at 37 °C for 30 minutes. After rinsing with PBS-CMF, 0.3 ml of the biotinylated HABP, diluted 1:100 in HABP-buffer was added to each experimental and control slide. All slides were incubated overnight at 4 °C. The slides were rinsed in PBS-CMF and transferred to 0.6% H_2O_2 in methanol at room temperature. After rinsing with PBS-CMF, staining was achieved using the substrate 3, 3' -diaminobenzidine (Peroxidase Substrate Kit, DAB SK 41000) (Vector, Burlingame, CA) for 5 minutes, followed by a rinse with dH_20. Slides were counterstained for 15 minutes in 0.25% methyl green, rinsed in dH_20 and dipped sequentially in 70%, 95%, and 100% ethanol, and xylene.

CD44 immunohistochemistry

The sections were deparaffinized and hydrated following standard procedures. The slides were then placed in 10 mM citrate buffer, pH 5.8 and incubated at 70% of full microwave power for 15 minutes. Endogenous peroxidase activity was blocked by incubating for 30 minutes in 2 ml of 0.6% H_2O_2 in methanol. After rinsing in PBS-CMF for 20 minutes, non-specific binding sites were blocked by incubation with 5% normal goat serum in filtered PBS-CMF for 30 minutes, at 37 °C.

The primary antibody used was the unconjugated rat anti-mouse CD44 mAb, IM7.8 IgG_{2b} (Pharmingen, San Diego, CA). The antibody, diluted 1:150 in PBS-CMF containing 5% normal goat serum, was incubated for 1 hour at 37 °C, then overnight at 4 °C. The secondary antibody, biotinylated goat anti-mouse IgG diluted in 5% normal goat serum, was incubated for 45 minutes at room temperature. Each one of the above steps was followed by three five minute washes in PBS-CMF, 0.1% Tween-20. Bound antibodies were visualized using an avidin-biotin horseradish peroxidase detection system.

All histochemistry was documented by photography using an Olympus Vanox AHBT3 Microscope (Olympus Co., Woodbury, NY), with an integrated Olympus C-35AD-4 camera and Kodak Gold Plus film (Eastman Kodak Co., Rochester, NY).

Reverse-transcriptase polymerase chain reaction (RT-PCR)

Tissue was dissected from the animals, and the mRNA extracted using RNA Track (Bioteck). The mRNA was used as template for the first strand synthesis of cDNA in a reaction mixture containing 1000 U Moloney murine leukemia virus reverse transcriptase, 50 µM random hexamer primer, 50 mM Tris-HCl pH 8.3, 75 mM KCl, 10 mM dithiothreitol, 3 mM MgCl2, 0.5 mM each of dGTP, dATP, dTTP and dCTP in 60 µl. The reactions were carried out at 37 °C for 90 minutes and then diluted 1:3 in water pretreated with DEPC.

Oligonucleotide primers were diluted to 40 µM in water. For RT-PCR, a modified hot start method was used. Three to 5 µl of cDNA were added to 30 µl of a master mix containing 0.8 µmol of each primer, 17 mM Tris-HCl pH 8.3, and 80 mM KCl. Water was added to a final volume of 40 µl. All reactions were overlaid with a light mineral oil and heated to 99 °C. After 10 minutes the reactions were cooled to 94 °C and a 10 µl volume containing 7 mM $Mg Cl_2$, 1mM each of dATP, dTTP, dGTP, and dCTP and 1.2 U Taq polymerase

added. The products of RT-PCR were separated on 2% agarose and visualized by UV light.

The primers used for amplification were as follows

Forward variant 0	5'-GCCAATTCTTTATCCGGAGCACCTTGGCC-3'
Forward variant 6	5'-ACCCCAAGTGAAGACTCCCATGT-3'
Forward variant 7	5'-GCCCACAACAACCATCCAAGTCA-3'
Reverse variant 8	5'-GCAGTAGGCTGAAGGGTTGTAC-3'
Reverse variant 11	5'-CGGGGTACCGGATCCATGAGTCACAGTGC-3'

Hyaluronic acid ELISA

A competitive ELISA was used to measure HA. HA (ICN, Irvine CA) (0.2 mg/ml) was bonded to 96-well microtiter plates (Corning Glassworks, Corning, NY). This was achieved by 24 h incubation with 0.184 mg/ml of N-hydroxylsulfosuccinimide and 1.23 mg/ml of 1-ethyl-3 dimethyl-anopropyl carbodiimide, at 4 °C. Non-specific binding was blocked by incubation with 300 µl/well of 0.6% nonfat milk, at 37 °C for 30 minutes. Prostate extract samples were incubated at 37 °C for 1 h, with an equal volume of biotinylated hyaluronic acid binding protein (HABP). The prostate extract-HABP mixture was added to the microtiter plate in aliquots of 100 µl and incubated at 37 °C for 1 h. Rinsing with PBS-0.5% Tween-20 washed away the HABP bound to the prostrate extract HA. The excess biotinylated HABP bound to the HA on the microtiter plate. A standard HA concentration curve was generated for each ELISA plate. The HABP bound to the plate was detected by coupling an avidin-biotin-peroxidase complex (Vector, Burlingame, CA) to an o-phenylenediamine substrate reaction. The absorbence at 492 nm was read on a Titertek Multiskan Plus spectrophotometer (Lab Systems, Helsinki, Finland). All readings were done in triplicate.

Protein Determination

2.2 RESULTS

Characterization of HABP

Hyaluronic acid binding protein (HABP) was extracted from nasal bovine cartilage, and was used as the primary reagent in HA-histochemistry, as well as in the hyaluronidase ELISA-like, and HA -ELISA. The specificity of the HABP was confirmed by analysis of the trypsinized and biotinylated protein eluate from the HA-Sepharose column using SDS-PAGE, and the blotting assay. The non-biotinylated HABP displayed a single band at a molecular weight of 45 kDa, and three different samples of the trypsinized biotinylated HABP displayed major bands at a molecular weight of about 45 kDa (Fig. 1 a, b)

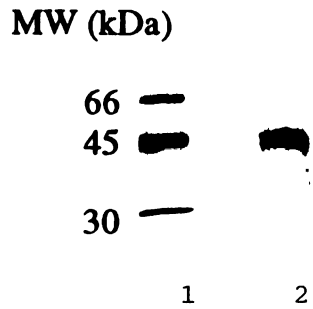

Figure 1

(a) HA binding analysis of the trypsinized and biotinylated fraction of HABP. Lane 1-molecular weight markers; Lane 2-HABP preparation.

Figure 1

(b) SDS polyacrylamide gel of the trypsinized and biotinylated fractions of the HA-binding cartilage extracts. Lanes 1, 2, 3, -three different preparations of biotinylated HABP; lane 4 -unbiotinylated HABP; lanes a and b molecular weight standards.

Quantification of HA

The total levels of HA that could be extracted from developing anterior mouse prostates, as well as the distribution of protein in the same organs were determined at 0-, 5-, 10- and 30-days-of-age. The relative HA concentration in μg/mg protein, in the developing anterior prostate, remained unchanged throughout the developmental ages studied (Table 1)

Age/days	0	5	10	30
Total [HA]/ ug/ml	0.93	0.98	1.32	1.45
Rel [HA] ug/mg Protein	0.89	0.92	0.92	0.93

Table 1 Quantification of HA in developing mouse prostate. HA was determined by the HA ELISA-like assay (Stern and Stern, 1992), and expressed as both total HA and relative units of HA

Distribution of HA

HA was localized in the prostate tissues at different stages of development using the biotinylated HABP as a histochemical stain (Fig. 2). During the early stages of development at 0 day postnatal (Fig. 2 a), HA was a prominent component of the stromal connective tissue, with no specific proximal-distal predilection. There was no HA associated with epithelial components. At 10 days (Fig. 2 b) and 14 days (not shown) postnatal, the intensity of HA staining in the stroma had decreased. HA staining was significantly more intense around the growing tips of the buds undergoing branching morphogenesis (see arrows), and less pronounced in the developmentally quiescent ductal regions of the ducts. These trends continued as development progressed through 30 days postnatal (Fig. 2 c), with the intensity of HA staining decreasing even further, and being practically undetectable at 60 days (Fig. 2 d).

CD44 immunostaining

To determine the localization of CD44, in prostatic development, sections were stained with anti CD44 mAb (Fig. 3). Localization was dependent on the developmental stage. In sections from embryonic prostate at 0 days (Fig 3 a), CD44 mAb stained the mesenchyme. The 0 day time-point coincided with the initiation of ductal branching which, in the mouse prostate, is a postnatal process. No expression was observed in the epithelium or associated with the basal lamina. At 10 days (Fig 3 b), CD44 was localized to the basolateral cell membranes of the epithelium, with no evidence of mesenchymal expression. The staining was generally uniform throughout the epithelium. This pattern was maintained through day 14 (not shown). CD44 became increasingly focalised to the developing distal tips of the epithelial ducts by 30 days (Fig 3 c). No immunostaining was evident at 60 days (Fig. 3 d). Background staining as determined by substituting biotinylated IgG for the anti-CD44 mAb was consistently negative (not shown).

Figure 2

Histochemical staining for HA. Staining was performed using the biotinylated HA-binding peptide and horseradish peroxidase. Methyl green counterstain was employed.

(a) 0-day-old prostate. The stroma shows uniformly intense staining for HA. HA is apparent only in the stroma. No HA is observed in the epithelium.

(b) 10-day-old, and **(c)** 30-day-old. The preponderance of HA is in the mesenchyme or stroma immediately adjacent to the growing buds or ductal tips, appearing to encompass the mesenchyme.

(d) 60-day-old. Staining is practically non-evident.

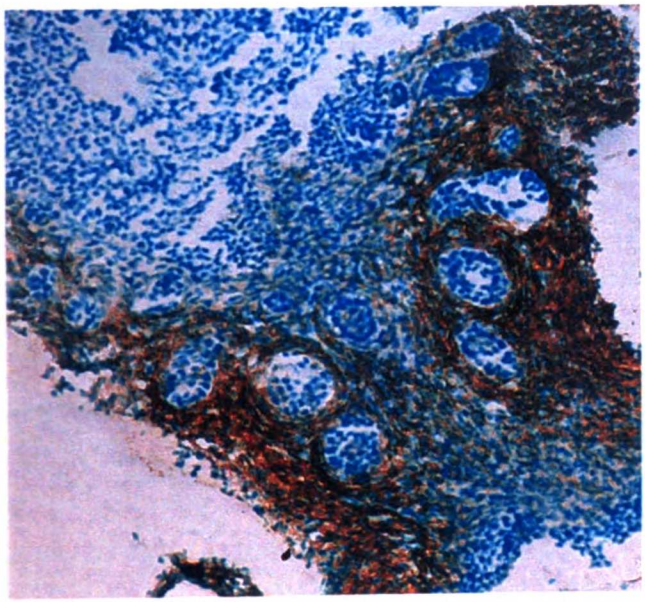

a

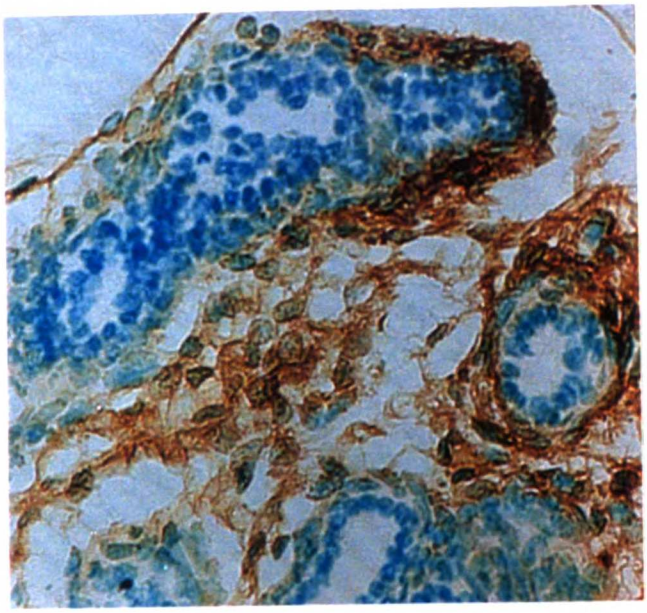

b

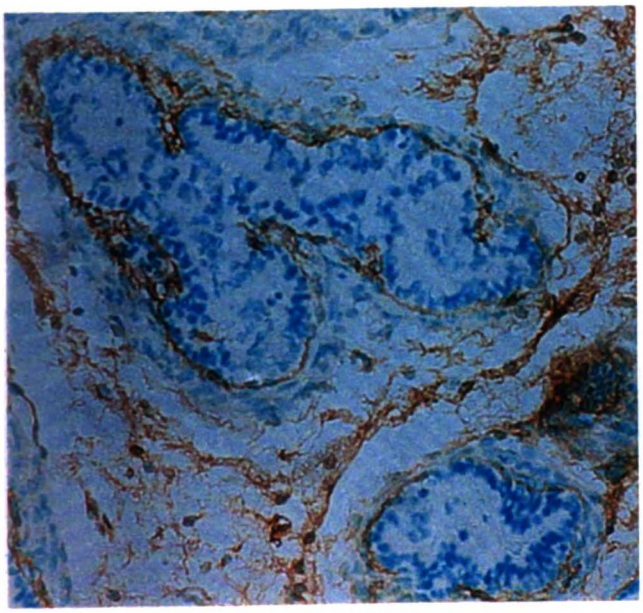

c

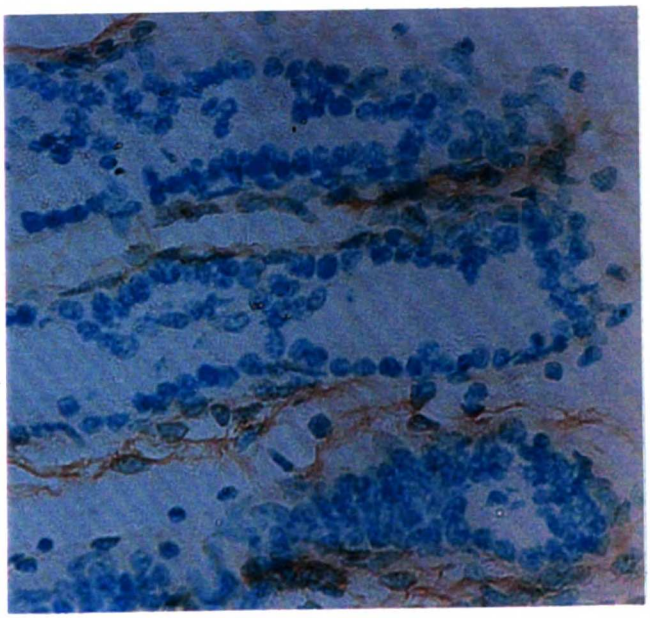

d

Figure 3

Immunolocalization of CD44 in the developing prostate. CD44 immunoreactivity was observed to undergo transition from mesenchyme to epithelium during the course of development.

(a) 0-day-old prostate showing immunostaining in mesenchymal tissue. **(b)** 10-day-old prostate showing strong immunostaining in the epithelial membrane. Staining in the mesenchyme was weak and diffuse.

(c) 15-day-old. CD44 immunostaining is reduced, confined to epithelial cell membrane, and predominantly on the distal ductal tips.

(d) 60-day-old. No immunostaining was evident at this time point.

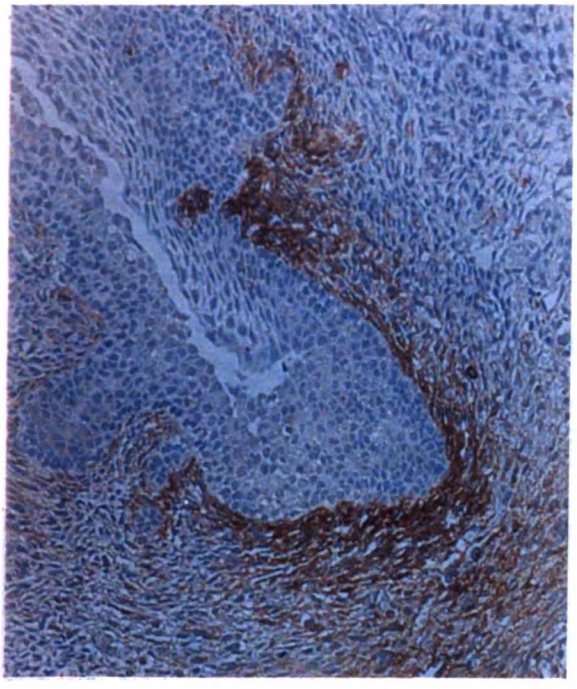

a

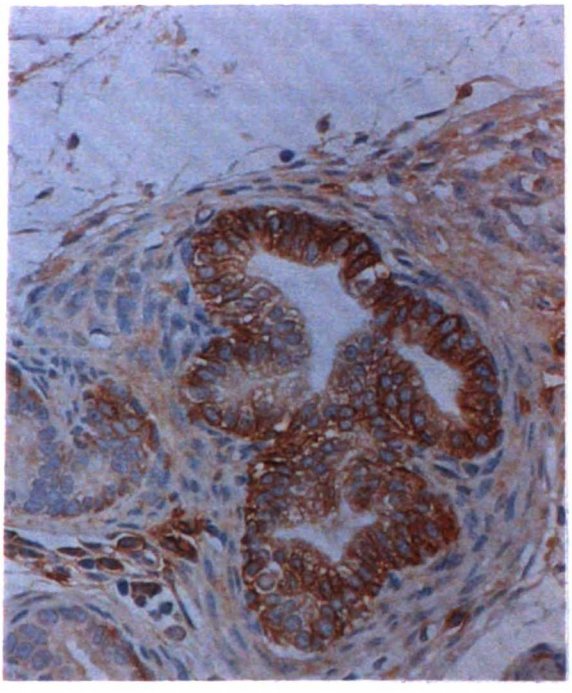

b

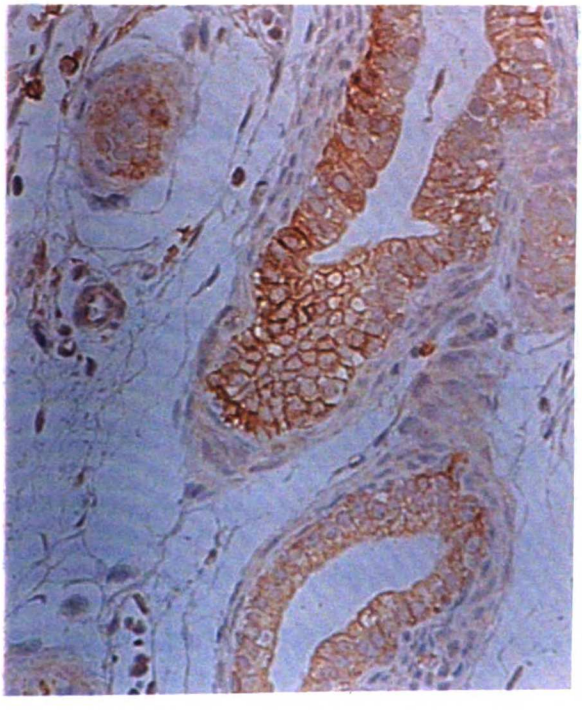

c

d

Immunoblot analysis of CD44 protein expression

The different isoforms of CD44 present in the developing prostate from 0 day to 30 days-of-age were examined by Western blotting with the mAb KM201 (Fig. 4). The predominant CD44 species expressed was detected at 85 kDa and corresponds to the CD44S isoform. The relative abundance of the 85 kDa form remained unchanged throughout the period studied. At 5 days-of-age, CD44 isoforms of approximately 116, and 160 kDa were detected, in addition to the 85 kDa form. This pattern of expression was maintained through day 10 and 15, however at 30 days-of-age and beyond, the higher molecular weight isoforms were of low abundance .

Subjecting the tissue samples to enzymatic digestion with chondroitin ABC lyase, followed by immunoblot analysis did not produce any alteration in the molecular weight of CD44 in all the samples analysed . This confirms that the high molecular weight isoforms were not products of modifications to glycosylation sites in the primary sequence of CD44, and suggests that they were products of exonal splicing among the variable exons.

RT-PCR analysis of CD44 splice variant expression

Reverse transcription polymerase chain reaction (RT-PCR) analysis was carried out to identify the pattern of CD44 splice variants expressed at the various timepoints in the developing anterior prostate. mRNA isolated from the anterior prostate was used to generate cDNAs, which were subsequently used as templates for PCR using amplimers specific for both constitutive and alternatively spliced exons (Fig. 5). Amplification and electrophoretic separation demonstrated PCR products, the sizes of which were consistent with the presence of mRNA in the anterior prostate encoding both CD44S, and alternatively spliced isoforms of CD44. cDNA amplified with primers FV0 and RV11 produced a product of 112 bp representative of CD44S, in which all the variable exons have been removed by alternative splicing (Fig. 5 A). This form of CD44 was consistently expressed

during the entire developmental period that was studied. Amplification by primers FV7 and RV8 produced a 161 bp product (Fig. 5 B) The variant 7 and 8-containing exons displayed a specific window of expression confined to between day 5 and day 10 of development .

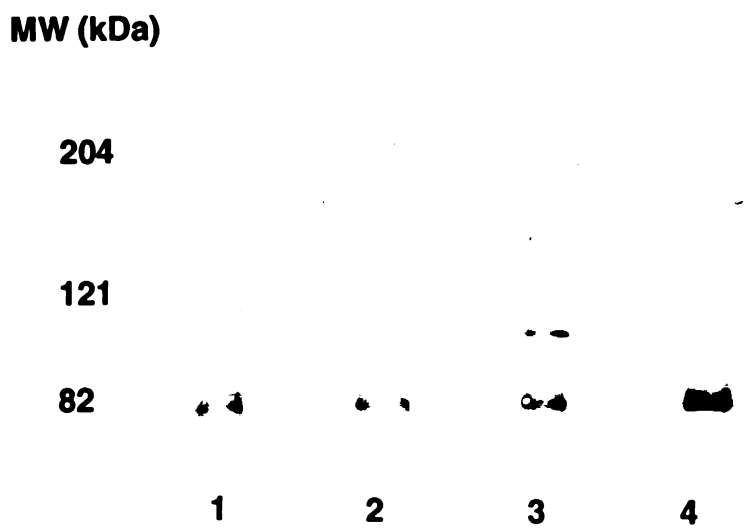

Figure 4

Western analysis of CD44 expressed by the developing anterior prostate at various ages of development. The predominant 85 kDa species (CD44S) was the only CD44 variant detected at day 0 (lane 1), and remained unchanged throughout the ages studied. At 5-days-of-age (lane 2), CD44 isoforms of approximately 116 and 160 kDa were also detected. This was maintained through days 10 and 15 (lanes 3 and 4 respectively).

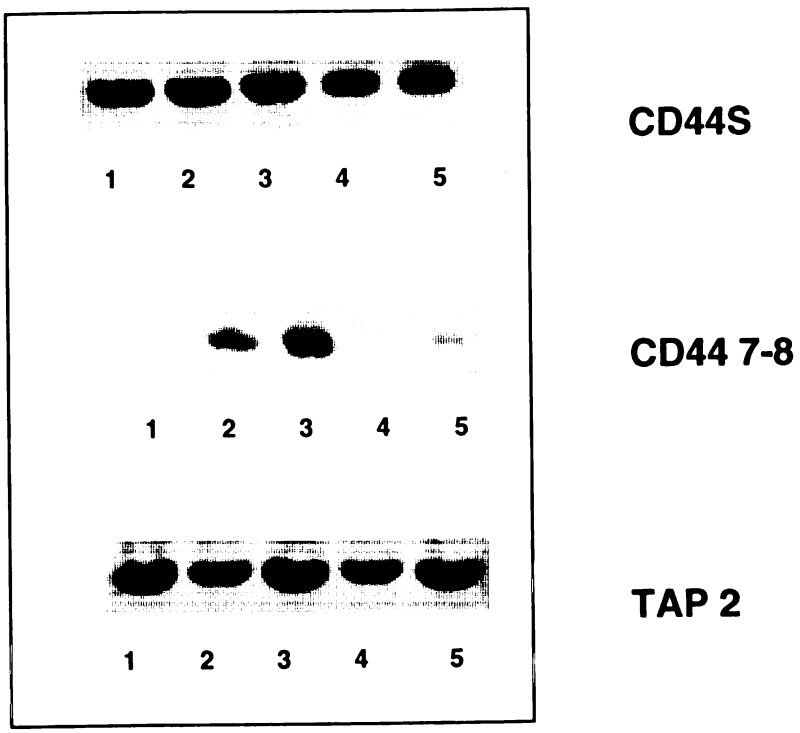

Figure 5

Detection of transcripts for CD44S (Fig 5 A), CD44 variants 7 and 8 (Fig 5 B), and control transcripts TAP 2 (Fig 5 C) at various ages in the development of the mouse anterior prostate (See Materials and Methods for techniques). Lane 1= 0 day, lane 2= 5 days, lane 3= 10 days, lane 4= 30 days, lane 5= 45 days

2.3 DISCUSSION

CD44 is the principal receptor for HA. Sequence analyses of CD44 indicate that the extracellular domain of CD44 contains homologies to the HA binding region of both aggrecan and cartilage link protein (Goldstein et al., 1989; Stamenkovic et al., 1989). A murine CD44 receptor for HA has been described (Miyake et al., 1990; Aruffo et al., 1990). Indeed Aruffo et al. (1990) confirmed HA to be the CD44 ligand by attenuating lymph node tissue reactivity to a soluble CD44 receptor immunoglobulin fusion protein following hyaluronidase treatment of the lymph node. The many important biological processes associated with HA, particularly in early embryology, tumor invasiveness, and tissue repair and remodeling, signify that the relationship between CD44 and HA is of special importance. It has become apparent that several different isoforms may be generated from the CD44 gene by alternative RNA splicing. Some of these alternative isoforms have distinct properties and ligands other than HA.

The mAbs KM201 and IM7.8 recognize all the isoforms of CD44. In this study, these antibodies were used to demonstrate that the HA-binding 85 kDa form of CD44 was predominantly expressed in the developing anterior prostate throughout the time-points studied 0-day to 20-days-of-age. Isoforms with higher molecular weight were observed in 10-, 15-, and 20-day-old organs. The presence of higher relative molecular weight CD44 forms has been explained by two distinct mechanisms; addition of chondroitin and heparan sulfate (Jalkanen et al., 1988; Lokeshwar and Bourguignon, 1991), as well as the presence of splice variants (Stamenkovic et al., 1989, He et al., 1992). In order to distinguish the mechanisms involved in our system, the samples were subjected to chondroitin ABC lyase digestion. This did not yield any changes in the relative molecular weight of the CD44. This investigation was extended by RT-PCR analysis using amplimers specific for several isoforms of CD44. This demonstrated that at specific timepoints, developing anterior prostate expressed, in addition to CD44S, alternatively

spliced isoforms of CD44. These timepoints were coincident with the detection of high relative molecular weight CD44 forms by immunoblotting.

The influence of an HA-rich ECM on resident cells is a product of both the hydration properties of HA (Comper and Laurent, 1978), and the interaction between HA and cell surface HA-binding proteins (Toole, 1990). This influences cellular processes critical to embryogenesis and morphogenesis, viz. cell shape, cell migration and cell proliferation. CD44-HA interactions influence cellular function by a number of different mechanisms. In the developing hair follicle a close correlation between the expression of CD44 and the absence of HA, both spatially and temporally, is demonstrated (Underhill, 1993). This suggests that the expression of CD44 by the inductive mesenchymal cells results in removal of HA. Similar observations have been made in other systems such as the developing lung, tooth and liver (Underhill et al 1993; Underhill, 1993). This phenomenon is reinforced by studies demonstrating that macrophages and fibroblasts that express CD44 do degrade HA (Culty et al., 1992). Apparently, HA binds to the cell surface and is taken up into the cell and degraded by lysosomal enzymes. In contrast to this, in the epidermis the patterns of expression of CD44 and HA are directly correlated. Both CD44 and HA are expressed in the early periderm, and in the stratum spinosum of the mature epidermis (Ahlo et al., 1989; Wang et al., 1992). A critical difference in the epidermis compared to the mesenchymal cells, is the expression by the keratinocytes of the 180 kDa isoform CD44E isoform which contains an extracellular insert which may change the molecule's affinity for HA (Brown et al., 1991; Stamenkovic et al, 1989; He et al, 1992). Thus, CD44 may be involved in functions other than the binding and degradation of HA.

The synthesis of HA is related directly to the rate of cell proliferation (Cohn et al, 1976; Matuoka et al., 1987) In the developing prostate, the rate of cell proliferation is particularly high in the distal tips of the developing ducts (Sugimura et al., 1986b). Our histochemical

data demonstrates that HA is associated with the proliferating prostatic ducts. The prostate expresses predominantly the 85 kDa CD44S form at all stages of development. This is the form that is characterized as the major HA receptor (Aruffo et al., 1990; Lesly et al., 1990; Miyake et al., 1990; Stamenkovic et al., 1989). Furthermore there is an obvious temporospatial regulation of CD44 expression directly correlated with the expression of HA circumscribing the distal ductal tips. The segregation of CD44 expression at ages 10-, 15 and 20-days to the apical and lateral aspects of the ductal epithelium is suggestive of a role for CD44-HA adhesion in cell-matrix interactions. The results of the CD44 immunoblots, CD44 immunohistochemistry and the RT-PCR analysis, taken together in conjunction with previous studies, suggest multiple functions of the CD44 expressed in the process of prostatic branching morphogenesis. The CD44S form regulates levels of HA by receptor-mediated internalization, as described by Culty et al. (1992) and Hall and Miyake (1992). Furthermore, cell surface-receptor mediated attachment to HA is directly implicated in morphogenesis (Banerjee and Toole, 1992). The expression of high relative molecular weight CD44 variants within a precise window of development suggests that these variants are involved in the "invasion" of the epithelial ducts into the mesenchyme. This would fit into the evolving paradigm that metastatic invasion during malignancy is a recapitulation of the molecular mechanisms involved in embryogenesis and morphogenesis. These CD44 variants have been shown to be of major importance for tumor dissemination in rat pancreas carcinoma (Gunthert et al., 1991; Seiter et al., 1993), in human colon cancer (Mulder et al., 1994) and mammary carcinoma (Kaufman et al., 1995). In addition to the interaction with ligands other than HA in the ECM, the exquisitely controlled expression of CD44 variants may confer to the molecule the ability to bind either soluble or membrane-bound molecules and to sequester cytokines or growth factors essential for regulated morphogenetic realignment of the epithelium. Monoclonal antibodies for the murine CD44 variants are not yet available, hence the use of RT-PCR to investigate the variety of CD44 isoforms expressed.

A critical aspect of our results is the demonstration of a presumptive role for HA and CD44 in the morphogenesis of an organ that is dependent on reciprocal epithelial-mesenchymal interactions. This extends the observations reported by Wheatley et al. (1993), who suggested that the role of CD44 in epithelia may be by a mechanism other than the binding of HA. In their seminal study, CD44 was detected in the apical ectodermal ridge and the odontogenic placodes in the presumptive jaws, regions in which HA-CD44 dependent morphogenesis had not been reported previously. They suggested that CD44 may act as an adhesion molecule binding a myriad of ECM ligands, or as a modulator of growth factor signaling. This latter concept was initially suggested by Tanaka et al. (1993), who showed that CD44 binds cytokines *in vitro*. Herein we demonstrate the expression of specific CD44 isoforms in prostatic epithelium during periods in which the epithelium is inducing smooth muscle differentiation. We interpret our results to mean that prostatic morphogenesis is mediating, in part, through modulation of CD44-HA interactions and other novel functions of CD44.

2.4 REFERENCES

Ahlo AM Underhill CB The hyaluronate receptor is preferentially expressed on proliferating epithelial cells. J Cell Biol 1989; 108: 1557-1565.

Aruffo A Stamenkovic I Melnick M Underhill CB Seed B CD44 is the principal cell surface receptor for hyaluronate. Cell 1990; 61:1303-1313.

Banerjee SD Toole BP Monoclonal antibody to chick embryo hyaluronan-binding protein: changes in distribution of binding protein during early brain development. Dev Biol 1991; 146:186-197.

Banerjee SD Toole BP Hyaluronan-binding protein in endothelial cell morphogenesis. J Cell Bio 1992; 119:643-652.

Banerjee SD Cohn RH Bernfield MR Basal lamina of embryonic salivary epithelia. Production by the epithelium and role in maintaining lobular morphology. J Cell Biol 1977; 73:445-463.

Barnes D Sato G Methods for growth of cultured cells in serum-free medium. Anal Biochem 1980; 102: 255-270.

Barnhart BJ Cox SH Kraemer PM Detachment variants of Chinese Hamster cells. Hyaluronic acid as a modulator of cell detachment. Exp Cell Res 1979; 119: 327.

Belsky E Toole BP Hyaluronate and hyaluronidase in the developing chick embryo kidney. Cell Diff 1983; 12:61-66.

Bernfield M Banerjee S The turnover of basal lamina glycosaminoglycan correlates with epithelial morphogensis. Dev Biol 1982; 90: 291-305.

Bernfield MR Banerjee SD Koda JE Rapraeger AC Remodelling of the basement membrane as a mechanism of morphogenetic tissue interactions. In: Trelstad RL, ed. The role of the Extracellular Matrix in Development. New York: A.R. Liss, 1984: 545-596.

Bernfield MR Cohn RH Banerjee SD Glycosaminoglycans and epithelial organ formation. Amer Zool 1973; 13:1067-1083.

Bernfield MR Wessells NK Intra-and extracellular control of epithelial morphogenesis. Symp Soc Dev Biol 1970; 29: 195-249.

Berry SJ Coffey DS Walsh PC Ewing LL The development of human benign prostatic hyperplasia with age. J Urology 1984; 132: 474-479.

Bertolami CN, Donoff RB Hyaluronidase activity during open wound healing in rabbits: A preliminary report. J Surg Res 1978; 25: 256-259.

Bissell MJ Hall HG Form and function in the mammary gland: the role of extracellular matrix. In: Neville CWD, ed. The Mammary Gland: Development, Regulation, and Function. New York: Plenum Press, 1987: 97-146.

Bourguignon LYW Lokeshwar VB He X Chen X Bourguignon GJ A CD44-like endothelial cell transmembrane glycoprotein (GP116) interacts with extracellular matrix and ankyrin. Mol Cell Bio 1992; 12: 4464-4471.

Branham W Sheehan D Zehr D Ridlon E Nelson C The postnatal ontogeny of rat uterine glands and age-related effects of 17 beta-estradiol. Endocrinology 1985; 117: 2229-2237.

Brown T Bouchard T St. John T Wagner E Carter WG Human keratinocytes express a new CD44 core protein (CD44E) as a heparin-sulfate intrinsic membrane proteoglycan with additional exons. J Cell Biol 1991; 113: 207-221.

Camp RL Kraus TA Birkeland ML Pure E High levels of CD44 expression distinguish virgin from antigen-primed B cells J Exp Med 1991; 173:763-766.

Carter WG and Wayner EA Characterization of the class III collagen receptor, a phosphorylated, transmembrane glycoprotein expressed in nucleated human cells. J Biol Chem 1988; 4193-4201.

Chung LWK Matsuura J Runner MN Tissue interactions and prostatic growth I. Induction of adult mouse prostatic hyperplasia by fetal urogenital sinus implants Biol of Reprod 1984; 31: 155-165.

Clarris BJ Fraser JRE On the pericellular zone of some mammalian cells *in vitro.* Exp Cell Res 1968; 49: 181-193.

Coffey DS Berry SJ Ewing LL An overview of current concepts in the study of benign prostatic hyperplasia. In: Rodgers CH, Coffey DS, Cunha GR, Grayhack JT, Hinman J, Horton R, eds. Benign Prostatic Hyperplasia. Washington, D.C.: U.S. Government Printing Office, 1987:1-14.

Coffey DS Pienta KJ New concepts in studying the control of normal and cancer growth of the prostate. In: Coffey DS, Bruchovsky N, Gardner WA, Resnick J, Karr JP, eds. Current Concepts and Approaches to the Study of Prostate Cancer. New York: A.R. Liss, 1987:p1-73.

Cohn RH Cassiman JJ Bernfield MR Relationship of transformation, cell density, and growth control to the cellular distribution of newly synthesized glycosaminoglycan. J Cell Bio 1976;71:280-294.

Comper WD Laurent TC Physiological function of connective tissue polysaccharides. Physiol Rev 1978; 58: 255-315.

Culty M Nguyen HA Underhill CB The hyaluronan receptor (CD44) particpates in the uptake and degradation of hyaluronan. J Cell Biol 1992; 116: 1055-1062.

Cunha GR Tissue interactions between epithelium and mesenchyme of urogenital and integumental origin. Anat Record 1972; 172: 529-534.

Cunha GR Age-dependent loss of sensitivity of female urogenital sinus to androgenic conditions as a function of the epithelial-stromal interaction in mice. Endocrinology 1975; 95: 665.

Cunha GR Development of the male urogenital tract. In: Rajfer J, ed. Urologic Endocrinology Philadelphia: WB Saunders Co, 1986: p 6-16.

Cunha GR Battle F Young P Brody J Donjacour A Hayashi N Kinbara H Role of epithelial-mesenchymal interactions in the differentiation and spatial organization of visceral smooth muscle Epith Cell Biol 1992; 1: 76-83.

Cunha GR and Chung LWK Stromal-epithelial interactions: I. Induction of prostatic phenotype in urothelium of testicular feminized (Tfm/y) mice. J Steroid Biochem 1981; 14: 1317-1321.

Cunha GR Donjacour PS Cooke PS Mee S Bigsby RM Higgins SJ Sugimura Y The endocrinology and developmental biology of the prostate. Endocrine Rev. 1987; 8:338-363.

Cunha GR Lung B The possible influences of temporal factors in androgenic reponsiveness of urogenital tissue recombinants from wild-type and androgen-insensitive (Tfm) mice. J Exp Zool 1978; 205: 181-194.

Cutler L The role of extracellular matrix in the morphogenesis and differentiation of salivary glands. Advs in Dent Res 1990; 4: 27-33.

Daniel CW Silberstein G B Postnatal development of the rodent mammary gland. In: M.C. Neville, ed. The Mammary Gland Development, Regulation and Function. New York: Plenum Press, 1987: 3-36.

De Cosse J Gossens CL Kuzma JF Breast Cancer: Induction of differentiation by embryonic tissue. Science 1973; 181: 1057-1058.

DeKlerk DP Coffey DS Quantitative determination of prostatic epithelial and stromal hyperplasia by a new technique. Biomorphometrics. Invest. Urol. 1978; 16: 240-245.

Delpeche B Halavent C Characterization and purification of a hyaluronic acid-binding glycoprotein, hyaluronectin. J Neurochem 1981; 36: 855-859.

Donjacour AA Cunha GR Assessment of prostatic protein secretion in tissue recombinants made of urogenital sinus mesenchyme and urothelium from normal or androgen-insensitive mice. Endocrinology 1993; 131: 2342-2350.

Dougherty GJ Lansdrop PM Cooper DL Humphries RK Molecular cloning of CD44R1 and CD44R2, two novel isoforms of the human CD44 lymphocyte "homing" receptor expressed by hemopoietic cells. J Exp Med 1991;174: 1-5.

English HF Drago JR Santen RJ Cellular response to androgen depletion and repletion in the rat ventral prostate: autoradiography and morphometric analysis. Prostate 1985; 7: 41-51.

Erickson CA and Turley EA Substrata formed by combinations of extracellular matrix components alter neural crest cell motility *in vitro* . J Cell Sci 1983; 61: 299-323.

Fenderson BA Stamenkovic I Aruffo A Localization of hyaluronan in mouse embryos during implantation, gastrulation and organogenesis. Differentiation 1993; 54: 85-98.

Fleming T P Molecular maturation of cell adhesion systems during mouse early development. Histochemistry 1994; 101:1-7.

Flikinger CJ The fine structure of the interstitial tissue of the rat prostate. Am J Anat 1972; 134: 107-125.

Fraser JR Laurent TC Turnover and metabolism of hyaluronan. In: The biology of hyaluronan. Ciba Foundation Symposium, Wiley, 1989. Vol 143.

Fujii H Cunha GR Norman JT The induction of adenocarcinomatous differentiation in neoplastic bladder epithelium by an embryonic prostatic inductor. J. Urol. 1982; 128: 858-861.

Gittinger JW Lasnitzki I The effect of testosterone metabolites on the fine structure of the rat prostate gland in organ culture. J Endocrinol 1972; 52: 459-464.

Goetnick PF Stirpe NS Tsonis PA. Carlone D The tandemly repeated sequences of cartilage link proteins contains the sites for interaction with hyaluronic acid. 1987; 105: 2403-2408.

Goldstein LA Zhou DHF Picker LJ Minty CN Bargatze RF Ding JF Butcher EC A human lymphocyte homing receptor, the Hermes antigen, is related to cartilage proteoglycan core and link proteins. Cell 1989; 56: 1063-1072.

Goodfellow PN Banting G Wiles MV Tunnacliffe A Parkar M Solomon E The gene, MIC4, which controls expression of antigen defined by monoclonal antibody F10.44.2, is on human chromosome 11. Eur J Immunol 1982; 12: 659-663.

Green SJ Tarone G Underhill CB Aggregation of macrophages and fibroblasts is inhibited by a monoclonal antibody to the hyaluronate receptor. Exp Cell Res. 1989;178:224-232.

Grobstein C. Tissue interactions in the morphogenesis of mouse embryonic rudiments in vitro. In: Rudnick D, ed. Aspects of Synthesis and Order in Growth. Princeton: Princeton University Press, 1954: 233-256.

Guan J Trevithick J Hynes R Fibronectin/integrin interaction induces tyrosine phosphorylation of a 120-kDa protein. Cell Regulation 1991; 2: 951-964.

Guntenhöner M Pogrel A Stern R A substrate-gel assay for hyaluronidase activity. Matrix 1992;12:388-396.

Gunthert U Hofman M Rudy W Reber S Zoller M Haussmann I Matzku S Wenzel A Ponta H Herrlich P A new variant of glycoprotein CD44 confers metastatic potential to rat carcinoma cells. Cell 1991; 65:13-24.

Haffen K Kedinger M Simon-Assmann P Mesenchyme-dependent differentiation of epithelial progenitor cells in the gut. J. Pediatr. Gastroenterol. Nutr. 1987; 6:14-23.

Hall BK Miyake T The membranous skeleton: The role of cell condensations in vertebrate skeletogenesis. Anat Embryol 1992; 186:107-124.

Hardwick C Hoare K Owens R Hohn HP Hook M Moore D Cripps V Austen L Nance DM Turley EA Molecular cloning of a novel hyaluronan receptor that mediates tumor cell motility. J Cell Biol 1992; 117:1343-1350.

Hay ED Interaction of embryonic surface and cytoskeleton with extracellular matrix. Am J Anat 1980;165: 1-12.

He Q Lesley J Hyman R Ishihara K Kincade PW Molecular isoforms of murine CD44 and evidence that the membrane proximal domain is not critical for hyaluronate recognition. J Cell Bio 1992; 119: 1711-1719.

Heider KH, Dammrich J, Skroch-Angel P Differential expression of CD44 splice variants in intestinal- and diffuse-type human gastric carcinomas and normal gastric mucosa. Cancer Res 1993; 53: 4197-4203.

Higgins SJ Young P Brody JR Cunha GR Induction of functional cytodifferentiation in the epithelium of tissue recombinants. I. Homotypic seminal vessicle recombinants. Development 1989a;106:219-234.

Higgins SJ Young P Cunha GR Induction of functional cytodifferentiation in the epithelium of tissue recombinants. II Instructive induction of Wolffian duct epithelia by neonatal seminal vessicle mesenchyme. Development 1989b; 106:235-250.

Hoare K Savani RC Wang C Yang B Turley E Identification of hyaluronan binding proteins using a biotinylated hyaluronan probe. Connect Tissue Res 1993; 30: 117-126.

Hyman R Lesley J Schulte R Somatic cell mutants distinguish CD44 expression and hyaluronic acid binding. Immunogenetics 1991; 33: 392-395.

Imagawa W Bandyopadhyay GK Nandi S Regulation of mammary epithelial cell growth in mice and rats. Endocrine Rev.1990;11:494-523.

Isacke CM Sauvage CA Hyman R Lesley J Schulte R Trowbridge IS Identification and characterization of the human Pgp-1 glycoprotein. Immunogenetics 1986; 23:326-332.

Imperato MJ Binienda Z Arthur A Mininberg DT Vaughan EJ Quimby FW The development of a male pseudohermaphroditic rat using an inhibitor of the enzyme 5 alpha-reductase. Endocrinology 1985; 116: 807-812.

Jalkanen S Jalkanen M Bargatze R Tammi M Butcher EC Biochemical properties of glycoproteins involved in lymphocyte recognition of high endothelial venules in man. J Immunol 1988;141:1615-1623.

Johansson R Niemi M DNA and protein synthesis of prostatic cultures in relation to histological response under the influence of testosterone and its metabolites. Acta Endocrinol. 1975; 78: 766-780.

Jost A Genetic and hormonal factors in sex differentiation of the brain. . Psychoneuroendocrinology 1953; 8: 183-193.

Jost A Hormonal factors in sex differentiation of mammalian foetus. Roy Soc Lond. Ser B 1970; 259: 119-130.

Jost A A new look at the mechanisms controlling sex differentiation in mammals. Johns Hopkins Med J 1972; 130: 38-53.

Jost A Genetic and hormonal factors in sex differentiation of the brain. . Psychoneuroendocrinology 1983; 8: 183-93.

Kaufmann M Heider KH Sinn HP von Minnckwitz G Ponta H Herrlich P CD44 variant exon epitopes in primary breast cancer and length of survival. Lancet 1995; 345: 615-619.

Kennel SJ Lankford TK Foote LJ Shinpock SG Stringer C CD44 expression on murine tissues. J Cell Sci 1993; 104(Pt 2)): 373-382.

Knudson CB Hyaluronan receptor-directed assembly of chondrocyte pericellular matrix. J Cell Biol 1993; 120: 825-834.

Knudson W Bartnik, E. Knudson CB Assembly of pericellular matrices by COS-7 cells transfected with CD44 homing receptor genes. Proc Natl Acad Sci USA 1993;90:4003-4007.

Knudson W Knudson CB Assembly of a chondrocyte-like pericellular matrix on non-chondrogenic cells. Role of the cell surface hyaluronan receptors in the assembly of apericellular matrix. J Cell Sci 1991; 99:227-235.

Knudson CB Toole BP Changes in the pericellular matrix during differntiation of limb bud mesoderm. Dev Biol 1985; 112: 308-318.

Knudson CB Toole BP Hyaluronate-cell interactions during differentiation of chick embryo mesoderm 1987 Dev Biol; 124:82-90.

Korach KS Insights from the study of animals lacking functional estrogen receptor. Science 1994; 266: 1524-1527.

Kratochwil K Dziadek M Lohler J Harbers K Jaenisch R Normal epithelial branching morphogenesis in the absence of collagen I. Dev Biol 1986; 117: 596-606.

Kratochwil K Tissue combination and organ culture studies in the development of the embryonic mammary gland. In: Gwatkin RBL, ed. Developmental Biology: A Comprehensive Synthesis. New York: Plenum Press., 1987: 315-334.

Kvist T N Finnegan CV The distribution of glycosaminoglycans in the axial region of the developing chick embryo. J Exp Zool 1970; 175: 221-258.

Lacy BE Underhill CB The hyaluronate receptor is associated with actin filaments. J Cell Biol 1987; 105: 1395-1404.

Laemmli UK Cleavage of structural proteins during the assembly of the head of bacteriophage T4. Nature 1970; 227:680-685.

Lasnitzki I Mizuno T Induction of the rat prostate gland by androgens in organ culture. Endocrinol 1977; 74: 47-55.

Lasnitzki I and Mizuno T Prostatic induction: interaction of epithelium and mesenchyme from normal wild-type mice and androgen-insensitive mice with testicular feminization. J Endocrinol. 1980; 85:423-428.

Lasnitzki I Whitaker RH Withycombe JFR The effect of steroid hormones on the growth pattern and RNA synthesis in human benign prostatic hyperplasia in organ culture. Br J Cancer 1975; 32: 168-178.

Laurent TC, Dahl LB, Reed RK. Catabolism of hyaluronan in rabbit skin takes place locally, in lymph nodes and liver. Exp Physiol 1991; 76:695-703.

Laurent TC Fraser JR The properties and turnover of hyaluronan. In: Functions of the proteoglycans. Wiley, Chichester Ciba Foundation Symposium, Wiley, 1986. Vol 124. 9-29.

Laurent C Johnson-Wells G Hellstrom S Engstrom-Laurent A Wells AF Localization of hyaluronan in various muscular tissues. A morphological study in the rat. Cell Tissue Res 1991; 263:201-205.

Lelongt B Makino H Dalecki TM Kanwar YS Role of proteoglycans in renal development. Dev Biol 1988; 128: 256-276.

Lesley J Hyman R CD44 can be activated to function as an hyaluronic acid receptor in normal murine T cells. Eur J Immunol 1992; 22:2719-2723.

Lesley J Schulte R Hyman R Binding of hyaluronic acid to lymphoid cell lines is inhibited by monoclonal antibodies against Pgp-1. Exp Cell Res 1990; 187: 224-233.

Lesley J and Trowbridge I S Genetic characterization of a polymorphic murine cell-surface glycoprotein. Immunogenetics 1982; 15:313-320.

Lindqvist U Chichibu K Delpech B Seven different assays of hyaluronan compared for clinical utility. Clin Chem 1992; 38(1):127-132.

Liotta LA Wewer U Rao NC Schiffman E Stracke M Guirguis R Thorgeirsson U Muschel R Sobel M Biochemical mechanisms of tumor invasion and metastases. Adv Exp Med Biol 1986; 233:161-169.

Lokeshwar VB, Bourguignon LY Posttranslational protein modification and expression of ankyrin binding site(s) in GP85 (Pgp-1/CD44) and its biosythetic precursors during T-lymphoma membrane biosynthesis. J Biol Chem 1991; 266:17983-17989.

Longaker MT, Chiu ES, Adzick NS, Stern M, Stern R. Studies in fetal wound healing: V. A prolonged presence of hyaluronic acid characterizes fetal wound fluid. Ann. Surg 1991; 213:292-296.

Mackenzie IC Hill WM Connective tissue influences on patterns of epithelial architecture and keratinization in skin and oral mucosa. Cell Tissue Res 1984; 235: 551-559.

Martikainen P Harkonen P Vanhala T Makela S Viljanen M Suominen J Multihormonal control of synthesis and secretion of prostatein in cultured rat ventral prostate. Endocrinology 1987; 121:604-611.

Martikainen P and Suominen J A morphometric analysis of rat ventral prostate in organ culture. Anat Rec 1983; 207: 279-288.

Matuoka K Mamba M Mitsui Y Hyaluronate synthetase inhibition by normal and transformed human fibroblasts during growth reduction. J Cell Bio 1987; 104: 1105-1115.

Matzku S Komitowski D Mildenberger M Zoller M Characterization of BSp73, a spontaneous rat tumor and its in vivo selected variants showing different metastasizing capacities. Invasion and Metastasis 1983; 3: 109-123.

Miyake K Underhill CB Lesley J Kincade PW Hyaluronate can function as a cell adhesion molecule and CD44 participates in hyaluronate recognition. J Exp Med 1990; 172: 69-75.

Mulder JW Kryut PM Sewnath M Oosting J Seldenrijk CA Weidema WF Oferhaus GJA Pals ST Colorectal cancer prognosis and expression of exon-v6-containing CD44 proteins. Lancet 1994; 344: 1470-1472.

McNeal JE Relationship of the origin of benign prostatic hypertrophy to prostatic structure of man and other mammals. In: Hinman FJ, ed. Benign Prostatic Hypertrophy. New York: Springer-Verlag, 1983: 152-166.

McNeal JE Prostate anatomy and BPH morphogenesis. Prog Clin Biol Res 1984;145: 27-54.

Meyer K Palmer JW The polysaccharide of the vitreous humor. J Biol Chem 1934; 107: 629-634.

Morriss-Kay GM Tuckett F Solursh M. The effects of *Streptomyces* hyaluronidase on tissue organization and cell cycle time in rat embryos. J Embryol Exp Morphol; 1986: 98:59-70.

Morris-Wiman J Brinkley LL Changes in mesenchymal cell and hyaluronate distribution correlate with in vivo elevation of the mouse mesencephalic neural folds Anat Rec 1990; 226: 383-395.

Nakanishi Y Nogawa H Hashimoto Y Kishi J Hayakawa T Accumulation of collagen III at the points of developing mouse submandibular epithelium. Development 1988; 104: 51-59.

Nakanishi Y Sugiura F Kishi J Hayakawa T Collagenase inhibitor stimulates cleft formation during early morphogenesis of mouse salivary gland. Dev Biol 1986; 113: 201-206.

Neame SJ Isacke CM Phosphorylation of CD44 in vivo requires both Ser323 and Ser325, but does not regulate membrane localization or cytoskeletal interaction in epithelial cells. Embo J 1992; 11: 4733-4738.

Neumann F Elger W Steinbeck H Antiandrogens and reproductive development. Phil Trans Roy Soc London Ser B 1970; 259: 179-184.

Nogawa H and Mizuno T Mesenchymal control over elongating and branching morphogenesis in salivary gland development. J Embryol Exp Morph 1981; 66: 209-221.

Norman JT Cunha GR Sugimura Y The induction of new ductal growth in adult prostatic epithelium in response to an embryonic prostatic inductor. Prostate 1986; 8:209-220.

Orkin RW Underhill CB, Toole BP Hyaluronate degradation in 3T3 and simian virus transformed 3T3 cells. J Biol Chem 1982; 257:5821-5826.

Pals ST Koopman G Heider KH CD44 splice variants: expression during lymphocyte activation and tumor progression. Behring Inst Mitt 1993; (92): 273-277.

Perides G Lane WS Andrews D Dahl D Bignami A Isolation and partial characterisation of a glial hyaluronate-binding protein. J Biol Chem 1989; 264: 5981-5987.

Picker LJ Terstappen LW Rott LS Streeter PR Stein H Butcher EC Differential expression of homing-associated adhesion molecules by T cell subsets in man. J Immunol 1990; 145: 3247-3255.

Prehm P Release of hyaluronate from eukaryotic cells. Biochem J 1990; 267: 185-189

Price D Normal development of the prostate and seminal vesicles of the rat with astudy of experimental postnatal modifications. Am J Anat 1936; 60:79-83.

Price D Ortiz E The role of fetal androgens in sex differentiation in mammals. In: DeHaan RL and Ursprung H eds. Organogenesis. New York: Holt, Reinhart and Winston, 1965:629-652.

Prins GS and Birch L Immunocytochemical analysis of androgen receptor along the ducts of the separate rat prostate lobes after androgen withdrawal and replacement. Endocrinology 1993; 132:169-178.

Prins GS Birch L The developmental pattern of androgen receptor expression in rat prostate lobes is altered after neonatal exposure to estrogen. Endocinol 1995; 136: 1303-1314.

Pure E Camp RL Peritt D Panettieri RA Jr. Lazaar AL Nayak S Defective phosphorylation and hyaluronate binding of CD44 with point mutations in the cytoplasmic domain. J Exp Med 1995; 181: 55-62.

Quackenbush EJ Vera S Greaves A Letarte M Confirmation by peptide sequence and co-expression on various cell types of the identity of CD44 and P85 glycoprotein. Mol Immunol 1990; 27:947-955.

Reed RK Laurent TC Taylor AE Hyaluronan in prenodal lymph from skin: changes with lymph flow. Am J Physiol 1990; 259: 1097-1100.

Roden L Campbell L Fraser JR Enzymatic pathways of hyaluronan catabolism. In: Whelan E, ed. The biology of hyaluronan. Ciba Foundation Symposium, Wiley, 1989. Vol 143.

Ruiz P Schwarzler C Gunthert U CD44 isoforms during differentiation and development. Bioessays 1995;17(1):17-24.

Sakakura T Mammary embryogenesis. In: Neville CW, ed. The Mammary Gland: Development, Regulation and Function. New York: Plenum Press, 1987: 37-66.

Santi RS Johansson R Some biochemical effects of insulin and steroid hormones on the rat prostate in organ culture. Exp Cell Res 1973; 77: 111-120.

Schoenwolf GC Fisher M Analysis of the effects of Streptomyces hyaluronidase on formation of the neural tube. J Emb Exp Morph 1983; 73:1-15.

Schor SL Schor AM Grey AM Chen J Rushton G Grant ME Ellis I Mechanism of action of the migration stimulating factor produced by fetal and cancer patient fibroblasts: Effect on hyaluronic acid synthesis. In Vitro Cell Dev Biol 1989; 25: 737-746.

Screaton GR Bell MV Bell JI Jackson DG The identification of a new alternative exon with highly restricted tissue expression in transcripts encoding the mouse Pgp-1 (CD44) homing receptor. Comparison of all 10 variable exons between mouse, human, and rat. J Biol Chem 1993; 268(17): 12235-12238.

Scott JE In: Greiling H and Scott JE, eds. Keratan sulfate; Chemistry, Biology, 1989: Biochemical Society, London 123-134.

Seiter S Arch R Reber S Komitowski D Hofmann M Ponta H Herrlich P Matzku S Zoller M Prevention of tumor metastasis formation by anti-variant CD44. J Exp Med 1993;177:443-455.

Stamenkovic I Amiot M Pesando JM Seed B A lymphocyte molecule implicated in lymph node homing is a member of the cartilage link protein family. Cell 1989; 56:1057-1062.

Shannon JM Cunha GR Autoradiographic localization of androgen binding in the developing mouse prostate. Prostate 1983; 4:367-373.

Shannon JM Cunha GR Vanderslice KD Autoradiographic localization of androgen recptors in the developing urogenital tract and mammary gland. Anat Rec 1981; 199: 232.

Smedstrod B Pertoft H Ericksson S Studies in vitro on the uptake and degradation of sodium hyaluronate in rat liver endothelial cells. Biochem J 1984; 223: 617-626.

Snedeker SM Brown CF DiAugustine RP Expression and functional properties of transforming growth factor a and epidermal growth factor during mouse mammary gland ductal morphogenesis. Proc. Natl. Acad. Sci. USA 1991 ; 88: 276-280.

Spooner BS Basset K Stokes B Sulfated glycosaminoglycan deposition and processing at the basal epithelial surface in branching and b-D-xyloside-inhibited embryonic salivary glands. Dev Biol 1985; 109: 177-183.

Spooner BS and Faubion JM Collagen involvement in branching morphogenesis of embryonic and salivary gland. Develop Biol 1980; 77:84-102.

Spooner BS Thompson-Pletscher HA Stokes B Basset KE Extracellular matrix involvement in epithelial branching morphogenesis, In: Steinberg MS ed . Developmental Biology: A comprehensive synthesis Plenum Press. New York. 1986 225-260.

Stamenkovic I Aruffo A Amist M Seed B The hematopoietic and epithelial forms of CD44 are distinct polypeptides with different adhesion potentials for hyaluronan bearing cells. EMBO J. 1991;10:343-347.

Stern M and Stern R An ELISA-like assay for hyaluronidase and hyaluronidase inhibitors. Matrix 1992;12:397-403.

Story MT Baeten LA Molter MA Lawson RK Influence of androgen and transforming growth factor beta on basic fibroblast growth factor levels in human prostate-derived fibroblast cell cultures. J. Urology 1990; 143: 241.

Sugimura Y Cunha G Bigsby R Androgenic induction of deoxyribonucleic acid synthesis in prostatic glands induced in the urothelium of testicular feminized (Tfm/y) mice. Prostate 1986a; 9: 217-225.

Sugimura Y Cunha G Donjacour A Morphogenesis of ductal networks in the mouse prostate. Biol. Reprod. 1986b; 34:961-971.

Takeda H Chang C Immunohistochemical and in situ hybridization analysis of androgen receptor expression during the development of the mouse prostate gland. J Endocrinol 1991;129:83-89.

Takeda H Mizuno T Lasnitzki I Autoradiographic studies of androgen-binding sites in the rat urogenital sinus and postnatal prostate. J Endocrinol 1985; 104: 87-92.

Takeda H Lasnitzki I Mizuno T Analysis of prostatic bud induction by brief androgen treatment in the fetal rat urogenital sinus. J Endocrinol 1986; 110: 467-470.

Tanaka Y Adams DH Hubscher S Hirano M Siebenlist U Shaw S T-cell adhesion induced by proteoglycan-immobilized cytokine MIP-1ß. Nature 1993; 361:79-82.

Terpe HJ Stark H Prehm P Gunthert U CD44 variant isoforms are expressed preferentially in basal epithelia of non-malignant human fetal and adult tissues. Histochemistry 1994; 101:79-89.

Thompson D Controlled growth *en masse* (Somatic growth) of embryonic chick tissue in vitro. Marcus Beck Laboratory Reports, No. 4 Proc R Soc. Med 1914; 7: 21-46

Toole BP Glycosaminoglycans in morphogenesis. In: Hay ED ed. Cell Biology of Extracellular Matrix Plenum Press, New York.1991, 259-294.

Toole BP Hyaluronan and its binding proteins, the hyaladherins. Curr. Opin. Cell Biol. 1990; 2: 839-844.

Toole BP Jackson G Gross J Hyaluronate in morphogenesis: inhibition of chondrogenesis in vitro. Proc Natl Acad Sci USA 1972; 69:1384-1386.

Toole BP Trelstad RL Hyaluronate production and removal during corneal development in the chick. Dev Biol 1971; 26: 28-35.

Trelstad RL Coulombre AJ Morphogenesis of the collagenous stroma in the chick cornea. J Cell Bio 1971; 50:840-58.

Trowbridge IF Lesley J Schulte R Hyman R Biochemical characterization and cellular distribution of a polymorphic murine cell-surface glycoprotein expressed on lymphoid tissues. Immunogenetics 1982; 15: 299-312

Turley EA Auersperg N A hyaluronate binding protein transiently codistributes with p21 k-ras in cultured cel lines. Exp Cell Res 1989; 182:340-348.

Turley EA Austin L Vandeligt K Clary C Hyaluronana and a cell-associated hyaluronan binding protein regulate the locomotion of ras-transformed cells. J Cell Biol 1991; 112:1041-1047.

Turley EA Brassel P Moore D A hyaluronan-binding protein shows a partial and temporally regulated codistribution with actin on locomoting chick heart fibroblasts. Exp Cell Res 1990; 187: 243-249.

Underhill CB The interaction of hyaluronate with the cell surface: the hyaluronate receptor and the core protein. In: The biology of hyaluronan. Ciba Foundation Symposium, Wiley, 1989. Vol 143.

Underhill CB Hyaluronan is inversely correlated with the expression of CD44 in the dermal condensation of the embryonic hair follicle. J Inv Derm 1993;101: 820-826

Underhill CB Toole BP Receptors for hyaluronate on the surface of parent and virus-transformed cell lines: Binding and aggregation studies. Exp Cell Res 1981;131:419-423.

Underhill CB Nguyen HA Shirazi M Culty M CD44 positive macrophages take up hyaluronan during lung development. Dev Biol 1993; 155:324-336.

Wang C Tammi M Tammi R Distribution of hyaluronan and its CD44 receptor in the epithelial human skin appendages. Dev Biol 1992;98: 105-112.

Wasner G Hennermann I kratochwil K Ontogeny of mesenchymal androgen receptors in the embryonic mouse mammary gland. Endocrinol 1983;113: 1771-80.

Weniger J Zeis A [Early secretion of testosterone by embryonic mouse testis]. contes Rendus Hebdomaires des Seance de L'Academie des Sciences. D: Sciences Naturelles 1972; 275 (13): 1431-3

Werb Z Proteinases and matrix degradation. In: Kelly R, ed. Textbook of Rheumatology. New York: Simon and Shuster, 1989:300-321.

Werb Z Tremble P Behrendtsen O Crowley E Damsky C Signal transduction through the fibronectin receptor induces collagenase and stromelysin gene expression. J Cell Biol 1989; 109: 877-889.

Wessells N In: W. A. Benjamin ed Tissue Interactions and Development. Menlo Park:, 1977.

Wheatley SC Isacke CM Crossley PH Restricted expression of the hyaluronan receptor, CD44, during postimplantation mouse embryogenesis suggests key roles in tissue formation and patterning. Dev 1993;119: 295-306

Wilson JD Griffin JE George FW Sexual differentiation: early hormone synthesis and action. Biol Reprod 1980; 22: 9-17.

Winter JSD Faiman C Reyes F Sexual endocrinology of fetal and perinatal life. In: Austin CR and Edwards RG eds. Mechanisms of sex differentiation in animals and man . New York Academic Press 1981; 205-254.

Wirth K Arch R Somasundaram C Expression of CD44 isoforms carrying metastasis-associated sequences in newborn and adult rats. Eur J Cancer 1993; 29A: 1172-1177.

Wolffe EJ Gause WC Pelfrey CM Holland SM Steinberg AD August JT The cDNA sequence of mouse Pgp-1 and homology to human CD44 cell surface antigen and proteoglycan core/link proteins. J Biol Chem 1990; 265: 341-347.

Yang B Yang BL Savani RC Turley EA Identification of a common hyaluronan binding motif in the hyaluronan binding proteins RHAMM, CD44 and link protein. Embo J 1994; 13:286-296.

Zimmermann DR Ruoslahti E Multiple domains of the large fibroblast proteglycan, versican. Embo J 1989; 8: 2975-2981.

Zhou DF Ding JF Picker LJ Bargatze R Tammi M Butcher EC Goeddel DV Molecular cloning and expression of Pgp-1. J Immunol 1989;143:3390-3395

CHAPTER III

EXTRACELLULAR HYALURONIC ACID IS A PREREQUISITE FOR DUCTAL BRANCHING MORPHOGENESIS OF THE MOUSE PROSTATE

3.0 INTRODUCTION

Hyaluronan (HA) is a large ECM polysaccharide with the repeating sequence of D-glucuronic acid and N-acetyl-D-glucosamine dissacharide units. HA is unique among GAGs in that it lacks a core protein, is non-sulfated, and can exist in chains that are thousands of disaccharides in length (Comper and Laurent, 1978). HA is the principal GAG of the ECM in a variety of mammalian tissues. It is bound both by specific cell surface receptors and by ECM structures and, as a result of a high net negative charge, it is extremely hydrophilic and attracts large volumes of water of hydration, forming hydrated gels. This property produces turgor pressure in the matrix, resulting in expansion of the extracellular space and facilitating penetration of migrating cells (Toole, 1971; Toole, 1990).

HA metabolism plays a major role in the normal development of several tissues. HA is believed to accumulate in regions of embryonic cell migration (Morriss and Solursh, 1978; Pintar, 1978) and to facilitate several developmental processes including differentiation of the cornea (Toole and Trelstad, 1971), and morphogenesis of heart valves (Markwald et al., 1978; Markwald et al, 1979; Nakamura and Manasek, 1981). HA facilitates embryonic cell behavior by stimulating cell proliferation and migration through the creation of a hydrated matrix that reduces cell-cell contact inhibition (Brecht at al, 1986). As the organ undergoes differentiation, the expanded ECM decreases, and the interstitium undergoes shrinkage coupled with the appearance of HA binding sites on cell surfaces. These receptors participate in the endocytosis of HA into lysosomes, and subsequent enzymatic degradation.

The principal vertebrate receptor for HA, CD44, is an integral plasma membrane glycoprotein involved in cell-cell and cell-matrix adhesion. CD44 was originally identified in NIH 3T3 fibroblasts, and was subsequently detected prominently on hematopoietic cells

(Trowbridge et al., 1982), and proliferating epithelial cells (Ahlo and Underhill, 1989). The predominant CD44 isoform has an approximate M_r of 80-90 x 10^3 (Trowbridge et al., 1982) and is denoted as CD44H or CD44S (CD44 standard). Sequence analysis of CD44 cDNAs from different species reveals homology in the extracellular amino terminus with the HA-binding domains of cartilage link and proteoglycan core proteins (Goldstein et al., 1989; Idzerda et al., 1989; Stamenkovic et al., 1989; Zhou et al 1989; Aruffo et al., 1990; Bosworth et al., 1991; Gunthert et al., 1991). A wide variety of the functions attributed to CD44 stem from its ability to bind HA (Aruffo et al., 1990; Culty et al., 1990; Miyake et al., 1990).

The prostate gland, under the influence of androgens, arises from solid epithelial buds from the endodermal urogenital sinus below the bladder (Cunha et al., 1987). The prostatic buds elongate into the mesenchyme, and undergo branching morphogenesis postnatally (Hayashi et al., 1991; Sugimura et al, 1986). Reciprocal mesenchymal-epithelial interactions are essential for prostatic development (Cunha et al., 1992; Cunha et al., 1987). UGM induces ductal morphogenesis, regulates epithelial proliferation and the expression of epithelial androgen receptors, and ultimately elicits prostate-specific secretory proteins (Cunha et al., 1980; Cunha et al., 1983; Donjacour and Cunha, 1993; Takeda et al; 1990). The epithelium of the developing prostate reciprocates by inducing the surrounding mesenchyme to differentiate into smooth muscle cells (Cunha et al., 1992).

The effects of androgens on prostatic epithelial development are mediated by paracrine influences from UGM. This has been studied utilizing Tfm/Y mice, genetic males that lack functional androgen receptors and are thus insensitive to androgens, and lack all male accessory sexual organs (Ohno, 1979; Wilson, 1992). Analysis of chimeric prostates with wild-type rat UGM and testicular feminized (Tfm) epithelium shows that the androgen receptor-negative Tfm epithelium is induced to undergo androgen-dependent changes, viz.

prostatic ductal morphogenesis, epithelial proliferation and simple columnar cytodifferentiation (Cunha and Lung, 1978; Donjacour and Cunha, 1993; Lasnitzki and Mizuno, 1980; Sugimura et al., 1986). These Tfm/wild-type tissue recombinant studies suggest that androgen targets the mesenchyme, which acts as a mediator of androgenic effects on developing prostate epithelium.

The general use of organ culture systems in experimental biology has evolved from the experiments of Thompson (1914), in which explanted organs from embryonic chicken were embedded in a plasma/embryo extract (Fell, 1976). Organ cultures of male accessory sex organs such as epididymis, seminal vesicle, prostate, and bulbourethral gland have been used to study the development and function of the male urogenital tract (Cooke et al, 1987; Lasnitzki, 1974; Lieber and Veneziale, 1980; Lung and Cunha, 1981; Vazquez et al., 1986). They have been used effectively to elucidate hormonal effects on the prostate, while excluding systemic influences (Gittinger and Lasnitzki, 1972; Lasnitzki, 1976; Lasnitzki et al., 1975; Martikainen and Suominen, 1983). This has been further facilitated by the development of serum-free culture media, facilitating the study of the effects of specific agents, without the influence of undefined serum factors.

The basic components of serum-free defined culture medium usually include insulin, and transferrin, as well as glucocorticoids (Barnes and Sato, 1980, Burleigh et al., 1980; Martikainen et al., 1987; Johansson and Niemi, 1975; Santi and Johansson, 1973). Testosterone is neccessary for the development of prostate in culture, and an optimum level of 10^{-8} M has been defined as being most effective (Johansson and Niemi, 1975).

The use of adult prostate organ cultures involves the surgical removal of the prostate, and its subsequent dicing into appropriately sized explants (1 mm^2). This *in vitro* adult system, however, elicits a distinctively elevated proliferative activity of the epithelium,

which does not correlate with the epithelial growth quiesence of adult prostate epithelium *in vivo*. Moreover, the use of minced adult prostatic tissue in organ culture ignores the known heterogeneity in growth and differentiation along the proximal-distal axis of prostatic ducts (Martikainen and Suominen, 1983; Sugimura et al., 1986). Thus, the interpretation of the results of such organ cultures are in part artifacts due to mechanical or surgical damage to the epithelial ducts The shortcomings associated with the adult prostate organ culture systems argue favorably for the choice of a method utilising intact neonatal Pprostatic ducts. These methods have been described and optimised sufficiently by the laboratory of G. Cunha (Lipschutz et al., 1996; Sugimura et al, 1986).

In the present study, the serum-free neonatal organ culture system has been adapted to elucidate the involvement of HA and HA-cell interactions in androgen-induced prostatic ductal branching morphogenesis.

3.1 MATERIALS AND METHODS

Animals

Male Balb/c mice less than 12 hours old were obtained from the Cancer Research Laboratory at the University of California (Berkeley, CA).

Organ culture

Mouse anterior prostates (AP) were maintained in an organ culture system modified from that previously described by Shima et al. (1990). The animals were sacrificed by decapitation, and the genital tract of each animal was removed *en bloc*. Further dissection to isolate the anterior prostate (AP) was performed in a watchmaker's depression slide, using a dissecting microscope, fine forceps, and a 27 1/2 gauge needle as a scalpel. Dissection was done in Dulbecco's Modified Eagle's (DME)/Ham's F-12, 50:50 (vol/vol) medium (Cell Culture Facility, University of California, San Francisco, CA). The APs were removed intact and cultured for six days on Millicell-CM filters (Millipore Corporation, Bedford, MA) floating in 1 ml of appropriate media in four-well culture dishes (Nunclon, Roskilde, Denmark). APs were cultured either in the presence or absence of testosterone. Appropriate caution was used to ensure that the glands were undamaged prior to being placed in culture. A basal medium of DME/Ham's F-12, 50:50, supplemented with insulin (10 µg/ml) (CCF, UCSF), and transferrin (10 µg/ml) (CCF, UCSF) was utilized in all the experiments. The medium was supplemented with testosterone (Sigma, St Louis, MO) dissolved in 100% ethanol at a concentration of 10^{-8} M, except in the testosterone (-) controls. Each floating gland was covered by a drop of media, which was about three times the volume of the gland. The organ cultures were maintained at 37 °C and 5% CO_2 in a humidified incubator, and the media changed every 2 days. Where indicated, neutralizing monoclonal antibody to CD44, HA oligosaccharides,

or hyaluronidase (plasma or *Streptomyces*) were added to the medium. Each experimental sample was comprised of at least three glands.

To ensure that hyaluronidase treatment in cultue was effective, histological sections of the APs cultured with the addition of hyaluronidase were further incubated with 100 TRU/ml *Streptomyces* hyaluronidase for 12 h at 37 °C and stained with bHABP. The staining was compared with similar sections that had not been incubated with the enzyme.

Immunoreagents

Anti CD44 monoclonal antibodies were obtained as described in chapter I. Briefly, the anti-CD44 monclonal antibodies (mAb), KM201 (IGg_1; Trowbridge et al., 1982) and IM7.8 (IgG_{2b} ; Miyake et al., 1990) generated in rats and directed against the HA receptor CD44 from mouse were obtained as hybridoma (American Type Culture Collection, Rockville, MD) and purified from ammonium sulfate fractions of the hybridoma culture supernatants.

Preparation of HA hexasaccharide

HA oligosaccharides were prepared by modifying the technique described by Banerjee and Toole (1991). HA (100 mg, Sigma type I) was incubated with bovine testicular hyaluronidase (Wydase®, Wyeth-Ayerst, Philadelphia, PA) in 30 ml of 0.05 M Na acetate, 0.15 M NaCl, pH 4.5, for 6 h at 37 °C. The digested products were separated by gel filtration over a Sephadex G-50 column (1.5 x 120 cm, flow rate 20 ml/h) (Pharmacia, Piscatawy, NJ) equilibrated with 0.1 M Na acetate buffer, pH 5.0. Fractions of 5 ml were collected and assayed for uronic acid, and for terminal N-acetylhexosamine. Uronic acid was assayed by carbazole reaction using the method of Bitter and Muir (1962). Briefly, 3 ml of sulfuric acid was cooled to 4 °C, and 0.5 ml of sample layered onto the acid and shaken vigorously. The tubes were then heated for 10 minutes in a boiling water

bath, cooled to room temperature, and 0.1 ml carbazole reagent added. The tubes were reheated for 15 minutes, cooled to room temperature, and the optical density read at 530 nm.

Terminal N-acetyl hexosamine was determined by Reissig's assay (Reissig et al., 1955). Briefly, 0.1 ml of sample, blank or standard, in 0.1 M formate, 0.15 M NaCl buffer was added to a test tube. To each tube was added 1 ml of KBO_4, and the tubes heated in a boiling water bath for 3 minutes, and then cooled to room temperature. Three ml of dimethylaminobenzaldhyde (DMAB) was added, and the tubes maintained at 36 °C for 20 minutes. Optical density was read at 585 nm.

The ratio of uronic acid to terminal hexosamine determines the average oligosaccharide length; a ratio of 3.0 representing a hexasaccharide. The fractions from Sephadex G-50 chromatography with a ratio of uronic acid to terminal hexosamine of between 2.8 and 3.2 were pooled and rechromatographed on Sephadex G-50. The fractions from the second run with a uronic acid to terminal hexosamine ratio of between 2.9 and 3.1 were pooled and used in experiments requiring HA hexosamines.

HA biotinylation

HA was dissolved in 0.1 M Mes pH 5.5 to a final concentration of 1 mg/ml, and stirred overnight at 4 °C. Biotin-hydrazide (Pierce, Rockford, Il) was added to the HA solution, to a final concentration of 1 mM. To this solution, fresh 1-ethyl-3-(3-dimethylaminopropyl) carbodiimide (EDC) (Sigma, St. Louis, MO) was added, to a final concentration of 0.03 mM, and incubated overnight at 4 °C with constant stirring.

Unlinked biotin was removed by dialysis using a Centricon-30® unit (Amicon, Beverley, MA) flushed with dH_20, followed by standard membrane dialysis against dH_20 for 24 h

with at least 3 changes of dH_2O. The biotinylated HA (bHA) was sterilized at 90 °C and stored at -20 °C.

HA-binding assay

Tissue homogenates (10 µg protein/lane), were electrophoresed on a 10% SDS polyacrylamide gel and the separated proteins were transfered onto nitrocellulose membrane (pore size: 0.40 µm) (Biorad, Hercules, CA) in the buffer 15.6 mM Tris, 120 mM glycine, pH 8.1. (Biorad, Hercules, CA). The unoccupied protein binding sites were blocked with 5% casein in PBS for 1 h at room temperature and the blots were incubated with bHA for 1 h at room temperature. The blots were washed in PBS with 0.1% Tween-20 (Fisher Scientific, Fair Lawn, NJ) for 1 h, and the signal detected with a horseradish peroxidase detection kit (Vector, Burlingame, CA). The blots probed with anti CD44 antibodies were rinsed with three changes of TBST (150 mM NaCl, 10 mM Tris-HCl, pH 8.0, 0.05% Tween-20) over 30 minutes, and followed by incubation with biotinylated secondary anti-rat IGg diluted 1:200 in TBST, for 60 minutes, and further rinsing in TBST. The signal was detected with a horseradish peroxidase detection kit (Vector, Burlingame, CA).

***Streptomyces* hyaluronidase**

Streptomyces hyaluronidase (Calbiochem, La Jolla, CA), an enzyme that specifically degrades HA, but does not adversely affect embryonic viability (Morriss-Kay et al., 1986) was preabsorbed with agarose-ovomucoid (Sigma, St. Louis, MO), 1 U/g agarose, overnight at 4 °C, to strip the enzyme of contaminating proteases. Agarose was precipitated by centrifugation.

Purification of plasma hyaluronidase

Human plasma hyaluronidase was purified from human plasma in collaboration with Greg Frost in the laboratory of R. Stern.

Five units (400 ml) of frozen human plasma were thawed and to this was added 0.02% NaN_3, 0.5 mM PMSF, 50 mM NaCl and 5% sucrose. Triton X-114 was added to 7.5%, and the solution stirred at 4 °C for 1 h and then centrifuged at 7000 rpm for 30 min at 4 °C. The supernatant fraction was warmed to 37 °C, and recentrifuged at 7000 rpm for 45 min. By vacuum suction, the detergent-poor phase was discarded and the detergent-rich phase reconstituted with 50 mM Hepes pH 7.5, 0.15 M NaCl, 0.02% NaN_3 to a final volume equal to the original plasma volume. The solution was warmed to 37 °C and centrifuged at 7000 rpm for 30 minutes, and the supernatant fraction decanted. This was repeated three times.

Fast flow S® Sepharose beads (Pharmacia, Upsala, Sweden) were equilibrated with 25 mM Mes pH 6.1, added to the sample and incubated overnight with gentle stirring. The beads were washed three times with 25 mM Mes pH 6.1, 46 mM octylglucoside, and the bound proteins, including hyaluronidase, eluted with 25 mM Mes pH 6.1, 46 mM octylglucoside, 0.3 M NaCl.

The eluate from the Fast flow S® step was added to activated hydroxyapatite beads (Biorad, Hercules, CA) equilibrated with the buffer 10 mM phosphate, pH 7.4, 25 mM NaCl, and incubated overnight. The sample was centrifuged and the supernatant fraction recovered. All the proteins except hyaluronidase bind to the hydroxyapatite beads.

All the steps were carried out at 4 °C. Hyaluronidase activity and protein purity were monitored by the hyaluronidase ELISA-like assay (Stern and Stern, 1992), and silver stained 12.5% SDS PAGE respectively, after each chromatographic step.

Substrate (HA)-gel assay

The substrate-gel assay for hyaluronidase was carried out as described by Guntenhöner et al. (1992). Samples were electrophoresed either on 7.5% polyacrylamide gel under native conditions, or on 12% SDS PAGE under denaturing conditions. Human umbilical cord HA (Sigma, St. Louis, Mo) was incorporated into the gel at a concentration of 0.17 mg/ml, as a substrate for hyaluronidase. Subsequent to electrophoresis, the gels were incubated in 0.1 M Na formate, 0.15 M NaCl, pH 4.6 (formate-NaCl buffer) at 37 °C for 16 h. This facilitated the digeston of HA in the gel. The SDS-PAGE were washed in a 3% solution of Triton X-100 at room temperature for 1 h and then incubated in formate-NaCl buffer for 16 h. The gels were stained sequentially with 0.5% Alcian blue and 0.15% Coomasie blue followed by destaining with 10% methanol and 10% acetic acid solution.

ELISA-like assay for hyaluronidase activity

The quantitative estimation of hyaluronidase activity was performed using an ELISA-like assay (Stern and Stern, 1992). HA (Sigma, St. Louis, Mo) was coated onto 96-well microtiter plates (Corning, Corning, NY) at a concentration of 0.1 mg/ml in 0.2 M carbonate buffer, pH 9.2, and the plates incubated for 24 h at 4 °C. All incubations were followed by three rinses in PBS containing 0.05% Tween-20 (Fisher Scientific, Fair Lawn, NJ), followed by addition of experimental samples. All assays were performed in triplicate. To establish pH optima for hyaluronidase activity, sample pH was adjusted with either formic acid or sodium hydroxide. Following sample hyaluronidase incubation, non-specific binding by subsequent reagents was blocked by incubating with 300 µl/well of ELISA blocking reagent (Boehringer Mannheim Biochemicals, Indianapolis, IN) for 30 minutes at 37 °C. The residual HA after enzymatic digestion was detected using biotinylated HABP. The signal was amplified by incubation with anti-keratan sulfate monoclonal antibody (ICN Biochemicals, Costa Mesa, CA), at a dilution of 1:1000 in PBS, for 30 minutes at room temperature. This was followed by incubation with

biotinylated anti mouse Ig (Vector, Burlingame, CA), 1:200 in PBS, for 30 minutes at room temperature. The biotinylated complex was detected with the avidin-biotin-peroxidase complex coupled to the substrate o-phenylenediamine (Cal Biochem, San Diego). Absorbance was read at 492 nm. A standard graph was prepared by plotting absorbance against units/ml of *Streptomyces* hyaluronidase. This standard graph was used to determine hyaluronidase activity in each sample, and the value was normalized to the protein content.

Image analysis

Wholemount images of the cultured glands were captured and digitized with a Dage-MTI CCD-72 TV camera (Olympus Co, Woodbury, NY) interfaced with a Macintosh Quadra 800 computer (Apple Cupertino, CA), and processed by image analysis software (NIH Image 1.41, Bethesda, MA). This software calculated perimeter and epithelial area of the explants from computer-generated binary images of the glands. Node number, a count of the number of branch points, was defined as the number of internal connections between three or more links in a computer-generated skeleton of the AP epithelial outline. This parameter, whose value is proportional to the complexity of ductal branching, was used to determine morphological complexity of each organ's epithelial shape. The complexity of the shape of the developing AP, form factor, was calculated as the ratio of area to perimeter (Form factor = 4π area/perimeter^2). The inverse of form factor was determined in order to achieve a direct correlation between morphological complexity and the value determined as form factor (1/form factor).

Statistical analysis

Descriptive statistics on mean and standard deviation were determined for all the quantitative parameters and displayed as histograms. Comparison of epithelial area, epithelial perimeter, node number, and inverse form factor were made by analysis of

variance (ANOVA) and intergroup difference determined by Fisher's multiple comparison test, with the level of significance set at $P<0.05$.

HA histochemistry

Mouse APs were harvested at 6 days of culture, fixed with paraformaldehyde, embedded in paraffin, sectioned, and mounted on polylysine coated glass slides for histological staining with HABP. The procedure used for HA histochemistry was identical to the one described in chapter II.

CD44 immunohistochemistry

Mouse APs harvested after 6 days of culture were fixed with paraformaldehyde, embedded in paraffin, and processed for immunohistochemistry as described in chapter II. The primary antibody used was the unconjugated rat anti-mouse CD44 mAb (Pharmingen, San Diego, CA).

All histochemistry was documented by integrated microscopic photography using the Olympus Vanox AHBT3 Microscope, and Olympus C-35AD-4 camera (Olympus Co., Woodbury, NY), and Kodak Gold Plus film (Eastman Kodak Co., Rochester, NY).

3.2 RESULTS

Purification of HA hexamer.

HA was digested with bovine testicular hyaluronidase. The digested products were separated by gel filtration over a Sephadex G-50 column equilibrated with the buffer 0.1 M Na acetate, pH 5.0. The fractions eluted were assayed for uronic acid, and for terminal N-acetylhexosamine. The fractions of HA oligosaccharides with a ratio of uronic acid to terminal hexosamine of 3.0, which represent the HA hexamer, were separated as shown in figures 1 a and b. The HA hexamer was utilized as a competitive inhibitor of the interaction between polymeric HA and cell surface HA-binding proteins.

Figure 1 (facing page)
Preparation of HA hexasaccharide. HA was digested with bovine testicular hyaluronidase. The digested products were separated by gel filtration over a Sephadex G-50 column and the fractions collected were assayed for uronic acid, and for terminal N-acetylhexosamine. Uronic acid was assayed by carbazole reaction using the method of Bitter and Muir (1962) **(Figure 1a)**. The ratio of uronic acid to terminal hexosamine presented in **Figure 1 b** is a measure of the average length of the oligosaccharide. The fractions with a ratio of 3.0 represent the HA hexamer.

a

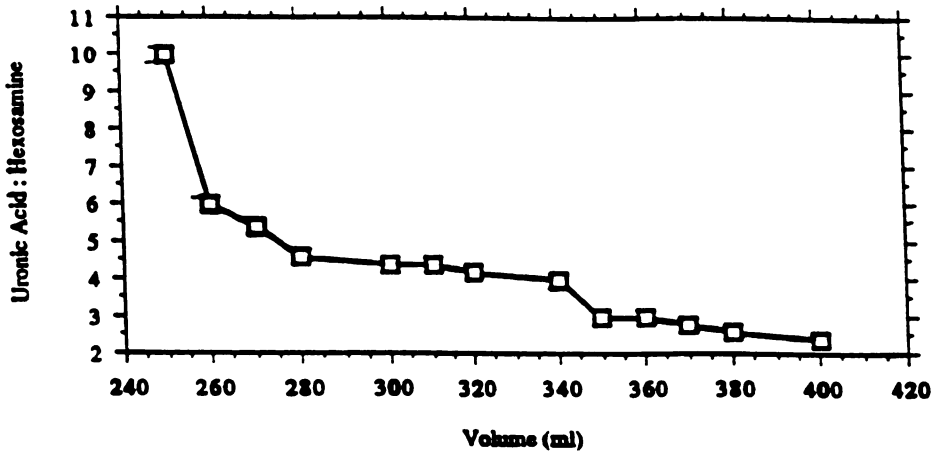
Uronic Acid : Hexosamine
11
10
9
8
7
6
5
4
3
2
240
260
280
300
320
340
360
380
400
420
Volume (ml)

b

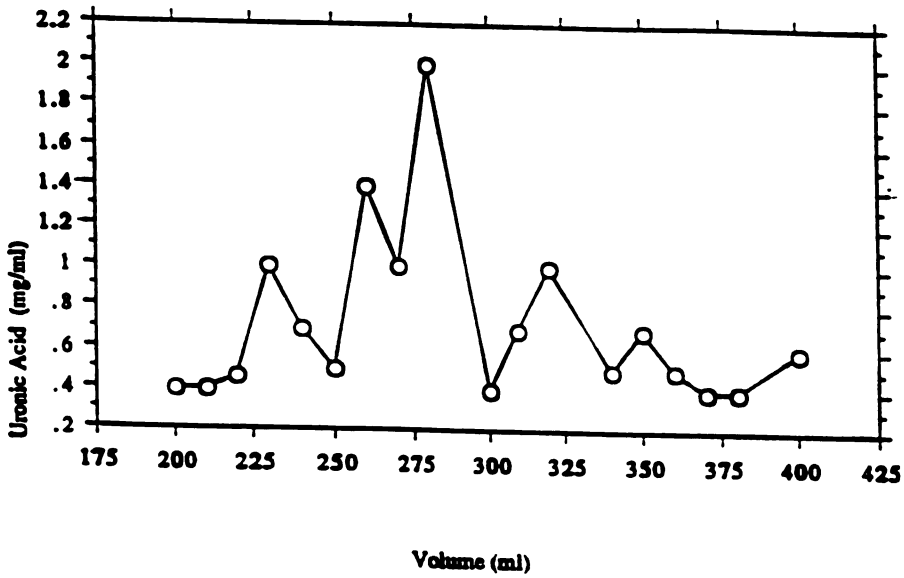
Uronic Acid (mg/ml)
2.2
2
1.8
1.6
1.4
1.2
1
.8
.6
.4
.2
175
200
225
250
275
300
325
350
375
400
425
Volume (ml)

Purification of hyaluronidase

Plasma hyaluronidase was purified to homogeneity as determined by SDS/PAGE , and HA-substrate gel electrophoresis (Figs. 2 and 3 respectively). A tabulation of the purification scheme for human plasma enzyme is shown in table 1. Starting with 2,100 ml of human plasma 1.5 μg of purified protein was obtained routinely. The recently developed HA-substrate gel electrophoresis was performed to further characterize the nature of plasma hyaluronidase activity; as well as to elucidate the HA degrading activity of *Streptomyces* hyaluronidase.

Table 1

Purification scheme for human plasma hyaluronidase

	Volume (ml)	Protein (mg/ml)	Total activity (rTRU)	Specific activity (rTRU/mg)
Starting material (Plasma)	2100	86	73500	0.4
Detergent phase	650	1.3	21450	22
Fast Flow-S	60	0.85	17880	350
Hydroxy-apatite unbound	15	0.0015	13610	604660

rTRU Relative turbidity reducing units

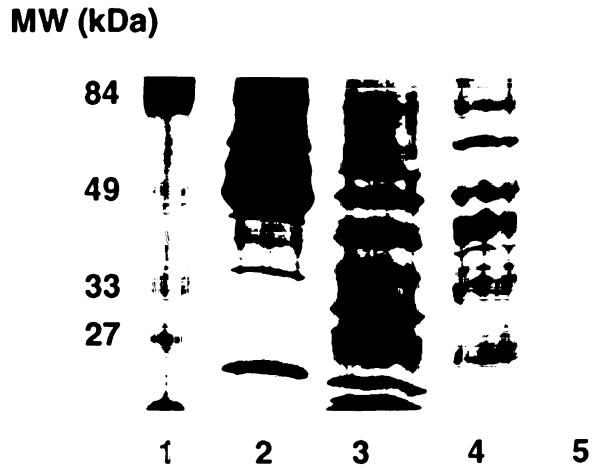

Figure 2

The purification scheme for human plasma hyaluronidase displayed on SDS/PAGE using 7.5% polyacrylamide and silver staining. Molecular weight standards are shown in lane 1. Lane 2 represents the starting material, human plasma ; the final detergent phase is in lane 3; purified human plasma hyaluronidase extracts from the Fast Flow-S purification step are in lane 4, and the final post-Hydroxyl-apatite purification product in lane 5.

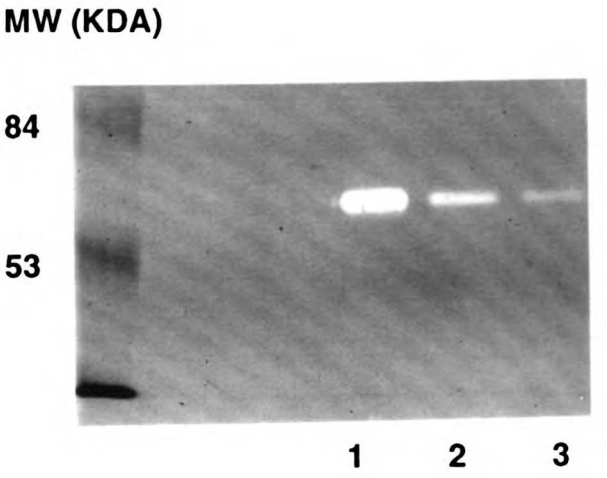

Figure 3a

Substrate gel electrophoresis of the final plasma hyaluronidase purification fractions. The fractions were pooled and electrophoresed on hyaluronic acid impregnated gel. Following electrophoresis, and activation of the enzymatic activity, the gel was stained with Alcian blue. The clear bands at a molecular weight of 57 kDa in lanes 1, 2 and 3 represent enzymatic activity of serial dilutions of purified hyaluronidase.

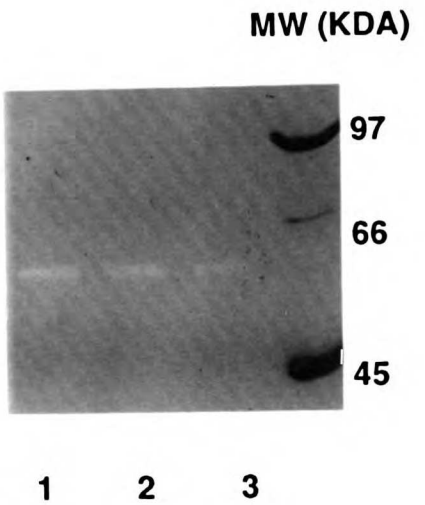

Figure 3b

Substrate gel electrophoresis of *Streptomyces* hyaluronidase. Lanes 1, 2, and 3 contain 1 µl, 0.5 µl, and 0.25 µl of *Streptomyces* hyaluronidase respectively.

Anterior prostates cultured with neutralizing anti CD44 antibodies

The anterior prostates (AP) of 0-day-old mice were cultured for six days. The four parameters assayed as a measure of ductal branching morphogenesis were epithelial area, epithelial perimeter, node number and form factor (Fig. 4). Form factor is a measure of shape complexity derived from the perimeter and area; the simplest shape being the circle with a form factor of one. Since form factor decreases as a shape achieves greater complexity, this parameter was computed as inverse form factor. Node number describes the number of branching points in a duct. At day 0, the AP was a simple unbranched epithelial anlagen surrounded by mesenchyme. At 6 days of culture in the presence of testosterone, the gland was significantly enlarged. In culture the AP is free of the influence of the surrounding seminal vesicle and its associated tissues. This, in addition to the limitations imposed by the organ culture system, result in the organ approximating a 2-dimensional pattern, compared to the 3-dimensional pattern achieved *in vivo* .

To determine the significance of CD44-mediated interactions in AP ductal branching morphogenesis, anti CD44 mAb was added to 0-day-old Balb/c mouse APs cultured with 10^{-8} M testosterone, and the parameters described above were analyzed. Anti CD44 mAb inhibited T-induced ductal branching morphogenesis (Figs. 4, 5). Addition of rat IgG of the same class as the anti CD44 mAb, but not recognizing CD44 had no effect on the branching morphogenesis.

In APs cultured with 50 ng/ml anti CD44 mAb plus T 10^{-8} M the epithelial area, epithelial perimeter, inverse form factor, and node number were 54.8 % ($P<0.0001$), 51.7% ($P<0.0001$), 48.9% ($P=0.006$), and 71.4% ($P=0.0139$), respectively, of the level achieved by optimum T alone. At a mAb concentration of 100 ng/ml, epithelial area was 37% ($P<0.0001$), epithelial perimeter 33.9% ($P<0.0001$), 1/FF 30.9% ($P<0.0017$), and number of nodes 15.2% ($P<0.0001$) of the values achieved in APs cultured with T

10^{-8} alone. Therefore, anti CD44 mAb significantly inhibited ductal branching morphogenesis. In cultures without testosterone, the mAB did not further reduce the epithelial parameters below the -T levels.

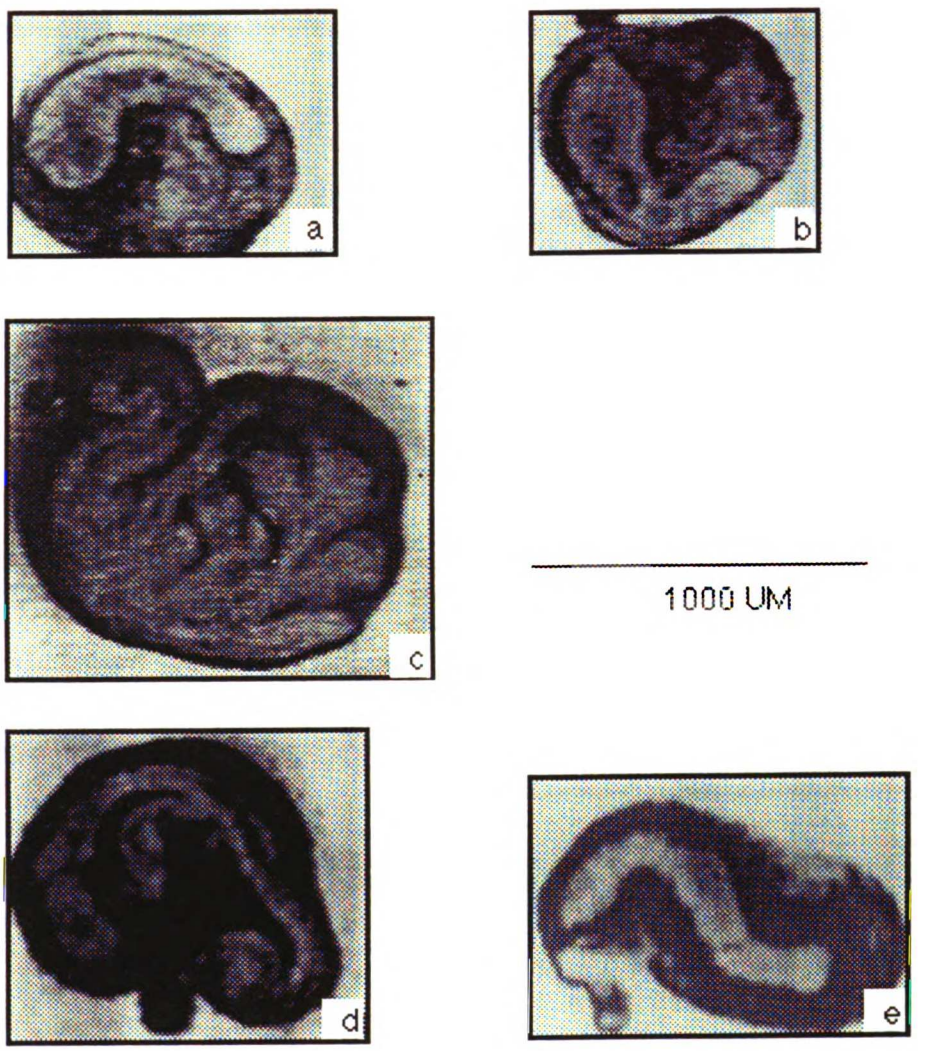

Figure 4

Representative images of mouse APs cultured for 6 days in serum-free medium **a.** day 0 before culture, **b.** without testosterone, **c.** with testosterone (10^{-8} M), **d.** with testosterone + 50 ng/ml anti CD44 mAb **e.** with testosterone (10^{-8} M) + 100 ng/ml anti CD44 mAb.

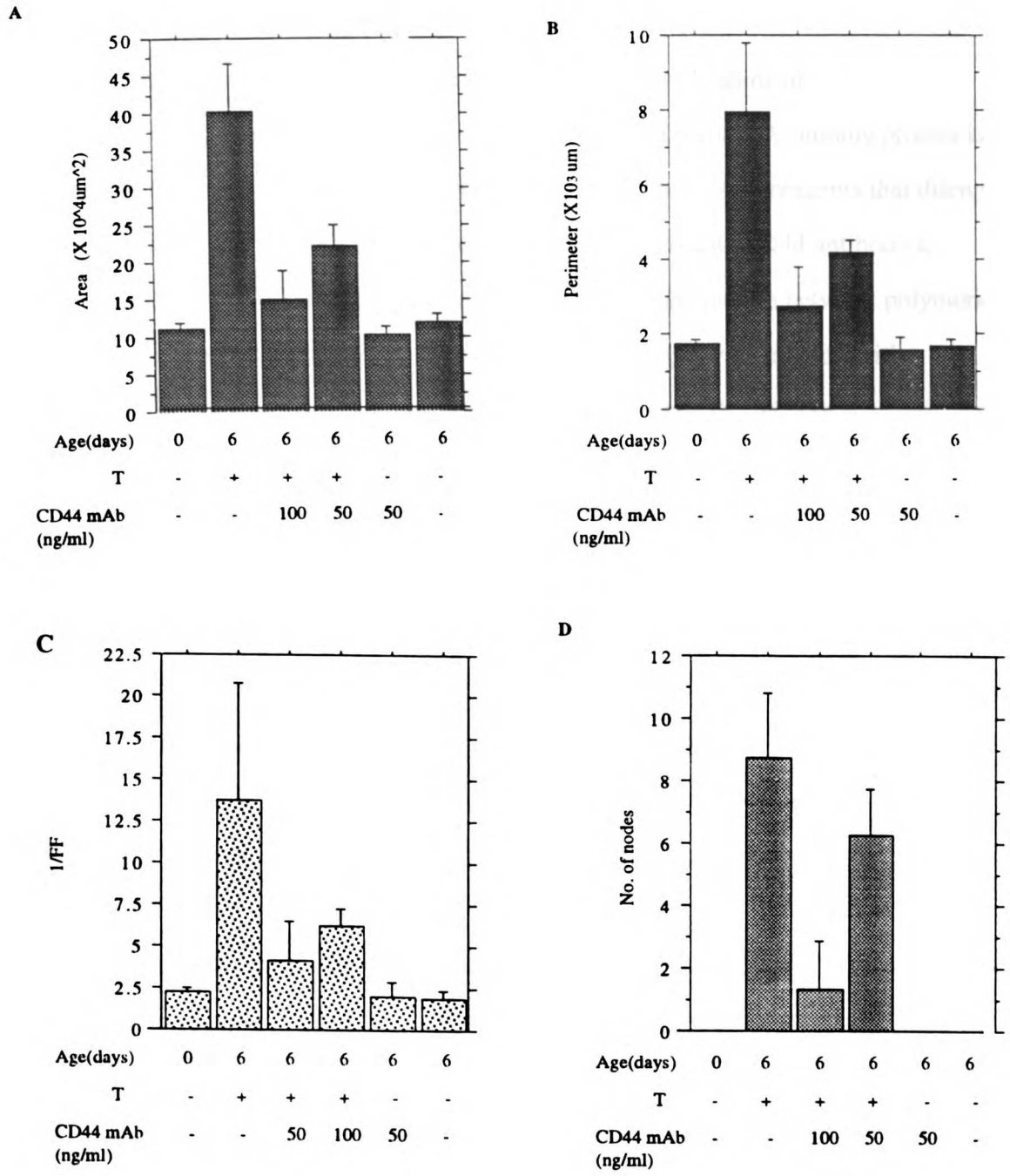

Figure 5

Effect of anti CD44 mAb on the morphogenesis of mouse APs following 6 days of incubation in serum-free medium. Four parameters of epithelial morphogenesis were investigated **A.** Epithelial area, **B.** Epithelial perimeter, **C.** Inverse form factor (1/FF), **D.** Node number.

Effect of HA hexamer on AP ductal branching morphogenesis

The results reported above suggest that interaction between HA and HA-binding protein is necessary for AP ductal branching morphogenesis. In that case, other reagents that disrupt interaction between HA and HA-binding protein, in addition to anti-CD44 antibodies, should affect branching. HA hexamer competitively inhibits interaction between polymeric HA and cell surface HA-binding proteins, while not competing for interaction with interstitial HA binding proteins (Underhill and Toole 1979; Hascall and Hascall, 1991; Yamagata, 1986).

HA hexamer was inhibitory to AP ductal branching morphogenesis (Figs. 6 and 7). At 80 ng/ml, partial inhibition was attained; node number decreased to 64.7% (P=0.0001), inverse form factor to 96.8 % (NS), epithelial perimeter to 84.3% (NS), and epithelial area to 73.4% (P=0.0118) compared to optimal T induced branching. At a higher concentration of HA hexamer (150 ng/ml), the same parameters were further reduced: epithelial area to 55.7% (P=0.0003), epithelial perimeter to 50.8% (P=0.0010), 1/FF to 46.4% (P=0.004), and node number to 11.8% (P<0.0001) of the optimal T induced levels. There was significant inhibition of ductal branching morphogenesis at 150 ng/ml. No effect was obtained by equivalent concentrations of Na uronate and N-acetylglucosamine.

Reactivity of the APs to anti CD44 mAb was significantly reduced in the cell membranes of organs treated with the hexamer. This suggests that, as well as competing for specific HA to HA- binding protein sites, the hexamer may cause its inhibitory effects by inducing loss of CD44 from the cell membranes.

On withdrawal of the hexamer, the APs resumed growth. This observation eliminates toxicity as the cause of the inhibitory effect.

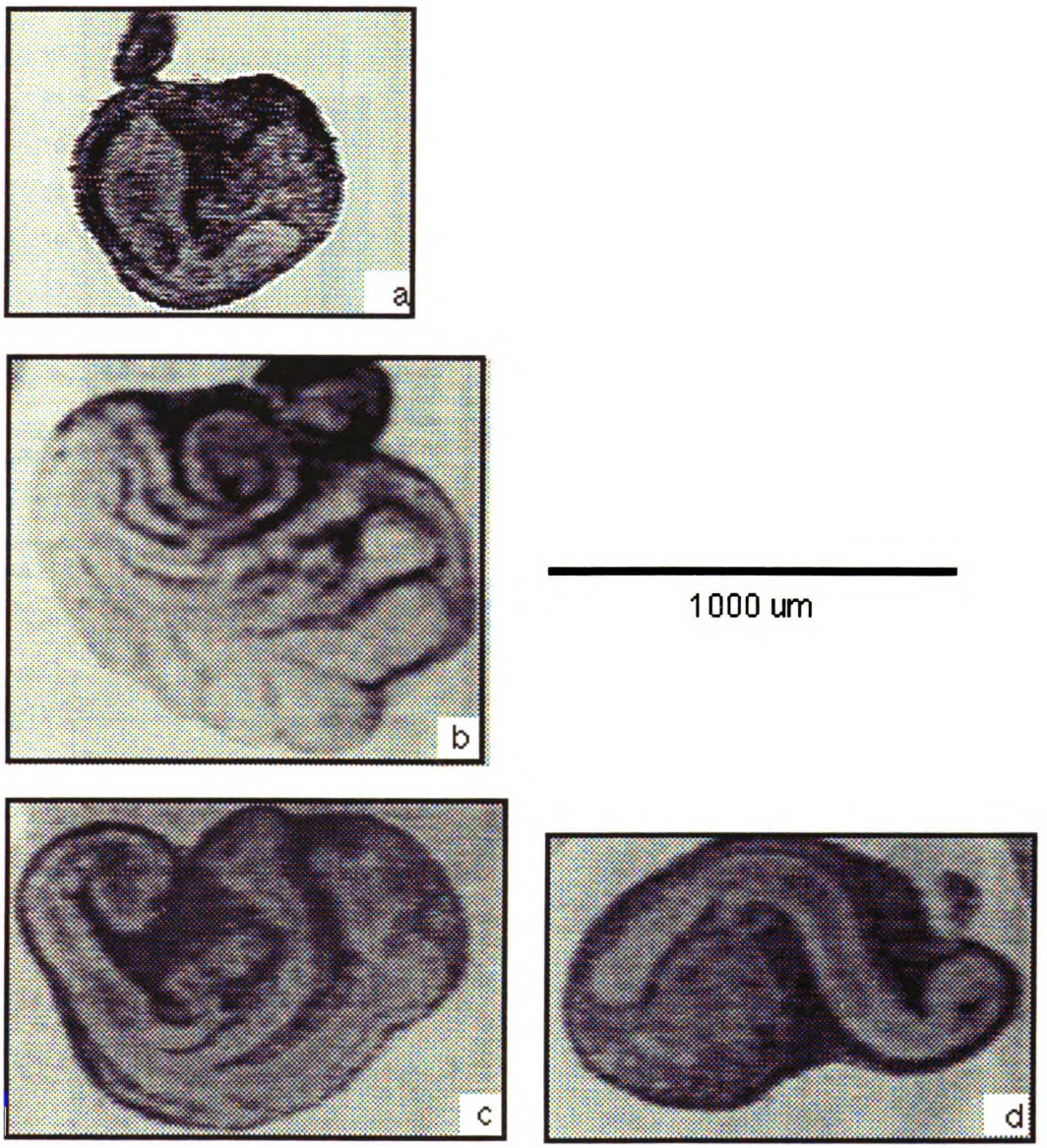

Figure 6

Representative images of mouse APs cultured for 6 days in serum-free medium **a.** without testosterone, **b.** with testosterone (10^{-8} M), **c.** with testosterone + 80 ng/ml HA hexamer, **d.** with testosterone (10^{-8} M) +150 ng/ml HA hexamer.

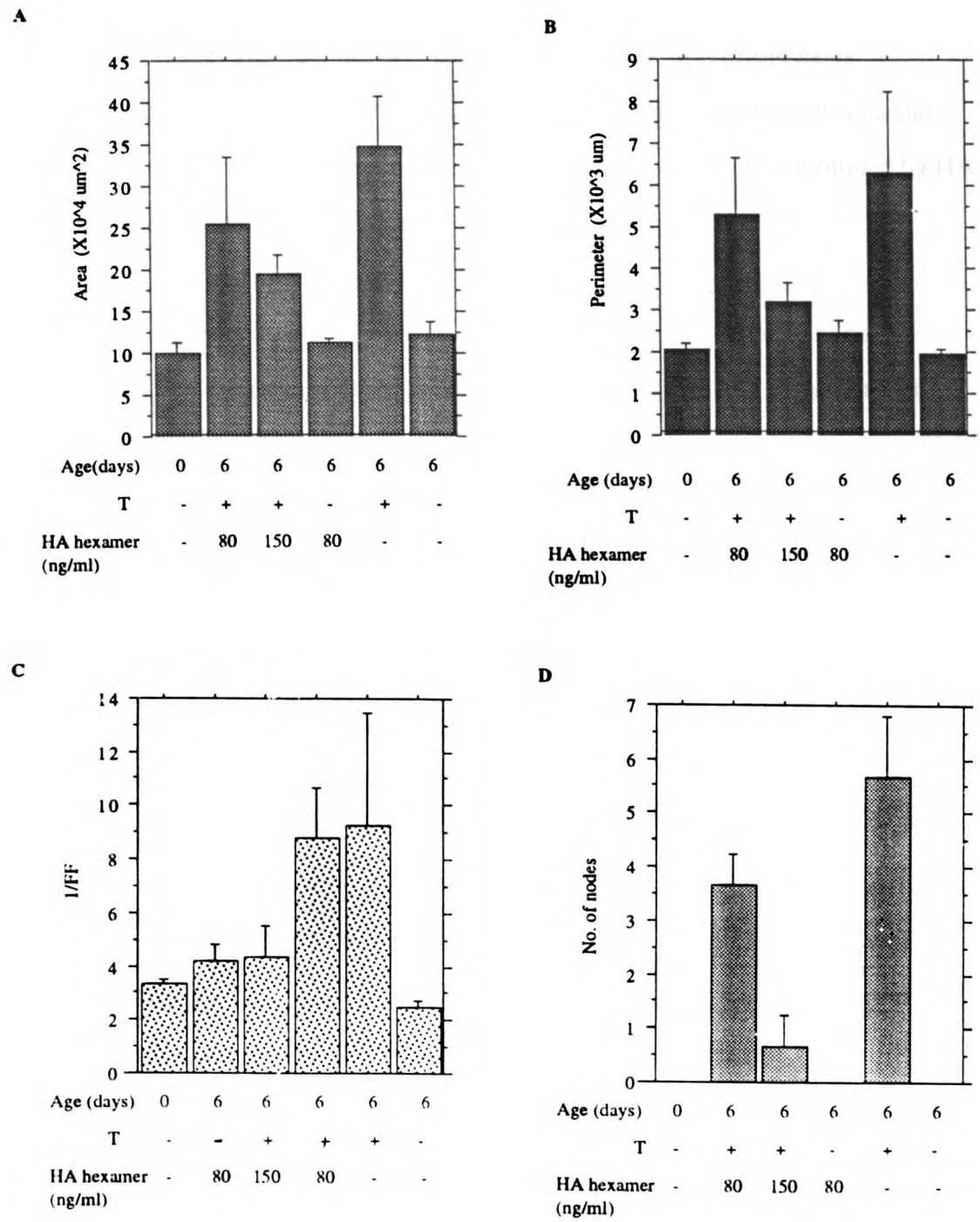

Figure 7

Effect of HA hexamer on the morphogenesis of mouse prostate APs following 6 days incubation in serum-free medium. Four parameters of epithelial morphogenesis were investigated **A.** Epithelial area, **B.** Epithelial perimeter, **C.** Inverse form factor (1/FF), **D.** Node number.

Effect of HA degradation on AP ductal branching morphogenesis

Treatment of cultured APs with 20 and 100 TRU/ml hyaluronidase (both plasma and *Streptomyces*) effectively removed HA from the developing organs as determined by HA histochemistry (Not shown)

APs were cultured with or without T 10^{-8} M in the presence or absence of either *Streptomyces* hyaluronidase (20 and 100 TRU/ml) (Figs. 8 and 9). *Stretpomyces* hyaluronidase distorted the pattern of branching at 20 TRU/ml; epithelial area was 71.5% (P=0.0004), epithelial perimeter 48.6% (P<0.0001), 1/FF 32.3% (P=0.0002) and node number 86.4% (P=0.011) of the values achieved when cultured with T 10^{-8} alone. At 100 TRU/ml eithelial area was 31.1% (P<0.0001), epithelial perimeter 37.8% (P<0.0001), 1/FF 25.5% (P<0.0001), and node number 9.1% (P<0.0001) of the optimal levels.

Plasma hyaluronidase displayed a similar pattern of distortion (Figs 10 and 11). At 20 TRU/ml, epithelial area was 72.3% (P=0.0024), epithelial perimeter 69.3% (P<0.0001), 1/FF 66.4 (P<0.0001), and node number 17.3% (P<0.0001) compared to the equivalent measures in cultures with T 10^{-8} alone. At a concentration of 100 TRU/ml, epithelial area was 40.1% (P<0.0001), epithelial perimeter 42.3% (P<0.0001), 1/FF 44.7% (P<0.0001) and node number was 13.0% (P<0.0001) of the optimal measures.

APs cultured with hyaluronidase and without T were equivalent to APs grown in the absence of T. Significantly, hyaluronidase treatment did not induce epithelial reduction to levels below those observed in the absence of T.

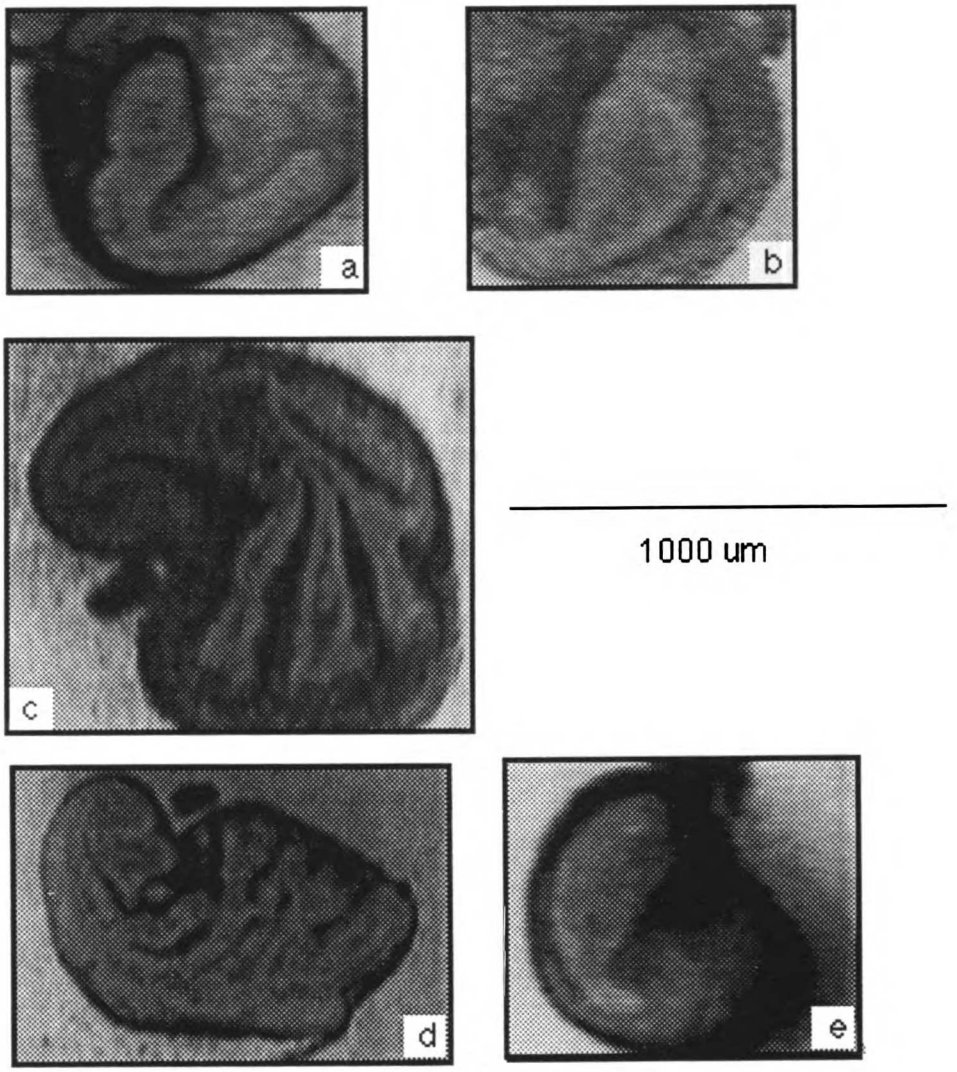

Figure 8 Representative images of mouse APs cultured for 6 days in serum-free medium **a**. day 0, before culture **b**. without testosterone. **c**. with testosterone (10^{-8} M) **d**. without testosterone + 20 TRU/ml *Streptomyces* hyaluronidase, and **e**. with testosterone (10^{-8} M) +100 TRU/ml *Streptomyces* hyaluronidase.

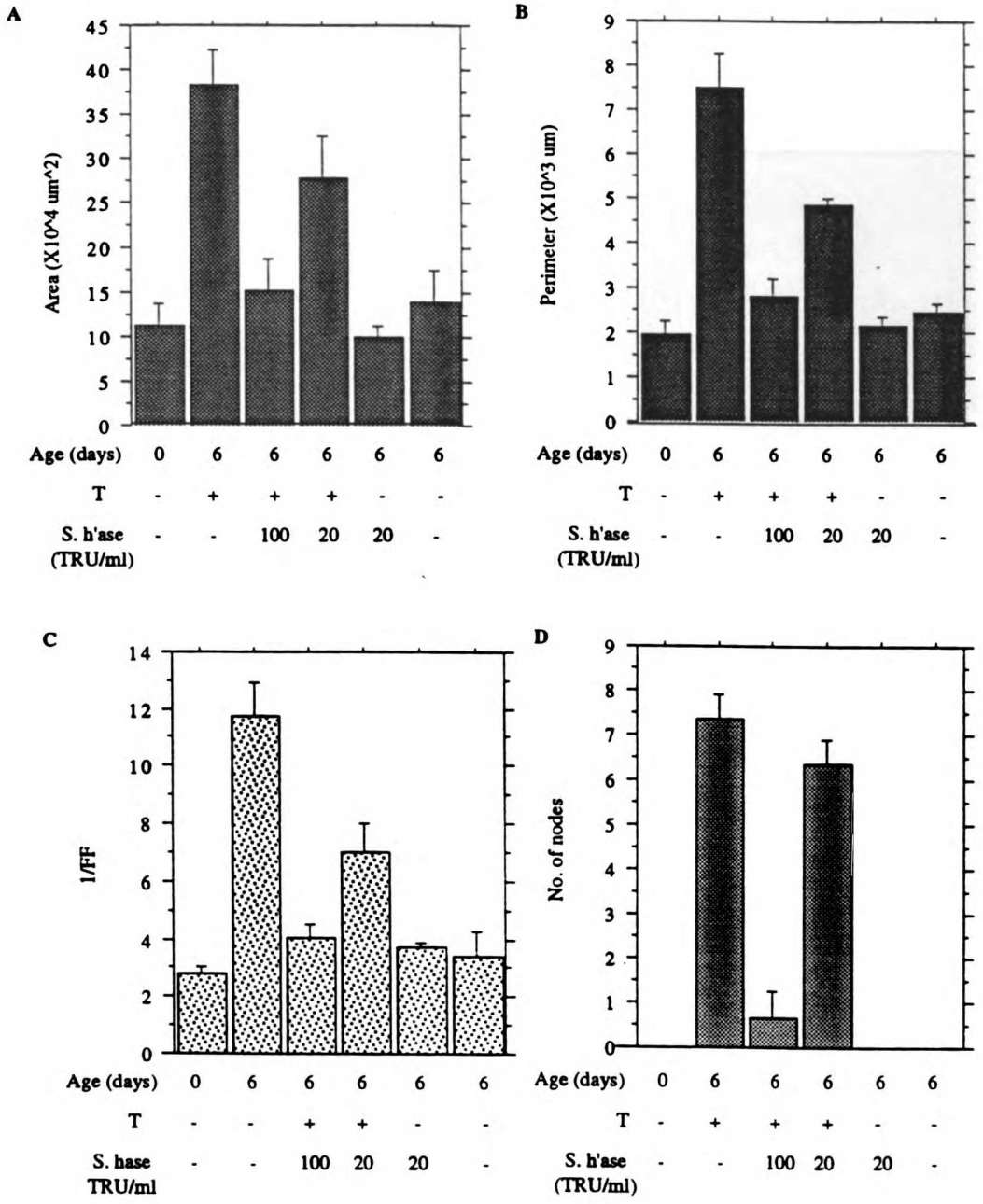

Figure 9

Effect of *Streptomyces* hyaluronidase on mouse prostate APs following 6 days incubation in serum-free medium. Four parameters of epithelial morphogenesis were assessed **A.** Epithelial area, **B.** Epithelial perimeter, **C.** Inverse form factor (1/FF), **D.** Number of nodes.

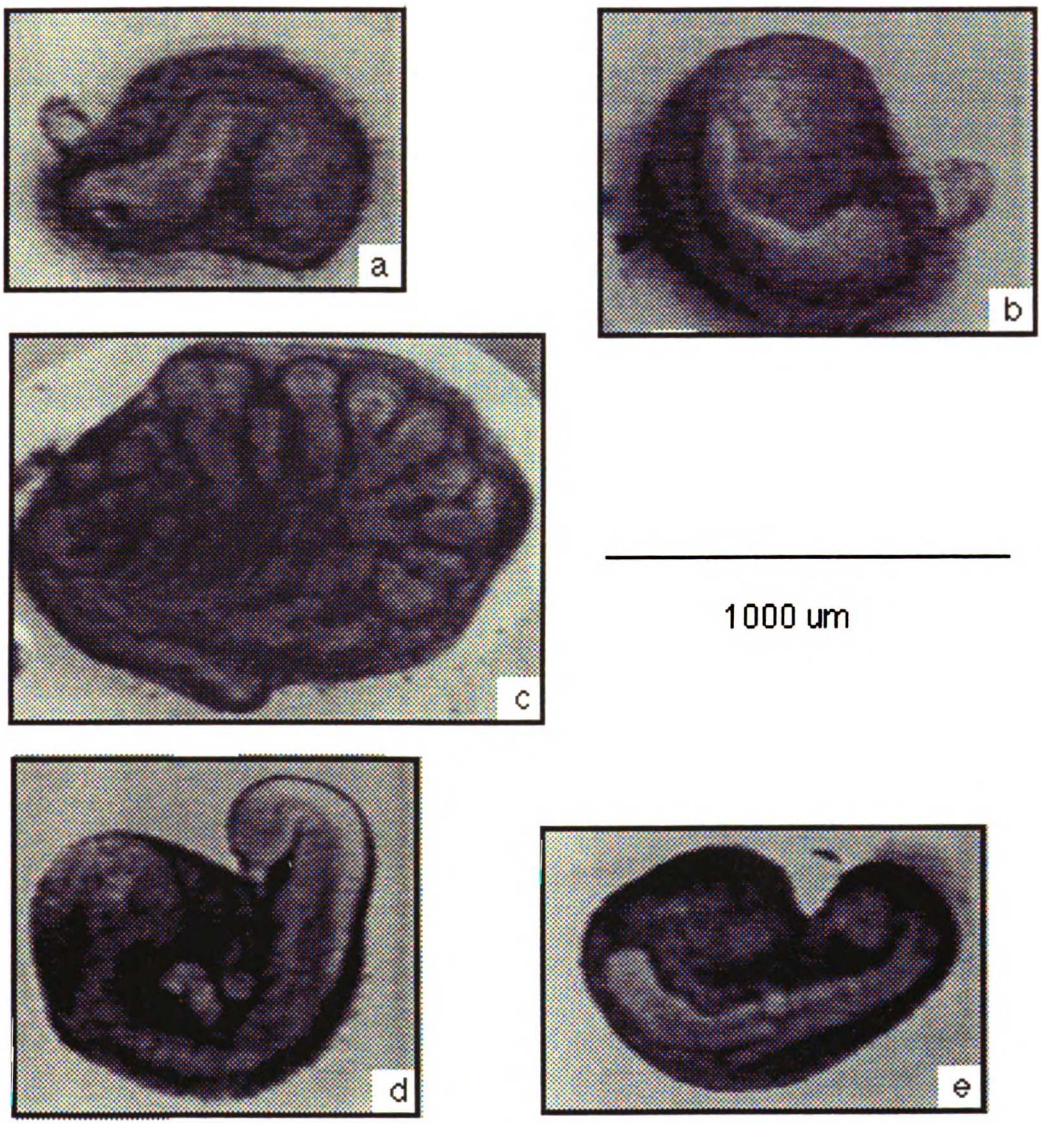

Figure 10 Representative images of mouse APs cultured for 6 days in serum-free medium **a.** day 0, before culture **b.** without testosterone. **c.** with testosterone (10^{-8} M) **d.** without testosterone + 20 TRU/ml plasma hyaluronidase, and **e.** with testosterone (10^{-8} M) +100 TRU/ml plasma hyaluronidase.

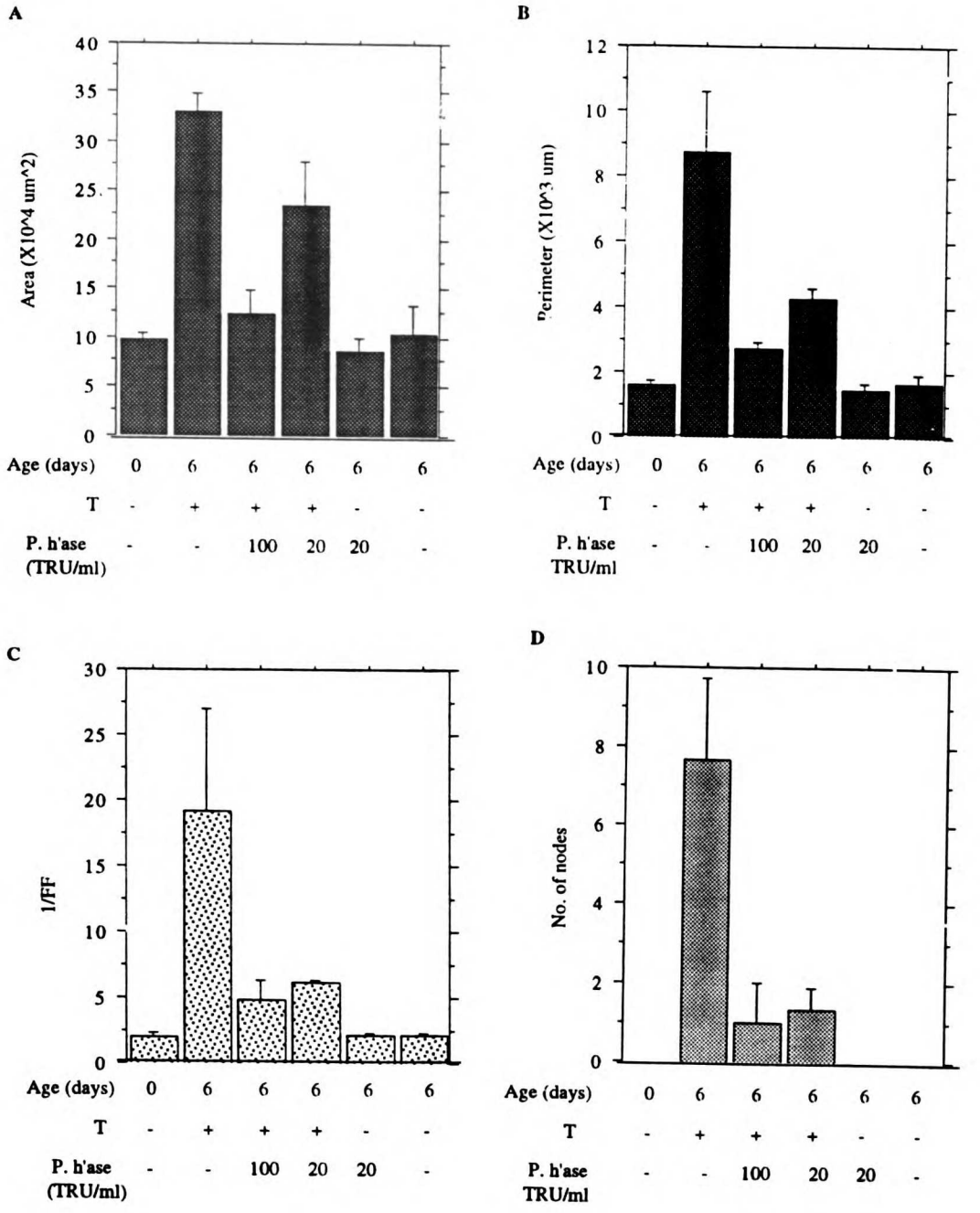

Figure 11 Effect of plasma hyaluronidase on mouse prostate APs following 6 days incubation in serum-free medium. Four parameters of epithelial morphogenesis were assessed **A.** Epithelial area, **B.** Epithelial perimeter, **C.** Inverse form factor (1/FF), **D.** Number of nodes.

3.4 DISCUSSION

As predicted, the development of AP using the serum-free organ culture system, was androgen-dependent, and ductal branching morphogenesis in this model replicates the *in vivo* development of the prostate. The novel contribution of this study lies in the application, for the first time, of computer-based morphometrics to analyze the effects of HA in a serum-free culture system of the developing neonatal prostate. This allows for the definition of the role of HA on prostatic development during the ductal branching phase, while eliminating experimental complications associated with systemic effects.

Four parameters of epithelial morphogenesis were used to determine the effects of various anti HA-cell interaction factors on the developing 0 day mouse AP. Epithelial area, epithelial perimeter, node number, and epithelial form factor (a parameter for shape complexity) were determined using the NIH Image software. These parameters are sufficient for the quantification of growth and ductal branching morphogenesis.

Prostatic development follows a sequence of events that begins with the undifferentiated UGS and leads to the fully functional adult organ. The UGS initiates as an undifferentiated prostatic anlagen. Under the influence of androgens, the anlagen becomes committed to form the prostate. The initial morphological indicator of this commitment is the formation of prostatic buds. Subsequently, with continued androgenic influence, the prostatic buds elongate, and undergo ductal branching morphogenesis, and growth. The pubertal phase is marked by the epithelium undergoing functional cytodifferentiation, hallmarked by the expression of prostate-specific secretory proteins. Growth and branching morphogenesis are part of this phase too. Although the adult phase is growth quiescent, it is androgen-dependent for the homeostasis of function and morphology. During adulthood the rate of cell proliferation is countered by the rate of cell death. Castration, and hence loss of androgen, results in the induction of apoptosis and loss of epithelial cells. The prostate

regresses, and loses its secretory function. Regeneration, both morphological and functional, can be achieved by the administration of androgens to castrated males.

The present study examines the function of HA in ductal growth and branching morphogenesis of the 0 day mouse prostate by comparing the effects of various anti HA-cell interaction factors. The time point studied is after prostatic ducts have emerged from the UGS. For the first time, we can effectively pose the question: Is HA necessary for ductal growth and branching morphogenesis of the prostate?

HA oligomer and CD44 mAb both inhibit branching morphogenesis of the prostate. The inhibition was reversible and not due to toxicity. The mechanism by which CD44 mAb inhibits ductal branching morphogenesis is presumably due to its specific binding to CD44 which in turn would block interaction of endogenous HA with the receptor CD44. Previous studies have shown that antibodies to HA-binding proteins block binding of exogenous HA to both soluble and membrane-bound HA-binding proteins (Banerjee and Toole, 1991; Banerjee and Toole, 1992). Several cells exhibit pericellular matrices that are dependent on both HA and HA-binding protein, and assembly of these matrices is inhibited by antibodies to HA-binding proteins and HA oligomers (Knudson and Knudson, 1991; Yu et al., 1992).

The HA oligomer (hexasaccharide) was used due to its ability to block HA-cell surface binding protein interactions competitively (Underhill and Toole, 1979). Although the precise mode of action of the oligomer in inhibiting ductal branching is not immediately clear, this study suggests that incorporation of the oligomer into the organ culture medium leads to reduction in membrane-associated CD44, and therefore to disruption of HA-CD44 interactions. Conceptually, it is possible that the loss of detectable CD44 following oligomer treatment is as a result of a blockade of the binding site by the occupying oligomer

(Banerjee and Toole, 1994). However, the low binding affinity of the oligomers to HA binding sites (Underhill and Toole, 1979), coupled with the multiple washing procedures prior to application of the antibody, precludes this possibility. The conclusion from this observation is that treatment with the HA oligomer results in interference with CD44-HA interaction, as well as loss in the receptor, leading to inhibition in branching morphogenesis. The results described above suggest that HA-CD44 interaction is necessary for prostatic ductal branching morphogenesis. Our previous results have shown that, by Western blot analysis, the anti CD44 antibodies KM201 and IM7.8 recognize a protein of molecular weight 85 kDa, expressed constituitively, and higher molecular weight, 116 kDa and 160 kDa isoforms that are expressed concomitantly with the initiation of branching morphogenesis. This, combined with the results showing that blocking the activity of endogenous CD44 with neutralizing monoclonal antibodies inhibited T-induced ductal branching morphogenesis, indicate that CD44 is expressed and is functional during the early postnatal period of prostatic development, and plays a significant role in the development of the mouse prostate. Ductal branching morphogenesis is certainly a very complex process. It is possible that variations in this development system might affect the definitions of the endpoints, and hence slight differences between the anti CD44-HA interaction reagents may not have been perceived. Further studies are required to determine precisely the dose-response effectiveness of both the antibodies and the hexasaccharide in the commitment of the UGS into prostatic differentiation, and in bud formation.

The expression of CD44 in the developing AP was assayed by RT PCR, and this highly sensitive method detected CD44 messenger RNA. This demonstrated that at specific timepoints, developing AP express alternatively spliced "invasive" isoforms of CD44, in addition to CD44s. The expression and alternative splicing of CD44 are clearly regulated in a tissue and differentiation stage specific manner. It can be speculated that this phenomenon results of transcriptional regulation. Mouse CD44 genes show a TATA box

at -31 to -35, and functional promoter activity as well as multiple negative regulatory elements which have been demonstrated by transfection assays (Shtivelman and Bishop, 1991). Both human and mouse genes have potential sites for the binding of SP-I transcription factor (Shtivelman and Bishop, 1991; Herrlich et al., 1993). The AP-I site at -109 to -115 in the mouse sequence is apparently functional, since mutation within this site reduces transcription of indicator genes in transfection assays, and reduces response to phorbol ester, and *fos* and *ras* mediated induction (Herrlich et al., 1993).

There is evidence that the cytoplasmic domains of HA receptors, CD44 included, are linked to the cytoskeleton (Lacy and Underhill, 1987; Turley et al., 1990; Lokeshwar and Bourguignon, 1991; Camp et al., 1991). There is also considerable evidence of CD44 phosphorylation, and HA receptor mediated signal transduction (Carter and Wayner, 1988; Kalomiris and Bourguignon, 1989; Camp et al., 1991). Phosphorylation of the cytoplasmic tail of CD44 is thought to affect cytoskeletal association. However, a review of the current data does not reveal a clear-cut line of interpretation. *In vitro* phosphorylation of the molecule enhances its affinity for ankyrin (Lokeshwar and Bourguignon, 1992). However it is not clear how these observations relate to events in intact cells. In macrophages, the detergent-insoluble fraction contains only nonphosphorylated CD44 (Camp et al., 1991). Activation of T lymphocytes by phorbol esters reduces the interaction of CD44 with the cytoskeleton (Geppert and Lipsky, 1991). Phorbol ester treatment of epithelial cells does not enhance phosphorylation in epithelial cells (Neame and Isacke, 1992). On the other hand, transient spikes in phosphorylation have been reported in macrophages following treatment with phorbol esters (Camp et al., 1993). Two well-conserved CD44 cytoplasmic serines (residues 323 and 325 in human CD44) can be phosphorylated (Isacke et al., 1986; Carter and Wayner, 1988; Neame and Isacke, 1992; Camp et al., 1993). Mutation of either of these serine residues significantly reduces phosphorylation (Neame and Isacke, 1992; Camp et al., 1993). Although deletion

of the cytoplasmic tail of CD44 prevented localization of the molecule to the basolateral membrane of transfected epithelial cells, mutation of serines 323 and 325 did not affect CD44 localization nor the association with the cytoskeleton (Neame and Isacke, 1992). In order to fully appreciate the role of CD44 in our system, it would be prudent to extend the present study beyond the expression of, and the function of CD44-HA interactions. Further detailed investigation should attempt to analyze the following: the functions of the splice variants of CD44 expressed; any potential dominant negative or secreted forms of CD44; and the internal signaling pathways.

At least three types of HA degrading enzymes or hyaluronidases exist, and they hydrolyze HA through different mechanisms (Meyer, 1971). The first group, the vertebrate hyaluronidases or endo-ß-N-acetyl-D-hexosaminidases degrade high molecular weight HA to the tetrasaccharide (Laurent, 1990). The second group are the bacterial hyaluronidases. These degrade HA to the disaccharide, and are also specific for HA degradation. The third group, represented by leech hyaluronidase, are essentially ß-endoglucuronidases (Hotez et al., 1994). In the present studies cultured AP organs were treated with either *Streptomyces* hyaluronidase or plasma hyaluronidase. The experiments in this phase were designed to explore the effect of degrading HA *in situ* by hyaluronidase, on androgen-induced prostate development. In both cases, hyaluronidase treatment of cultured AP effectively removed HA from the mesenchyme. HA degradation resulted in a dramatic attenuation of branching. These findings provide insights into the essential function of HA accumulation in the ontogeny of normal prostatic ductal branching morphogenesis. The presence of HA in the developing prostate extracellular matrix is necessary for ductal branching morphogenesis, and absence of HA is associated with substantial alterations in the branching. The observation that branching did not take place after treatment with hyaluronidase is consistent, at least in principle, with observations in other biological systems, principally in the developing endocardial cushions (Baldwin et al.,1994;

Bernanke and Markwald, 1982). It has been observed that incorporation of HA into the collagen gel bioassay of endocardial cushion formation creates a two-fold increase in the epithelial-mesenchymal transformation of atrioventricular canal endothelial cells (Barnake and Markwald, 1982), while treatment with hyaluronidase had an inhibitory effect on epithelial mesenchymal transformation in the same model (Krug et al., 1985).

Apoptosis (programmed cell death) is a mechanism operative in several cellular functions, including tissue remodeling and involution during embryogenesis, cell growth control, neoplastic cell growth regulation, and T-cell repertoire development (Goldstein et al., 1991; Kerr et al., 1972; Bursh et al., 1992; Arends et al., 1990). Recent studies by Ayroldi et al. (1995) show that CD44 stimulation by HA or anti CD44 mAbs result in inhibition of apoptosis induced by anti CD3 mAbs or treatment with dexamethasone on the 3DO T-cell line. This inhibiting effect is dose dependent and specific. Apoptosis induced by ultra violet light, a p53-dependent apoptotic pathway, is not inhibited by anti CD44 mAbs, nor is the action by CD44 mAbs dependent on bcl-2 oncoproteins. This suggests that CD44 uses a specific pathway to inhibit apoptosis. Other evidence shows that during peripheral T lymphocyte depletion by apoptosis, CD44- cells are selectively eliminated, whereas CD44+ memory T cells are selectively activated (Howie et al., 1994). This observation strongly suggests that CD44 contributes a survival, anti-apoptotic signal to T-cells, and presumably to other cells too. The adult prostate is dependent on androgens for the maintenance of both morphology and function, and castration leads to apoptosis of the prostatic epithelium, followed by regression of the gland (Kyprianou and Isaacs, 1989; Lee, 1981). On the contrary, androgen deprivation in the newborn rat prostate does not result in loss of epithelial area (Hayward et al., 1995). Newborn prostates maintained for 6 six days *in vitro* in the absence of androgens retain the same epithelial area as at the initiation of culture. This suggests that the epithelium of the 0 day AP without testosterone does not undergo apoptosis. The prostate is composed of several distinctive cell types at

various stages of differentiation. Stem cells are pluripotent. Amplifying cells arise from the stem cells and have a more limited potential. Transit cells, which derive from the amplifying cell have a low proliferative potential. Postmitotic cells are terminally differentiated and incapable of cell division. Stem cells and amplifying cells do not require androgen, while both transit cells and postmitotic cells are dependent on androgens for their survival. Evidently, the newborn mouse prostatic epithelial ducts are primarily stem and amplifying cells that are not dependent on androgen for survival.

The results of our studies indicate that disrupting HA-CD44 interaction is a potent way of inhibiting T-induced prostatic ductal branching morphogenesis and epithelial growth. However, this does not appear to be achieved by the induction of apoptosis in the 0 day prostate. At low concentrations of anti CD44 mAbs and the HA hexasaccharide, with optimal T, ductal branching morphogenesis was distorted, but epithelial area was maintained at a level comparable to that of control prostates grown only with T. This means that in response to disrupted HA-cell interactions, the 0 day AP did not undergo apoptosis. At high concentrations of anti CD44 mAbs and HA hexasaccharide in the presence of T, ductal branching morphogenesis was significantly inhibited. However, epithelial area was still comparable to that of glands at the initiation of culture, indicating that interrupting the HA-cell interaction did not induce apoptosis, although T-induced increase in epithelial area was completely inhibited.

How universal is the process of ductal branching morphogenesis? and therefore how widely can we interpret our results ? Salivary gland epithelium grown in Matrigel undergoes ductal branching morphogenesis in the absence of mesenchyme when cultured with EGF or TGF (Nogawa and Takahishi, 1991). On the other hand, the same system does not work with lung epithelium (Nogawa and Takaaki, 1995). This suggests that, while the principles involved in the process of ductal branching morphogenesis may be the

same in different organs, the specific molecules and molecular mechanisms involved may be different. The results presented here are therefore applicable for prostate development, and would have to be tested in other organs undergoing ductal branching morphogenesis.

The development of the prostate involves non-uniform proliferation of the epithelium and requires both stimulation and inhibition of branching in order to achieve the appropriate pattern during ductal branching morphogenesis. Ductal tip epithelium has a higher rate of proliferation than the proximal ducts (Prins and Birch, 1995; Sugimura et al., 1986). Endogenous HA may function in the local facilitation of branching around the ductal tips of the developing gland by regulating ECM localization, and hence deposition and degradation. Distortion of T-induced ductal branching produced by the reagents in this study could be due to disruption of HA- mediated ductal tip cellular proliferation.

Absence of effective HA presence distorts the delicately controlled regulation, resulting in significant changes on the ductal branching pattern.

CHAPTER III - APPENDIX

Statistical analysis of data from the prostate organ culture studies

Table 2 Statistical comparisons, following treatment of the *in vitro* mouse anterior prostate cultures with various reagents. Descriptive statistics on mean and standard deviation were determined for all the quantitative parameters. Comparison of **A.** epithelial area, **B.** epithelial perimeter, **C.** node number, and **D.** inverse form factor were made by analysis of variance (ANOVA) and intergroup difference determined by Fisher's multiple comparison test, with the level of significance set at $P<0.05$. S= statistically significant P-value.

Table 2a Treatment with anti CD44 antibodies

Table 2b Treatment with HA hexamer

Table 2c Treatment with *Streptomyces* hyaluronidase

Table 2d Treatment with plasma hyaluronidase

Fisher's PLSD for Area (um^2)
Effect: Treatment
Significance Level: 5 %

	Mean Diff.	Crit. Diff	P-Value	
0 d, 6 d +T	-292868.000	52959.863	<.0001	S
0 d, 6 d anti CD44 100 ng /ml +T	-40413.168	57203.190	.1529	
0 d, 6 d anti CD44 50 ng/ml w/o T	6818.695	57203.190	.8029	
0 d, 6 d anti CD44 50 ng/ml +T	-113356.102	52959.863	.0004	S
0 d, 6 d w/o T	-9145.042	57203.190	.7380	
6 d +T, 6 d anti CD44 100 ng /ml +T	252454.832	57203.190	<.0001	S
6 d +T, 6 d anti CD44 50 ng/ml w/o T	299686.695	57203.190	<.0001	S
6 d +T, 6 d anti CD44 50 ng/ml +T	179511.897	52959.863	<.0001	S
6 d +T, 6 d w/o T	283722.958	57203.190	<.0001	S
6 d anti CD44 100 ng /ml +T, 6 d anti CD44 50 ng/ml w/o T	47231.863	61152.783	.1205	
6 d anti CD44 100 ng /ml +T, 6 d anti CD44 50 ng/ml +T	-72942.934	57203.190	.0159	S
6 d anti CD44 100 ng /ml +T, 6 d w/o T	31268.127	61152.783	.2930	
6 d anti CD44 50 ng/ml w/o T, 6 d anti CD44 50 ng/ml +T	-120174.797	57203.190	.0004	S
6 d anti CD44 50 ng/ml w/o T, 6 d w/o T	-15963.737	61152.783	.5861	
6 d anti CD44 50 ng/ml +T, 6 d w/o T	104211.061	57203.190	.0015	S

Fisher's PLSD for Perimeter (um)
Effect: Treatment
Significance Level: 5 %

	Mean Diff.	Crit. Diff	P-Value	
0 d, 6 d +T	-6205.425	1392.418	<.0001	S
0 d, 6 d anti CD44 100 ng/ml +T	-957.622	1503.984	.1948	
0 d, 6 d anti CD44 50 ng/ml +T	-2419.210	1392.418	.0021	S
0 d, 6 d anti CD44 50 ng/ml w/o T	155.632	1503.984	.8284	
0 d, 6 d w/o T	62.898	1503.984	.9302	
6 d +T, 6 d anti CD44 100 ng/ml +T	5247.803	1503.984	<.0001	S
6 d +T, 6 d anti CD44 50 ng/ml +T	3786.215	1392.418	< 0001	S
6 d +T, 6 d anti CD44 50 ng/ml w/o T	6361.057	1503.984	<.0001	S
6 d +T, 6 d w/o T	6268.323	1503.984	<.0001	S
6 d anti CD44 100 ng/ml +T, 6 d anti CD44 50 ng/ml +T	-1461.588	1503.984	.0560	
6 d anti CD44 100 ng/ml +T, 6 d anti CD44 50 ng/ml w/o T	1113.253	1607.826	.1607	
6 d anti CD44 100 ng/ml +T, 6 d w/o T	1020.520	1607.826	.1961	
6 d anti CD44 50 ng/ml +T, 6 d anti CD44 50 ng/ml w/o T	2574.842	1503.984	.0024	S
6 d anti CD44 50 ng/ml +T, 6 d w/o T	2482.108	1503.984	.0031	S
6 d anti CD44 50 ng/ml w/o T, 6 d w/o T	-92.733	1607.826	.9038	

Fisher's PLSD for Number of nodes
Effect: Treatment
Significance Level: 5 %

	Mean Diff.	Crit. Diff	P-Value	
0 d, 6 d +T	-8.750	1.913	<.0001	S
0 d, 6 d anti CD44 100 ng/ml +T	-1.333	2.066	.1892	
0 d, 6 d anti CD44 50 ng/ml +T	-6.250	1.913	<.0001	S
0 d, 6 d anti CD44 50 ng/ml w/o T	0	2.066	•	
0 d, 6 d w/o T	0	2.066	•	
6 d +T, 6 d anti CD44 100 ng/ml +T	7.417	2.066	<.0001	S
6 d +T, 6 d anti CD44 50 ng/ml +T	2.500	1.913	.0139	S
6 d +T, 6 d anti CD44 50 ng/ml w/o T	8.750	2.066	<.0001	S
6 d +T, 6 d w/o T	8.750	2.066	<.0001	S
6 d anti CD44 100 ng/ml +T, 6 d anti CD44 50 ng/ml +T	-4.917	2.066	.0001	S
6 d anti CD44 100 ng/ml +T, 6 d anti CD44 50 ng/ml w/o T	1.333	2.209	.2178	
6 d anti CD44 100 ng/ml +T, 6 d w/o T	1.333	2.209	2178	
6 d anti CD44 50 ng/ml +T, 6 d anti CD44 50 ng/ml w/o T	6.250	2.066	<.0001	S
6 d anti CD44 50 ng/ml +T, 6 d w/o T	6.250	2.066	< 0001	S
6 d anti CD44 50 ng/ml w/o T, 6 d w/o T	0	2.209	•	

Fisher's PLSD for 1/FF
Effect: Treatment
Significance Level: 5 %

	Mean Diff.	Crit. Diff	P-Value	
0 d, 6 d +T	-11.495	4.982	.0002	S
0 d, 6 d anti CD44 100 ng/ml +T	-1.888	5.381	.4661	
0 d, 6 d anti CD44 50 ng/ml +T	-4.030	4.982	.1052	
0 d, 6 d anti CD44 50 ng/ml w/o T	.199	5.381	.9381	
0 d, 6 d w/o T	.296	5.381	.9082	
6 d +T, 6 d anti CD44 100 ng/ml +T	9.607	5.381	.0017	S
6 d +T, 6 d anti CD44 50 ng/ml +T	7.465	4.982	.0060	S
6 d +T, 6 d anti CD44 50 ng/ml w/o T	11.694	5.381	.0003	S
6 d +T, 6 d w/o T	11.791	5.381	.0003	S
6 d anti CD44 100 ng/ml +T, 6 d anti CD44 50 ng/ml +T	-2.142	5.381	.4094	
6 d anti CD44 100 ng/ml +T, 6 d anti CD44 50 ng/ml w/o T	2.087	5.752	.4513	
6 d anti CD44 100 ng/ml +T, 6 d w/o T	2.184	5.752	.4310	
6 d anti CD44 50 ng/ml +T, 6 d anti CD44 50 ng/ml w/o T	4.229	5.381	.1146	
6 d anti CD44 50 ng/ml +T, 6 d w/o T	4.326	5.381	.1072	
6 d anti CD44 50 ng/ml w/o T, 6 d w/o T	.097	5.752	.9719	

Figure 2a

Fisher's PLSD for Area (um^2)
Effect: Treatment with HA hexamer
Significance Level: 5 %

	Mean Diff.	Crit. Diff	P-Value	
0 d, 6 d + hexamer 150 ng/ml +T	-93139.887	68648.521	.0114	S
0 d, 6 d + hexamer 80 ng/ml -T	-11418.363	64214.811	.7087	
0 d, 6 d + hexamer 80ng/ml +T	-154972.113	68648.521	.0003	S
0 d, 6 d +T	-247576.893	68648.521	<.0001	S
0 d, 6 d -T	-22277.196	64214.811	.4691	
6 d + hexamer 150 ng/ml +T, 6 d + hexamer 80 ng/ml -T	81721.523	64214.811	.0163	S
6 d + hexamer 150 ng/ml +T, 6 d + hexamer 80ng/ml +T	-61832.227	68648.521	.0739	
6 d + hexamer 150 ng/ml +T, 6 d +T	-154437.007	68648.521	.0003	S
6 d + hexamer 150 ng/ml +T, 6 d -T	70862.691	64214.811	.0329	S
6 d + hexamer 80 ng/ml -T, 6 d + hexamer 80ng/ml +T	-143553.750	64214.811	.0003	S
6 d + hexamer 80 ng/ml -T, 6 d +T	-236158.530	64214.811	<.0001	S
6 d + hexamer 80 ng/ml -T, 6 d -T	-10858.832	59451.363	.7011	
6 d + hexamer 80ng/ml +T, 6 d +T	-92604.780	68648.521	.0118	S
6 d + hexamer 80ng/ml +T, 6 d -T	132694.917	64214.811	.0006	S
6 d +T, 6 d -T	225299.697	64214.811	<.0001	S

Fisher's PLSD for Perimeter (um)
Effect: Treatment with HA hexamer
Significance Level: 5 %

	Mean Diff.	Crit. Diff	P-Value	
0 d, 6 d + hexamer 150 ng/ml +T	-1144.460	1602.438	.1479	
0 d, 6 d + hexamer 80 ng/ml -T	-416.261	1498.944	.5609	
0 d, 6 d + hexamer 80ng/ml +T	-3254.027	1602.438	.0007	S
0 d, 6 d +T	-4241.077	1602.438	<.0001	S
0 d, 6 d -T	105.754	1498.944	.8819	
6 d + hexamer 150 ng/ml +T, 6 d + hexamer 80 ng/ml -T	728.199	1498.944	.3151	
6 d + hexamer 150 ng/ml +T, 6 d + hexamer 80ng/ml +T	-2109.567	1602.438	.0135	S
6 d + hexamer 150 ng/ml +T, 6 d +T	-3096.617	1602.438	.0010	S
6 d + hexamer 150 ng/ml +T, 6 d -T	1250.214	1498.944	.0953	
6 d + hexamer 80 ng/ml -T, 6 d + hexamer 80ng/ml +T	-2837.766	1498.944	.0012	S
6 d + hexamer 80 ng/ml -T, 6 d +T	-3824.816	1498.944	<.0001	S
6 d + hexamer 80 ng/ml -T, 6 d -T	522.015	1387.752	.4333	
6 d + hexamer 80ng/ml +T, 6 d +T	-987.050	1602.438	.2076	
6 d + hexamer 80ng/ml +T, 6 d -T	3359.781	1498.944	.0003	S
6 d +T, 6 d -T	4346.831	1498.944	<.0001	S

Fisher's PLSD for No. of nodes
Effect: Treatment with HA hexamer
Significance Level: 5 %

	Mean Diff.	Crit. Diff	P-Value	
0 d, 6 d + hexamer 150 ng/ml +T	-.667	.936	.1489	
0 d, 6 d + hexamer 80 ng/ml -T	0.000	.876	•	
0 d, 6 d + hexamer 80ng/ml +T	-3.667	.936	<.0001	S
0 d, 6 d +T	-5.667	.936	<.0001	S
0 d, 6 d -T	0.000	.876	•	
6 d + hexamer 150 ng/ml +T, 6 d + hexamer 80 ng/ml -T	.667	.876	.1248	
6 d + hexamer 150 ng/ml +T, 6 d + hexamer 80ng/ml +T	-3.000	.936	<.0001	S
6 d + hexamer 150 ng/ml +T, 6 d +T	-5.000	.936	<.0001	S
6 d + hexamer 150 ng/ml +T, 6 d -T	.667	.876	.1248	
6 d + hexamer 80 ng/ml -T, 6 d + hexamer 80ng/ml +T	-3.667	.876	<.0001	S
6 d + hexamer 80 ng/ml -T, 6 d +T	-5.667	.876	<.0001	S
6 d + hexamer 80 ng/ml -T, 6 d -T	0.000	.811	•	
6 d + hexamer 80ng/ml +T, 6 d +T	-2.000	.936	.0004	S
6 d + hexamer 80ng/ml +T, 6 d -T	3.667	.876	<.0001	S
6 d +T, 6 d -T	5.667	.876	<.0001	S

Fisher's PLSD for I/FF
Effect: Treatment with HA hexamer
Significance Level: 5 %

	Mean Diff.	Crit. Diff	P-Value	
0 d, 6 d + hexamer 150 ng/ml +T	-.867	3.227	.5736	
0 d, 6 d + hexamer 80 ng/ml -T	-1.055	3.019	.4659	
0 d, 6 d + hexamer 80ng/ml +T	-5.464	3.227	.0027	S
0 d, 6 d +T	-5.898	3.227	.0015	S
0 d, 6 d -T	.860	3.019	.5508	
6 d + hexamer 150 ng/ml +T, 6 d + hexamer 80 ng/ml -T	-.188	3.019	.8955	
6 d + hexamer 150 ng/ml +T, 6 d + hexamer 80ng/ml +T	-4.597	3.227	.0086	S
6 d + hexamer 150 ng/ml +T, 6 d +T	-5.031	3.227	.0048	S
6 d + hexamer 150 ng/ml +T, 6 d -T	1.727	3.019	.2400	
6 d + hexamer 80 ng/ml -T, 6 d + hexamer 80ng/ml +T	-4.409	3.019	.0073	S
6 d + hexamer 80 ng/ml -T, 6 d +T	-4.843	3.019	.0040	S
6 d + hexamer 80 ng/ml -T, 6 d -T	1.915	2.795	.1637	
6 d + hexamer 80ng/ml +T, 6 d +T	-.434	3.227	.7771	
6 d + hexamer 80ng/ml +T, 6 d -T	6.324	3.019	.0005	S
6 d +T, 6 d -T	6.758	3.019	.0003	S

Figure 2b

Fisher's PLSD for Area
Effect: Treatment with S. h'ase
Significance Level: 5 %

	Mean Diff.	Crit. Diff	P-Value	
0 d, 6 d	-270428.340	60156.388	<.0001	S
0 d, 6 d + S. h'ase 100 TRU/ml +T	-41395.483	60156.388	.1596	
0 d, 6 d + S. h'ase 20 TRU/ml +T	-164928.427	60156.388	<.0001	S
0 d, 6 d + S. h'ase 20 TRU/ml w/o T	12266.520	60156.388	.6647	
0 d, 6 d w/o T	-29250.973	60156.388	.3103	
6 d, 6 d + S. h'ase 100 TRU/ml +T	229032.857	60156.388	<.0001	S
6 d, 6 d + S. h'ase 20 TRU/ml +T	105499.913	60156.388	.0024	S
6 d, 6 d + S. h'ase 20 TRU/ml w/o T	282694.860	60156.388	<.0001	S
6 d, 6 d w/o T	241177.367	60156.388	<.0001	S
6 d + S. h'ase 100 TRU/ml +T, 6 d + S. h'ase 20 TRU/ml +T	-123532.943	60156.388	.0008	S
6 d + S. h'ase 100 TRU/ml +T, 6 d + S. h'ase 20 TRU/ml w/o T	53662.003	60156.388	.0758	
6 d + S. h'ase 100 TRU/ml +T, 6 d w/o T	12144.510	60156.388	.6679	
6 d + S. h'ase 20 TRU/ml +T, 6 d + S. h'ase 20 TRU/ml w/o T	177194.947	60156.388	<.0001	S
6 d + S. h'ase 20 TRU/ml +T, 6 d w/o T	135677.453	60156.388	.0004	S
6 d + S. h'ase 20 TRU/ml w/o T, 6 d w/o T	-41517.493	60156.388	.1585	

Fisher's PLSD for Perimeter
Effect: Treatment with S. h'ase
Significance Level: 5 %

	Mean Diff.	Crit. Diff	P-Value	
0 d, 6 d	-5541.137	806.317	<.0001	S
0 d, 6 d + S. h'ase 100 TRU/ml +T	-818.030	806.317	.0472	S
0 d, 6 d + S. h'ase 20 TRU/ml +T	-3237.017	806.317	<.0001	S
0 d, 6 d + S. h'ase 20 TRU/ml w/o T	-184.167	806.317	.6277	
0 d, 6 d w/o T	-459.137	806.317	.2384	
6 d, 6 d + S. h'ase 100 TRU/ml +T	4723.107	806.317	<.0001	S
6 d, 6 d + S. h'ase 20 TRU/ml +T	2304.120	806.317	<.0001	S
6 d, 6 d + S. h'ase 20 TRU/ml w/o T	5356.970	806.317	<.0001	S
6 d, 6 d w/o T	5082.000	806.317	<.0001	S
6 d + S. h'ase 100 TRU/ml +T, 6 d + S. h'ase 20 TRU/ml +T	-2418.987	806.317	<.0001	S
6 d + S. h'ase 100 TRU/ml +T, 6 d + S. h'ase 20 TRU/ml w/o T	633.863	806.317	.1124	
6 d + S. h'ase 100 TRU/ml +T, 6 d w/o T	358.893	806.317	.3513	
6 d + S. h'ase 20 TRU/ml +T, 6 d + S. h'ase 20 TRU/ml w/o T	3052.850	806.317	<.0001	S
6 d + S. h'ase 20 TRU/ml +T, 6 d w/o T	2777.880	806.317	<.0001	S
6 d + S. h'ase 20 TRU/ml w/o T, 6 d w/o T	-274.970	806.317	.4718	

Fisher's PLSD for No. of nodes
Effect: Treatment with S. h'ase
Significance Level: 5 %

	Mean Diff.	Crit. Diff	P-Value	
0 d, 6 d	-7.333	.726	<.0001	S
0 d, 6 d + S. h'ase 100 TRU/ml +T	-.667	.726	.0687	
0 d, 6 d + S. h'ase 20 TRU/ml +T	-6.333	.726	<.0001	S
0 d, 6 d + S. h'ase 20 TRU/ml w/o T	0.000	.726	•	
0 d, 6 d w/o T	0.000	.726	•	
6 d, 6 d + S. h'ase 100 TRU/ml +T	6.667	.726	<.0001	S
6 d, 6 d + S. h'ase 20 TRU/ml +T	1.000	.726	.0111	S
6 d, 6 d + S. h'ase 20 TRU/ml w/o T	7.333	.726	<.0001	S
6 d, 6 d w/o T	7.333	.726	<.0001	S
6 d + S. h'ase 100 TRU/ml +T, 6 d + S. h'ase 20 TRU/ml +T	-5.667	.726	<.0001	S
6 d + S. h'ase 100 TRU/ml +T, 6 d + S. h'ase 20 TRU/ml w/o T	.667	.726	.0687	
6 d + S. h'ase 100 TRU/ml +T, 6 d w/o T	.667	.726	.0687	
6 d + S. h'ase 20 TRU/ml +T, 6 d + S. h'ase 20 TRU/ml w/o T	6.333	.726	<.0001	S
6 d + S. h'ase 20 TRU/ml +T, 6 d w/o T	6.333	.726	<.0001	S
6 d + S. h'ase 20 TRU/ml w/o T, 6 d w/o T	0.000	.726	•	

Fisher's PLSD for 1/FF
Effect: Treatment with S. h'ase
Significance Level: 5 %

	Mean Diff.	Crit. Diff	P-Value	
0 d, 6 d	-8.986	1.188	<.0001	S
0 d, 6 d + S. h'ase 100 TRU/ml +T	-1.295	1.188	.0351	S
0 d, 6 d + S. h'ase 20 TRU/ml +T	-5.042	1.188	<.0001	S
0 d, 6 d + S. h'ase 20 TRU/ml w/o T	-.948	1.188	.1079	
0 d, 6 d w/o T	-.666	1.188	.2455	
6 d, 6 d + S. h'ase 100 TRU/ml +T	7.691	1.188	<.0001	S
6 d, 6 d + S. h'ase 20 TRU/ml +T	3.944	1.188	<.0001	S
6 d, 6 d + S. h'ase 20 TRU/ml w/o T	8.038	1.188	<.0001	S
6 d, 6 d w/o T	8.320	1.188	<.0001	S
6 d + S. h'ase 100 TRU/ml +T, 6 d + S. h'ase 20 TRU/ml +T	-3.746	1.188	<.0001	S
6 d + S. h'ase 100 TRU/ml +T, 6 d + S. h'ase 20 TRU/ml w/o T	.348	1.188	.5359	
6 d + S. h'ase 100 TRU/ml +T, 6 d w/o T	.629	1.188	.2711	
6 d + S. h'ase 20 TRU/ml +T, 6 d + S. h'ase 20 TRU/ml w/o T	4.094	1.188	<.0001	S
6 d + S. h'ase 20 TRU/ml +T, 6 d w/o T	4.376	1.188	<.0001	S
6 d + S. h'ase 20 TRU/ml w/o T, 6 d w/o T	.282	1.188	.6149	

Figure 2c

Fisher's PLSD for Area
Effect: Treatment
Significance Level: 5 %

	Mean Diff.	Crit. Diff	P-Value	
0 d, 6 d	-233030.920	43187.675	<.0001	S
0 d, 6 d + P. h'ase 100 TRU/ml +T	-27465.450	43187.675	.1927	
0 d, 6 d + P. h'ase 20 TRU/ml +T	-138622.403	43187.675	<.0001	S
0 d, 6 d + P. h'ase 20 TRU/ml -T	11606.164	40398.371	.5456	
0 d, 6 d -T	-7196.277	43187.675	.7246	
6 d, 6 d + P. h'ase 100 TRU/ml +T	205565.470	43187.675	<.0001	S
6 d, 6 d + P. h'ase 20 TRU/ml +T	94408.517	43187.675	.0004	S
6 d, 6 d + P. h'ase 20 TRU/ml -T	244637.084	40398.371	<.0001	S
6 d, 6 d -T	225834.643	43187.675	<.0001	S
6 d + P. h'ase 100 TRU/ml +T, 6 d + P. h'ase 20 TRU/ml +T	-111156.953	43187.675	<.0001	S
6 d + P. h'ase 100 TRU/ml +T, 6 d + P. h'ase 20 TRU/ml -T	39071.614	40398.371	.0569	
6 d + P. h'ase 100 TRU/ml +T, 6 d -T	20269.173	43187.675	.3291	
6 d + P. h'ase 20 TRU/ml +T, 6 d + P. h'ase 20 TRU/ml -T	150228.567	40398.371	<.0001	S
6 d + P. h'ase 20 TRU/ml +T, 6 d -T	131426.127	43187.675	<.0001	S
6 d + P. h'ase 20 TRU/ml -T, 6 d -T	-18802.441	40398.371	.3330	

Fisher's PLSD for Perimeter
Effect: Treatment
Significance Level: 5 %

	Mean Diff.	Crit. Diff	P-Value	
0 d, 6 d	-7161.937	1330.906	<.0001	S
0 d, 6 d + P. h'ase 100 TRU/ml +T	-1129.043	1330.906	.0898	
0 d, 6 d + P. h'ase 20 TRU/ml +T	-2669.717	1330.906	.0008	S
0 d, 6 d + P. h'ase 20 TRU/ml -T	91.329	1244.948	.8765	
0 d, 6 d -T	-91.323	1330.906	.8844	
6 d, 6 d + P. h'ase 100 TRU/ml +T	6032.893	1330.906	<.0001	S
6 d, 6 d + P. h'ase 20 TRU/ml +T	4492.220	1330.906	<.0001	S
6 d, 6 d + P. h'ase 20 TRU/ml -T	7253.266	1244.948	<.0001	S
6 d, 6 d -T	7070.613	1330.906	<.0001	S
6 d + P. h'ase 100 TRU/ml +T, 6 d + P. h'ase 20 TRU/ml +T	-1540.673	1330.906	.0265	S
6 d + P. h'ase 100 TRU/ml +T, 6 d + P. h'ase 20 TRU/ml -T	1220.372	1244.948	.0540	
6 d + P. h'ase 100 TRU/ml +T, 6 d -T	1037.720	1330.906	.1159	
6 d + P. h'ase 20 TRU/ml +T, 6 d + P. h'ase 20 TRU/ml -T	2761.046	1244.948	.0004	S
6 d + P. h'ase 20 TRU/ml +T, 6 d -T	2578.393	1330.906	.0011	S
6 d + P. h'ase 20 TRU/ml -T, 6 d -T	-182.652	1244.948	.7563	

Fisher's PLSD for No. of nodes
Effect: Treatment
Significance Level: 5 %

	Mean Diff.	Crit. Diff	P-Value	
0 d, 6 d	-7.667	1.647	<.0001	S
0 d, 6 d + P. h'ase 100 TRU/ml +T	-1.000	1.647	.2123	
0 d, 6 d + P. h'ase 20 TRU/ml +T	-1.333	1.647	.1039	
0 d, 6 d + P. h'ase 20 TRU/ml -T	0.000	1.541	•	
0 d, 6 d -T	0.000	1.647	•	
6 d, 6 d + P. h'ase 100 TRU/ml +T	6.667	1.647	<.0001	S
6 d, 6 d + P. h'ase 20 TRU/ml +T	6.333	1.647	<.0001	S
6 d, 6 d + P. h'ase 20 TRU/ml -T	7.667	1.541	<.0001	S
6 d, 6 d -T	7.667	1.647	<.0001	S
6 d + P. h'ase 100 TRU/ml +T, 6 d + P. h'ase 20 TRU/ml +T	-.333	1.647	.6691	
6 d + P. h'ase 100 TRU/ml +T, 6 d + P. h'ase 20 TRU/ml -T	1.000	1.541	.1843	
6 d + P. h'ase 100 TRU/ml +T, 6 d -T	1.000	1.647	.2123	
6 d + P. h'ase 20 TRU/ml +T, 6 d + P. h'ase 20 TRU/ml -T	1.333	1.541	.0842	
6 d + P. h'ase 20 TRU/ml +T, 6 d -T	1.333	1.647	.1039	
6 d + P. h'ase 20 TRU/ml -T, 6 d -T	0.000	1.541	•	

Fisher's PLSD for 1/FF
Effect: Treatment
Significance Level: 5 %

	Mean Diff.	Crit. Diff	P-Value	
0 d, 6 d	-17.088	5.501	<.0001	S
0 d, 6 d + P. h'ase 100 TRU/ml +T	-2.834	5.501	.2859	
0 d, 6 d + P. h'ase 20 TRU/ml +T	-4.100	5.501	.1314	
0 d, 6 d + P. h'ase 20 TRU/ml -T	-.035	5.146	.9885	
0 d, 6 d -T	-.102	5.501	.9688	
6 d, 6 d + P. h'ase 100 TRU/ml +T	14.254	5.501	<.0001	S
6 d, 6 d + P. h'ase 20 TRU/ml +T	12.988	5.501	.0002	S
6 d, 6 d + P. h'ase 20 TRU/ml -T	17.053	5.146	<.0001	S
6 d, 6 d -T	16.987	5.501	<.0001	S
6 d + P. h'ase 100 TRU/ml +T, 6 d + P. h'ase 20 TRU/ml +T	-1.266	5.501	.6274	
6 d + P. h'ase 100 TRU/ml +T, 6 d + P. h'ase 20 TRU/ml -T	2.799	5.146	.2610	
6 d + P. h'ase 100 TRU/ml +T, 6 d -T	2.732	5.501	.3027	
6 d + P. h'ase 20 TRU/ml +T, 6 d + P. h'ase 20 TRU/ml -T	4.065	5.146	.1117	
6 d + P. h'ase 20 TRU/ml +T, 6 d -T	3.998	5.501	.1404	
6 d + P. h'ase 20 TRU/ml -T, 6 d -T	-.067	5.146	.9781	

Figure 2d

CHAPTER IV

SUMMARY

4.1 INTRODUCTION

In the preceding chapters, a series of studies have been described identifying, characterizing, and evaluating the expression and role of HA and CD44 in a model of the developing prostate gland. These studies were undertaken as a result of the poor understanding of the function of HA in the developing prostate and in prostate cancer. In this chapter, a synopsis of the major findings of this study is outlined and a critique provided. The clinical and scientific implications are evaluated, and future research areas suggested.

4.2 SUMMARY

The developmental program followed by the prostate goes through a cascade of events that lead to ductal branching morphogenesis. The mesenchyme, on instructions from androgens, induces the epithelium and elicits the patterns of ductal branching morphogenesis. ECM components are involved in these epithelial mesenchymal interactions that are decisive in prostatic development. The data presented in this study provide strong evidence that HA is involved in the patterning of the AP lobe of the mouse prostate, and suggest a critical function for HA and CD44 interactions in prostate branching morphogenesis.

In addition to definitively defining spatial and temporal control of the histochemical distribution of HA and CD44, anti CD44 mAbs and HA hexamers reduce branching morphogenesis. The inhibitory effects in our model may be explained by the inhibition of CD44-HA binding, preventing the cells from adhering to, and migrating on an established matrix. Previously cell-HA interactions have been documented as being involved in the regulation of cell behavior in several ways, including aspects of cell proliferation (Brecht et al., 1986), adhesion (Knudson, 1990; Culty et al., 1990; Lesley et al., 1990; Miyake et al., 1990; Aruffo et al 1990), migration (Turley et al., 1985; Schor et al., 1989), and

differentiation (Kujawa et al., 1986; Toole et al., 1990). It is also conceptually possible that the reagents may also affect the deposition of HA or the ordering of the ligand into specific configurations. The further use of specific inhibitors of HA synthesis and matrix assembly in our model of murine prostate branching morphogenesis is likely to provide deeper insight into the role of HA-CD44 interactions in prostatic development.

Tumor metastasis is the ultimate result of cellular malignancy, and is the cause of cancer deaths. The mechanisms that play a role in controlling metastatic potential involve a myriad of cellular and biochemical events. These include, but are not limited to, interaction of tumor cells with the host cells, as well as several different components of the ECM (Zetter, 1990; Stetler-Stevenson et al., 1993; Liotta and Stetler-Stevenson, 1991). In the initial stages of tumor invasion, tumor cells secrete specific ECM-degrading enzymes in order to penetrate the basement membrane. Subsequent to this event, tumor-vascular endothelium interactions facilitate entry of tumor cells into the circulation. Upon arrest in the target organs, the tumor cells re-invade new territory by reactivating the interaction with the stroma and the endothelium (Liotta and Stetler-Stevenson, 1991). In addition to being a significant player in physiological functions, HA also plays an important role in several pathophysiological conditions. In a number of tumors, levels of HA are elevated 10-20 fold, suggesting a role for HA in tumor progression (Knudson et al., 1989; Pauli and Knudson, 1988). The increased levels of HA in tumor tissues is produced by fibroblasts in the stroma, in response to paracrine signals from the tumor cells (Knudson et al., 1989; Knudson et al., 1984). In tumor tissue, HA expands on hydration and opens up tissue spaces for cell migration. HA also promotes cell migration by very specific interactions with cell surface receptors, principally CD44 (Thomas et al., 1993). It has also been demonstrated that HA, by forming a halo around tumor cells, allows these cells to avoid immune surveillance (Hobarth et al., 1992).

Angiogenesis is a process that is critical for tumor progression. There is substantial evidence to suggest that components of the ECM play a major role in regulating key events in angiogenesis such as endothelial cell proliferation, migration, and formation of the lumen (McCormick and Zetter, 1992). The ECM may sequester potent angiogenic factors such as basic fibroblast growth factor (bFGF), which stimulates endothelial cell proliferation and migration (Kandel et al, 1991; Nguyen et al., 1993). Significantly, HA has been documented to play an active role in the process of angiogenesis (West et al, 1985). Small fragments (4-20 disaccharide units) of HA are angiogenic *in vivo*. Fragments of 10-15 disaccharide units promote endothelial cell proliferation, migration and tubule formation (Lokeshwar and Bourguignon, 1993; Banerjee and Toole, 1992). This suggests that regulated degradation of HA may be important in the processes of tumor metastasis and angiogenesis.

The coordinated actions of both HA and hyaluronidases are significant in embryonic development, vasculogenesis, and immune surveillance (Toole, 1991). The elevated expression of hyaluronidase in tumor tissue has been demonstrated in the urine of Wilm's tumor patients (Stern et al., 1991). More recently, and very relevant to our studies, hyaluronidase has been demonstrated in the ECM associated with benign prostatic hyperplasia, and prostate cancer, compared to normal adult prostate (Lokeshwar et al., 1996). It is possible that tumor cells and developing embryonic organs, secrete controlled elevated levels of hyaluronidase which result in controlled digestion of HA into fragments that promote both angiogenesis and the invasive potential of both tumor cells and cells undergoing active proliferation as in morphogenesis. Experiments to provide direct proof of this important observation will be possible once the cloning of hyaluronidase, which is at an advanced stage in our laboratory, is accomplished. In embryonic development, degradation of the HA-rich matrix by hyaluronidase corresponds to the arresting of cellular movement and the onset of differentiation. Hyaluronidase has been documented to

function as an anti-cancer agent and has been used clinically in conjunction with other chemotherapeutic drugs such as mitomycin C, vindesine and doxorubicin in the treatment of bladder cancer, and head and neck tumors (Schumer et al., 1990; Beckenlehner et al., 1992). The original basis for this treatment modality was that the HA halo around tumors blockaded penetration of chemotherapeutics (Hobarth et al., 1992). A shift in this paradigm is suggested by our studies. It is suggested that sensors on embryonic and tumor cell surfaces respond to changing levels of HA and this modulates the cell phenotype and behavior. CD44 may function as the sensor. Indeed, significant data generated in the human breast cancer SCID mouse model suggest that hyaluronidase is a potent anti-cancer agent. These observations further suggest that hyaluronidase performs this function by modulating the CD44-splice variant repertoire, in response to the degradation of cancer cell-associated HA (Stern R, Personal communication). Parallel studies involving prostate cancer models are currently being pursed.

Since different cell types express and respond to growth factors in different ways, it might be expected that there would be mechanisms in place to control growth factor expression and activity. Certain ECM components, including GAGs have patterns of expression that collaborate in the creation of distinct cellular closets that regulate proliferation and differentiation (Knudson and Toole, 1985; Goldstein et al., 1986; Baldwin and Solursh, 1989). Accumulation of GAGs influences not only the properties of the ECM, but also exert a wider sphere of influence by mediating the availability of cytokines (Nathan and Sporn, 1991). It is well documented that bFGF binds to heparin, an interaction that is prerequisite for activation of the bFGF cell surface receptor (Klagsburn and Baird, 1991; Rapraeger et al., 1991). In addition, several interleukins bind selectively to acidic polysaccharides, suggesting that under certain physiological conditions, there is retention of some cytokines through a low affinity interaction with GAGs. Locci et al. (1995) have demonstrated that HA is involved in modulating TGF β activity. In their model, the

stimulatory effects of TGF β upon embryonal fibroblasts GAG synthesis is suppressed by the presence of high molecular weight HA. Preincubation of TGFβ with high molecular weight HA considerably reduces its effect on thymocyte proliferation, while digestion of the TGF β-HA complex with hyaluronidase prior to being added to thymocytes restores the inhibitory capacity of TGF β. It has been established unequivocally that TGFβ functions as a potent regulator of ECM formation and maintenance (Roberts and Sporn, 1990). TGFβ-HA interaction may prevent binding of the growth factor to its receptors, and thus provide an additional level for regulating the ECM. The additional data from our studies further suggests that the developmental regulation of HA and its differential localization *in vivo*, contributes to the regulation of growth factor activity. Further studies are needed to characterize the effects of HA on TGF β, and other growth factors.

The concept that hyaluronic acid and CD44 play critical roles in prostatic development is a hypothesis that has been explored in this work. An appealing aspect of this idea is that it links developmental biology with observations that have, and are continuing to evolve in relation to the tumorigenic process. The gist of this work, in suggesting an integration between normal development and carcinogenesis, provides a basis for novel therapeutics to neoplasms, as well as potential prognostic indicators for prostatic (and other parencymal organ) oncopathologies.

4.3 REFERENCES

Ahlo AM Underhill CB The hyaluronate receptor is preferentially expressed on proliferating epithelial cells. J Cell Biol 1989; 108: 1557-1565.

Arends MJ Morris RG Willie AH Apoptosis: The role of endonuclease. Am J Pathol 1990; 136:593-602.

Aruffo A Stamenkovic I Melnick M Underhill C Seed B CD44 is the principal cell surface receptor for hyaluronate. Cell 1990; 61:1303-1313.

Ayroldi E Cannarile L Migliorati G Bartoli A Nicoletti I Riccardi C CD44 (Pgp-1) inhibits CD3 and dexamethasone-induced apoptosis. Blood 1995; 86:2672-2678.

Baldwin HS Lloyd TR Solursh M Hyaluronate degradation affects ventricular function of the early post looped embryonic rat heart in situ. Circ Res 1994; 74:244-252.

Banerjee SD Toole BP Monoclonal antibody to chick embryo hyaluronan-binding protein: changes in distribution of binding protein during early brain development. Dev Biol 1991; 146:186-197.

Banerjee SD Toole BP Hyaluronan-binding protein in endothelial cell morphogenesis. J Cell Biol 1992; 119:643-652.

Barnes D and Sato G Methods for growth of cultured cells in serum-free medium. Anal Biochem 1980; 102:255-270.

Bernanke DH Markwald RR Migratory behavior of cardiac cushion tissue cells in a collagen-lattice culture system. Dev biol 1982; 91:235-45.

Bitter T and Muir H A modified uronic acid carbazole reaction. Anal Biochem 1962; 4: 330-334.

Bosworth BT St John T Gallatin WM Harp JA Sequence of the bovine CD44 cDNA: comparison with human and mouse sequences. Mol Immunol 1991; 28:1131-1135.

Brecht M Mayer U Schlosser E Prehm P Increased hyaluronate synthesis is required for fibroblast detachment and mitosis. Biochem J 1986; 239:445-450.

Burleigh D Reich E Strickland S The culture of hormone-dependent epithelial cells from the rat ventral prostate. Mol Cell Endocrinol 1980; 19:183-191.

Bursh W Oberhammer F, Schulte-Hermann R Cell death by apoptosis and its protective role against disease. Trends Pharmacol Sci 1992; 131:245.

Camp RL Kraus TA Pure E Variations in the cytoskeletal interaction and posttranslational modification of the CD44 homing receptor in macrophages. J Cell Biol 1991; 115:1283-1292.

Camp RL Kraus TA Birkeland ML Pure E High levels of CD44 expression distinguish virgin from antigen-primed B cells. J Exp Med 1991; 173:763-766.

Camp RL Scheynius A Johansson C Pure E CD44 is necessary for optimal contact allergic responses but is not required for normal leukocyte extravasation. J Exp Med 1993; 178:497-507.

Carter WG Wayner EA Characterization of the class III collagen receptor, a phosphorylated transmembrane glycoprotein expressed in nucleated human cells. J Biol Chem 1988; 263:4193-201.

Comper WD Laurent TC Physiological function of connective tissue polysaccharides. Physiol Rev 1978; 58:255-315.

Cooke PS Young PF Cunha GR Androgen dependence of growth and epithelial morphogenesis in neonatal mouse bulbourethral glands. Endocrinology 1987; 121: 2153-2160.

Cooke PS Young PF Cunha GR A new model system for studying androgen-induced growth and morphogenesis in vitro: The bulbourethral gland. Endocrinology 1987; 121:2161-2170.

Culty M Miyake K Kincade PW The hyaluronate receptor is a member of the CD44 (H-CAM) family of cell surface glycoproteins [published erratum appears in J Cell Biol 1991 Feb;112(3):following 513]. J Cell Biol 1990; 111:2765-2774.

Cunha GR Battle F Young P Brody J Donjacour A Hayashi N Kinbara H Role of epithelial-mesenchymal interactions in the differentiation and spatial organization of visceral smooth muscle Epith Cell Biol 1992; 1: 76-83.

Cunha GR Lung B The possible influence of temporal factors in androgenic responsiveness of urogenital tissue recombinants from wild-type and androgen-insensetive (Tfm) mice J Exp Zool 1978; 105:181-194.

Cunha GR Reese BA Sekkingstad M Induction of nuclear androgen-binding sites in epithelium of the embryonic urinary bladder by mesenchyme of the urogenital sinus. Endocrinology 1980; 107:1767-1770.

Cunha GR Chung LWK Shannon JM Taguchi O Fujii H Hormone-induced morphogenesis and growth: Role of mesenchymal-epithelial interactions. Rec Prog Hormone Res 1983; 39:559-598.

Cunha GR Donjacour AA Cooke PS The endocrinology and developmental biology of the prostate. Endocrine Rev. 1987; 8:338-363.

Donjacour AA and Cunha GR Assessment of prostatic protein secretion in tissue recombinants made of urogenital sinus mesenchyme and urothelium from normal or androgen-insensitive mice. Endocrinology 1993;131:2342-2350.

Fell HB The development of organ culture. In: Ball M and MA Monnickendam MA (eds) Organ culture in biomedical research. Cambridge University Press, Cambridge 1976 p 2-13.

Geppert TD Lipsky PE Association of various T cell-surface molecules with the cytoskeleton. Effect of cross-linking and activation. J Immunol 1991; 146:3298-3305.

Gittinger JW Lasnitzki I The effect of testosterone metabolites on the fine structure of the rat prostate gland in organ culture. J Endocrinol 1972;52: 459-464.

Golstein P Ojcius DM Young DM Cell death mechanisms and the immune system. Immunol Rev 1991; 121:129.

Goldstein LA Zhou DF Picker LJ Minty CN A human lymphocyte homing receptor, The hermes antigen is related to cartilage proteoglycan core and link proteins. Cell 1989; 56:1063-1072.

Guntenhöner M Pogrel A Stern R A substrate-gel assay for hyaluronidase activity. Matrix 1992; 12:388-396.

Gunthert U Hofmann M Rudy W A new variant of glycoprotein CD44 confers metastatic potential to rat carcinoma cells. Cell 1991; 65:13-24.

Hascall VC and Hascall GK Proteoglycans In: Hay ED (ed). Cell biology of the extracellular matrix. New York. Plenum Press 1991 p 468.

Hayashi N Sugimura Y Kawamura J Donjacour AA Cunha GR Morphological and functional heterogeneity in the rat prostatic gland. Biol Reprod 1991; 45:308-321.

Herrlich P Zoller M Pals ST Ponta H CD44 splice variants: metastases meets lymphocytes. Immun Today 1993; 14:395-399.

Hobarth K Maier U Marberger M Topical chemoprophylaxis of superficial bladder cancer with mitomycin C and adjuvant hyaluronidase. European Urology 1992;21:206-210.

Hotez P Cappello M Hawdon J Beckers C Sakanari J Hyaluronidases of the gastrointestinal invasive nematodes Ancylostoma caninum and Anisakis simplex: possible functions in the pathogenesis of human zoonoses. J inf Dis 1994; 170: 918-926.

Howie SE Sommerfield AJ Gray E Harrison DJ Peripheral T lymphocyte depletion by apoptosis after CD4 ligation in vivo: Selective loss of CD44- and activating memory T cells. Clin Exp Immunol 1994;95: 195-206.

Goldstein LA Zhou DF Picker LJ Minty CN A human lymphocyte homing receptor, The hermes antigen is related to cartilage proteoglycan core and link proteins. Cell 1989; 56:1063-1072.

Isacke CM Sauvage CA Hyman R Lesley J Schulte R Trowbridge IS Identification and characterization of the human Pgp-1 glycoprotein. Immunogenetics 1986; 23:326-32.

Johansson R and Niemi M DNA and protein synthesis of prostatic cultures in relation to histological response under the influence of testosterone and its metbolites. Acta Endocrinol 1975; 78:766-780.

Jost A Problems of fetal endocrinology: The gonodal and hypophyseal hormones. Rec Prog Horm Res 1953; 8:379-418.

Kalomiris EL and Bourbuignon LY Lymphoma protein kinase c is associated with the transmembrane glycoprotein, GP85, and may function in GP85-ankyrin binding. J Biol Chem 1989; 264: 8113-8119.

Kerr JFR Willie AH Currie AR Apoptosis: A basic biological phenomenon with wide - ranging implications in tissue kinetics. Br J Cancer 1972; 26:239-245.

Knudson W Biswas C Li XQ Nemec RE Toole BP The role and regulation of tumor-associated hyaluronan. In: The biology of hyaluronan. Ciba Foundation Symposium, Wiley, 1989. Vol 143.

Knudson W Knudson CB. Assembly of a chondrocyte-like pericellular matrix on non-chondrogenic cells. Role of the cell surface hyaluronan receptors in the assembly of a pericellular matrix. J Cell Sci 1991; 99:227-235.

Krug EL Runyan RB Markwald RR Protein extracts from early embryonic hearts initiate cardiac endothelial cytodifferentiation. Dev Biol 1985; 112: 414-426.

Kujawa MJ Carrino DA Caplan AI Substrate-bonded hyaluronic acid exhibits a size-dependent stimulation of chondrogenic diffeentiation of stage 24 limb mesenchymal cells in culture. Dev Biol 1986;114: 519-528.

Kyprianou N, Isaacs JT. Expression of transforming growth factor-ß in the rat ventral prostate during castration-induced programmed cell death. Molecular Endocrinol 1989; 3:1515-1522.

Lacy BE, Underhill CD. The hyaluronate receptor is associated with actin filaments. J. Cell Biol 1987;105:1395-1404.

Lasnitzki I The action of androgens on rat prostate glands in organ culture. In: Balls M and Monnickendam MA (eds). Organ culture in biomedical research. Cambridge University Press. Cambridge. 1976; p 241-256.

Lasnitzki I The prostate in organ culture. In: Brandes D (ed). Male Accessory Sex Organs: Structure and Function. New York: Academic Press. 1974:348-382.

Lasnitzki I and Mizuno T Prostatic induction: interaction of epithelium and mesenchyme from normal wild-type mice and androgen-insensitive mice with testicular feminization. J Endocrinol. 1980; 85:423-428.

Lasnitzki I Whitaker RH Withycombe JFR The effect of steroid hormones on the growth pattern and RNA synthesis in human benign prostatic hyperplasia in organ culture. Br J Cancer 1975; 32: 168-178.

Laurent UB Fraser JR Disappearance of concentrated hyaluronan from the anterior chamber of monkey eyes. Exp Eye Res 1990; 51:65-69.

Lee C Physiology of castration-induced regression in rat prostate. Prog in Clin and Biol Res 1981; 75A:145-159.

Lee C Sensibar JA Dudek SM Hiipakka RA Liao S Prostatic ductal system in rats: regional variation in morphological and functional activities. Biol Reprod 1990; 43: 1079-1086.

Lieber MM Veneziale CM Cell and organ culture of male accessory sex organs. Adv. Sex Hormone Res. 1980; 4:73-118.

Lokeshwar VB Bourguignon LY Post-translational protein modification and expression of ankyrin-binding site(s) in GP85 (Pgp-1/CD44) and its biosynthetic precursors during T-lymphoma membrane biosynthesis. J Biol Chem 1991; 266:17983-17989.

Lokeshwar VB Bourguinon LY The lymphoma transmembrane glycoprotein GP85 is a novel guanine nucleotide-binding protein which regulates GP85 (CD44) -ankyrin interaction. J Biol Chem 1992; 267:22073-22078.

Lokeshwar VB Lokeshwar BL Pham HT Block NL Association of elevated levels of hyaluronidase, a matrix-degrading enzyme, with prostate cancer progression. Can Res 1996;56:651-657.

Lung B, Cunha GR. Development of seminal vesicles and coagulating glands in neonatal mice. 1. The morphogenetic effects of various hormonal conditions. Anat. Rec. 1981; 199:73-88.

Markwald RR Fitzharris TP Bank H Bernanke DH Structural analyses on the matrical organization of glycosaminoglycans in developing endocardial cushions. Dev Biol 1978; 62:292-316.

Markwald RR Fitzharris TP Bolender DL Bernanke DH Structural analysis of cell matrix association during morphogenesis of atrioventricular cushion tissue. Dev Biol 1979; 69:634-654.

Martikainen P Harkonen P Vanhala T Makela S Viljanen M Suominen J Multihormonal control of synthesis and secretion of prostatein in cultured rat ventral prostate. Endocrinology 1987; 121:604-611.

Martikainen P and Suominen J A morphometric analysis of rat ventral prostate in organ culture. Anat Rec 1983; 207: 279-288.

McCormick BA Zetter BR Adhesive interactions in angiogenesis and metastasis. Pharmac and Ther 1992;53:239-260

Meyer K Hyaluronidases. In Boyer PD (ed) The Enzymes. Academic Press, New York and London.1971 vol 2:307-320 .

Miyake K Medina KL Hayashi S Ono S Hamaoka T Kincade PW Monoclonal antibodies to Pgp-1/CD44 block lympho-hemopoiesis in long-term bone marrow cultures. J Exp Med 1990; 171:477-488.

Miyake K Underhill CB Lesley J Kincade PW Hyaluronate can function as a cell adhesion molecule and CD44 participates in hyaluronate recognition. J Exp Med 1990; 172:69-75.

Moriss-Kay GM and Solursh M Regional differences in mesenchymal cell morphology and glycosaminoglycans in early neural-fold stage rat embryos. J Embryol Exp Morphol 1978; 46:37-52.

Morriss-Kay GM Tuckett F Solursh M The effects of Streptomyces hyaluronidase on tissue organization and cell cycle time in rat embryos. J Embryol Exp Morph 1986; 98:59-70.

Nakamura A Manasek FJ An experimental study of the relation of cardiac jelly to the shape of the early chick embryonic heart. J Embryol Exp Morphol 1981; 65:235-256.

Neame SJ, Isacke CM Phosphorylation of CD44 in vivo requires both Ser323 and Ser325, but does not regulate membrane localization or cytoskeletal interaction in epithelial cells. Embo J; 11: 4733-4738.

Nogawa H Takaaki I Branching morphogenesis of embryonic mouse lung epithelium in mesenchyme-free culture. Development 1995; 121: 1015-1022.

Nogawa H Takahashi Y Substitution for mesenchyme by basement-membrane-like substratum and epidermal growth factor in inducing branching morphogenesis of mouse salivary gland. Development 1991; 112:855-861.

Nguyen M Watanabe H Budson AE Richie JP Folkman J Elevated levels of angiogenic peptide basic fibroblast growth factor in urine of bladder cancer patients. J NCI 1993;85(3): 241-242.

Ohno S Major Sex Determining Genes. New York: Springer-Verlag, 1979.

Pauli BU Knudson W Tumor invasion: a consequence of destructive and compositional matrix alterations. Human Pathology 1988;19:628-639.

Pintar JE Distribution and synthesis of glycosaminoglycans during quail neural crest morphogenesis. Dev Biol 1978; 67:444-464.

Pratt RM Larsen MA Johnstone MC Migration of cranial neural crest cells in a cell-free hyaluronate-rich matrix. Dev Biol 1975; 44:298-305.

Prins GS Birch L The developmental pattern of androgen receptor expression in rat prostate lobes is altered after neonatal exposure to estrogen. Endocrinology 1995; 136: 1303-1314.

Reissig JL Strominger JL Leloir LR A modified colometric method for the estimation of N-acetylamino sugars. Biol Chem 1955; 217:959-966.

Santi RS Johansson R Some biochemical effects of insulin and steroid hormones on the rat prostate in organ culture. Exp Cell Res 1973; 77: 111-120.

Shima H Tsuji M Young PF Cunha GR Postnatal growth of mouse seminal vesicle is dependent on 5a-dihydrotestosterone . Endocrinology 1990; 127:3222-3233.

Shtivelman E Bishop JM Expression of CD44 is repressed in neuroblastoma cells. Mol Cell Biol 1991; 11(11):5446-5453.

Stamenkovic I, Amiot M, Pesindro JM A lymphocyte molecule implicated in lymph node homing is a member of the cartilage link protein family. Cell 1989; 56:1057-1062.

Stern M and Stern R An ELISA-like assay for hyaluronidase and hyaluronidase inhibitors. Matrix 1992; 12:397-403.

Stetler-Stevenson WG Aznavoorian S Liotta LA Tumor cell interactions with the extracellular matrix during invasion and metastasis. Ann Rev Cell Bio 1993;9:541-573.

Sugimura Y Cunha G Bigsby R Androgenic induction of deoxyribonucleic acid synthesis in prostatic glands induced in the urothelium of testicular feminized (Tfm/y) mice. Prostate 1986; 9: 217-225.

Sugimura Y Cunha AA Donjacour RM Bigsby RM Brody JR Wholemount autoradiography study of DNA synthetic activity during postnatal development and androgen induced regeneration in the mouse prostate. Biol Reprod 1986; 34: 985-995.

Thompson D Controlled growth *en masse* (Somatic growth) of embryonic chick tissue in vitro. Marcus Beck Laboratory Reports, No. 4 Proc R Soc. Med 1914; 7: 21-46.

Toole BP Hyaluronan and its binding proteins, the hyaladherins. Curr Opin Cell Biol. 1990; 2: 839-844.

Toole BP Gross J The extracellular matrix of the regenerating newt limb: Synthesis and removal of hyaluronate prior to differentiation. Dev Biol 1971; 25:57-77.

Toole BP Trelstad RL Hyaluronate production and removal during corneal development in the chick. Dev Biol 1971; 26: 28-35.

Toole BP Turner RE Banerjee SD Hyaluronan-binding protein in chondrogenesis and angiogenesis in the developing limb. Prog Clin Biol Res 1993; 383B:437-444.

Trowbridge IF Lesley J Schulte R Hyman R Biochemical characterization and cellular distribution of a polymorphic murine cell-surface glycoprotein expressed on lymphoid tissues. Immunogenetics 1982; 15:299-312.

Turley EA bowman P Kytryk MA Effects of hyaluronate binding proteins on cell motile and contact behaviour. J Cell Sci 1985;78:133-145.

Turley EA Brassel P Moore D A hyaluronan-binding protein shows a partial and temporally regulated codistribution with actin on locomoting chick heart fibroblasts. Exp Cell Res 1990; 187:243-249.

Underhill CB Toole BP Binding of hyaluronate to the surface of cultured cells. J Cell Biol 1979; 82:475-484.

Vazquez MH de Larminat MA Blaquier JA Effect of androgen on androgen receptos in cultured human epididymis. J Endocrinol 1986;111-122.

West DC Hampson IN Arnold F Kumar S Angiogenesis induced by degradation products of hyaluronic acid. Science 1985; 228:1324-1326.

Wilson JD Syndrome of androgen resistance. Biol. Reprod. 1992; 46:168-173.

Wilson JD Griffin JE Leshin M George FW Role of gonodal hormones in the development of the sexual phenotypes Human Genetics 1981; 58:78-84.

Yamagata M Yamada KM Yoneda S Suzuki S Kimata K Chondroitin sulfate proteoglycan (PG-M-like proteoglycan) is involved in the binding of hyaluronic acid to cellular fibronectin. J Biol Chem 1986; 261:13526-13533.

Yu Q, Banerjee SD, Toole BP. The role of hyaluronan-binding protein in assembly of pericellular matrices. Dev Dyn 1992; 193:145-151.

Zhou DF Ding JF Picker LJ Bargatze RF Butcher EC Goeddel DV Molecular cloning and expression of Pgp-1: The mouse homology of the human H-CAM (Hermes) lymphocyte homing receptor. J Immunol 1989; 143:3390:3395.

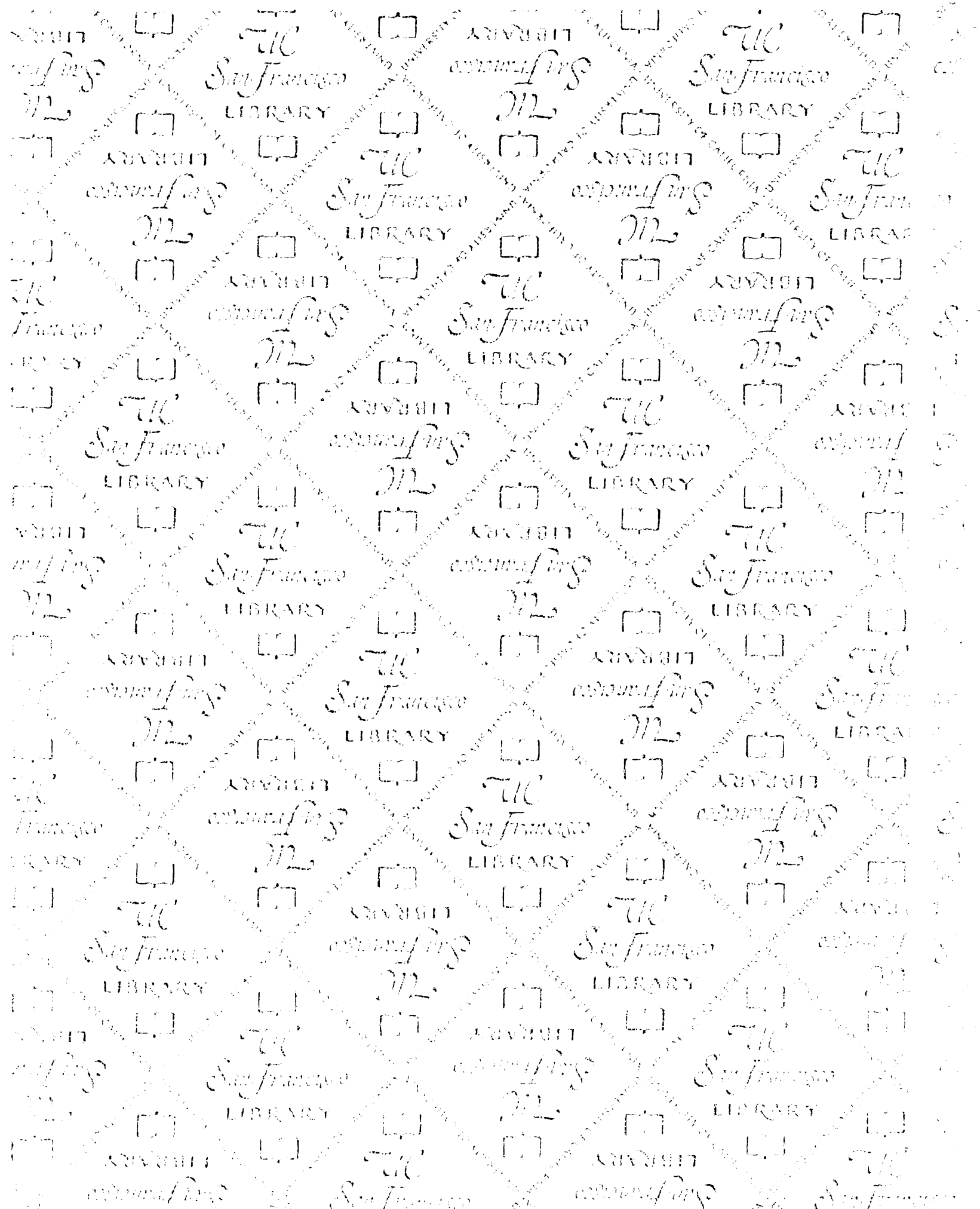
The San Francisco
LIBRARY